DIFFERENTIAL GUT MICROBIOTA AND FERMENTATION METABOLITE RESPONSE TO CORN BRAN ARABINOXYLANS IN DIFFERENT CHEMICAL AND PHYSICAL FORMS

by

Xiaowei Zhang

A Dissertation

Submitted to the Faculty of Purdue University

In Partial Fulfillment of the Requirements for the degree of

Doctor of Philosophy

Department of Food Science

West Lafayette, Indiana

May 2019

THE PURDUE UNIVERSITY GRADUATE SCHOOL
STATEMENT OF COMMITTEE APPROVAL

Dr. Bruce Hamaker, Chair
Department of Food Science
Dr. Bradley Reuhs
Department of Food Science
Dr. Kee-Hong Kim
Department of Food Science
Dr. Liping Zhao
Department of Biochemistry and Microbiology, Rutgers University

Approved by:

Dr. Arun Bhunia
Head of the Graduate Program

For my beloved wife
Yueheng

ACKNOWLEDGMENTS

I would like to express my special gratitude to my major adviser, Dr. Bruce Hamaker, for his valuable guidance, support and mentorship during my research and study at Purdue University. He not only enlarged my academic knowledge, but also taught me how to think differently and creatively. I would also like to thank my committee advisors Dr. Bradley Reuhs, Dr. Kee-Hong Kim, and Dr. Liping Zhao, for their great suggestions and wonderful insights. Also, special thanks to Dr. Osvaldo Campanella for his advices and thoughts on rheology study.

I would like to thank my friends at Purdue, Xin, Tong, Dongdong, Jing, Fei, Yongkai, Ziyun, Changping, Xingyun, Yezhi, Jingfan, Xingjian, Dongqi, Fangting and Chen, for their supports and care all the way long.

I would like to thank all my lovely lab members, Dr Mohammed Chegni, Dr. Elizabeth Pletsch, Dr. Yunus Tuncil, Dr. Xin Nie, Dr. Fang Fang, Dr. Byounghoo Lee, Dr. Cheng Li, Dr. Bin Zhang, Tianming, Anna, Leigh, Pablo, Jongbin, and especially to Dr. Tingting Chen, for her great help during my research and manuscript writing.

Lastly, I would like to thank my families. They gave me endless love and great supports throughout my life. Special thanks to my lovely wife Yueheng, thank her for unconditional support, encouragement and love throughout my PhD study that made the completion of this thesis possible.

TABLE OF CONTENTS

LIST OF TABLES

LIST OF FIGURES

ABSTRACT

Author: Zhang, Xiaowei. PhD
Institution: Purdue University
Degree Received: May 2019
Title: Differential Gut Microbiota and Fermentation Metabolite Response to Corn Bran Arabinoxylans in Different Chemical and Physical Forms
Committee Chair: Bruce Hamaker

As a major part of the dietary fiber classification, plant polysaccharides often have chemically complex structures which may differ by genera and species, and perhaps even by genotype and growing environment. Arabinoxylans from cereal cell walls are known to differently impact human gut microbiota composition and fermentation metabolites due to variability in chemical structure, though specificities of structure to these functions are not known at the level of genotype × environment. In the first study, corn bran arabinoxylan (CAX) extracted from 4 genotypes × 3 growing years at the Purdue Agronomy Farm was compared in human fecal fermentations to test the hypotheses that, 1) CAXs extracted from brans from different corn genotypes and grown over different years (environments) show distinct structures, and 2) these cause differences in gut microbiota response and fermentation metabolites. Monosaccharides and linkage analysis revealed that CAXs had different structures and the differences were genotype-specific, but not significantly due to environment. PCA analysis revealed that both short chain fatty acid production and the microbial community shifted also in a genotype-specific way. Thus, small structural changes, in terms of sugar and linkage compositions, cause significant changes in fermentation response showing very high specificity of structure to gut microbiota function.

Insoluble fermentable cell wall matrix fibers have been shown to support beneficial butyrogenic *Clostridia*, but have restricted use in food products due to their insoluble character.

In the second study, a soluble fiber matrix was developed that exhibited a similar fermentation effect as fermentable insoluble fiber matrices. Low arabinose/xylose ratio CAX was extracted with two concentrations of sodium hydroxide to give soluble polymers with relatively low and high residual ferulic acid (CAX-LFA and CAX-HFA). After laccase treatment to make diferulate crosslinks, soluble matrices were formed with average size of 3.5 to 4.5 mer. *In vitro* human fecal fermentation of CAX-LFA, CAX-HFA, soluble crosslinked ~3.5 mer CAX-LFA (SCCAX-LFA), and ~4.5 mer SCCAX-HFA revealed that the SCCAX matrices had slower fermentation property and higher butyrate proportion in SCCAX-HFA. 16S rRNA gene sequencing showed that SCCAX-HFA promoted OTUs associated with butyrate production including Unassigned *Ruminococcacea*e, Unassigned *Blautia*, *Fecalibacterium prausnitzii*, and Unassigned *Clostridium*. This is the first work showing the fabrication of soluble crosslinked fiber matrices that favors growth of butyrogenic bacteria.

Moreover, these same SCCAXs exhibited an interesting gel forming property on simple pH reduction, which is similar in gelling property to low acyl gellan gum, though is differently readily soluble in water. Both of the SCCAXs formed gels at pH 2, with SCCAX-HFA forming the stronger gel. Gels showed shear-thinning behavior and a thermal and pH reversible property. A gel forming mechanism was proposed involving noncovalent crosslinking including hydrogen bonds and hydrophobic interaction among the SCCAX complexes. This mechanism was supported by structural characterization of SCCAX complexes using a Zeta-sizer and FT-IR spectroscopy. SCCAX-HFA could be used in low sugar gels and has the above property of promoting butyrogenic bacteria in the gut.

In conclusion, gut microbiota responds differentially to CAXs with various fine structures. This probably due to dietary fiber-gut microbiota relationships have been evolved over time to be

highly specific. Forming soluble fiber matrices could be a good strategy to promote butyrogenic bacteria and improve gut health, in a readily usable form in beverages.

CHAPTER 1. INTRODUCTION

Nowadays, it is accepted that the state of the human gut microbiome is associated with many diseases, including type II diabetes, obesity, cardiovascular diseases, cancer, and even neurodegenerative disorders (Cani, 2017). Dietary fibers are the major dietary substrates for gut bacteria growth. Dietary fiber-gut microbiota relationships have evolved to be highly specific due to substrate sensing and enzymatic adaptions that best equip certain species or strains to utilize varied fiber structures (Hamaker & Tuncil, 2014; Larsbrink et al., 2014; Martens, Kelly, Tauzin, & Brumer, 2014; E. D. Sonnenburg et al., 2010). Therefore, small differences in the dietary fiber structures may affect the gut microbiota differently.

1.1 Hypothesis and Objectives

Arabinoxylans, the main non-starch polysaccharide in cereals, are heteroglycans composed of a β-1,4-linked xylan backbone with single arabinose branches or containing more complex branched structures with arabinose, galactose, glucuronic acid, and xylose. In bran cell walls, they are usually highly crosslinked with ferulic acid. Arabinoxylans (AX) from cereal cell walls are known to differently impact human gut microbiota composition and fermentation metabolites due to variability in structure. Corn bran, which accounts for 2% of the corn kernel weight, is an important by-product of the maize industry. There are ~68% of CAX in purified corn bran (Y. Li & Yang, 2016). Compared with rice and sorghum AX, CAX had highly branched and very complex structures (Chen et al., 2017; Rumpagaporn et al., 2015). Here, we hypothesized that CAX extracted from different corn genotypes and environments (growing years) would show different structures and these differences in structure would affect fermentation characteristics by human gut microbiota (Chapter 3). To test this hypothesis, CAX were extracted from 4

genotypes × 3 growing years at the Purdue Agronomy Farm. The structures, including monosaccharides and linkage composition of CAX, were analyzed by GC and GC-MS. CAX were then investigated in *in vitro* fecal batch fermentation for their impact on gut microbiota composition and metabolites. After realizing the importance of the chemical forms of CAX on gut microbiota, the second study was conducted to evaluate whether the differences in physical forms of CAX would affect gut microbiota composition and fermentation products. Insoluble fermentable cell wall matrix fibers have been shown to support beneficial butyrogenic gut *Clostridia*, but have restricted use in food products. We hypothesized that a soluble fiber matrix would have similar butyrogenic effects. To test the hypothesis, CAX with low arabinose/xylose ratio as well as esterified ferulic acid was crosslinked using laccase to form soluble crosslinked CAX (SCCAX) matrices. Then, SCCAX and CAX were fermented by gut bacteria *in vitro*. Butyrate production and butyrate-producing bacteria were analyzed by GC and 16S rRNA gene sequencing, respectively (Chapter 4). In a subsequent study, we found an interesting gelling property of SCCAX at low pH. In this study, we hypothesized that SCCAX-HFA would form a stronger gel than SCCAX-LFA, as they had denser structure and would form denser network structure to hold water. Since the gel was formed when lowering pH, we hypothesized that hydrogen bonding was probably involved in the gel formation. To test this hypothesis, G' and G'' of the gel was examined using a rheometer. The gel structure was measured with cryo-SEM. The structural feature of SCCAX were determined by HPSEC, HPLC, FT-IR, and a zeta-potential analyzer (Chapter 5).

CHAPTER 2. LITERATURE REVIEW

2.1 Impact of gut microbiota composition on human health

The human gut is colonized with a large and complex microbial community with functions that contribute to our systemic metabolism and have an effect on health and disease (Rowland et al., 2018). A growing work about the relationship among host diet, the composition of the gut microbiota, and host physiology has emerged. Essential functions of the gut microbiome include fermenting indigestible food components into absorbable metabolites, synthesizing vitamins and producing short chain fatty acids (SCFA), stimulating and regulating the immune system, increasing gut barrier function, and outcompeting pathogen colonization (Heintz-Buschart & Wilmes, 2018). Many studies have revealed that dysbiosis of the gut microbiota ecosystem is associated with a multitude of diseases including irritable bowel disease, obesity, type 2 diabetes and cardiovascular disease (Everard & Cani, 2013; Louis, Hold, & Flint, 2014; Patterson et al., 2016; Shreiner, Kao, & Young, 2015; Simren et al., 2013). Overall, gut microbiota composition has a profound impact on human health.

2.2 Contribution of diet to gut microbiota composition

2.2.1 Vegetarian and Western diets

Human gut microbiota composition is affected by many factors, including general lifestyle, host genetics, early bacteria colonization, medications, as well as diet (Graf et al., 2015). As the major energy source of gut bacteria, diet is a key factor that determines gut microbiota composition. Dietary patterns, such as vegetarian and Western diets, have different effects on the microbiota community structure. For instance, Western diets led to an underrepresentation of *Prevotella*, which was the ‘discriminatory taxon’ between Americans and Africans, and Venezuelans and

Malawians (De Filippo et al., 2010; Ou et al., 2013; Yatsunenko et al., 2012), accompanied by an overall decline in the biodiversity of human gut microbiota (J. L. Sonnenburg & Backhed, 2016).

2.2.2 Long-term and short-term diets

Gut microbiota composition is affected by both long-term and short-term diets. Long-term diets are strongly associated with gut microbiota enterotypes, where the *Prevotella* enterotype is associated with a plant-based diet and the *Bacteroides* enterotype is associated with diet high in animal fat and protein (Arumugam et al., 2011; G. D. Wu et al., 2011). Enterotype is a biomarker of the gut microbiota which might enable a better understanding of the link between diet and health outcome, and it might be used as a factor in personalized nutrition and obesity management (Christensen, Roager, Astrup, & Hjorth, 2018). The two enterotypes respond to environmental change differently. *Prevotella* enterotype subjects were found to lose body weight from a high fiber diet by increased SCFAs, while similar effects were not found in *Bacteroides* enterotypes (Hjorth et al., 2019; Hjorth et al., 2018). As the *Bacteroides* enterotype has comparatively lower biodiversity, it may show decreased resilience to environmental change (Vieira-Silva et al., 2016). In order to increase the response of the high fiber diet for the *Bacteroides* enterotype, one strategy may be to modulate the gut microbiota composition to respond more to fibers, perhaps by switching the community from the *Bacteroides* to *Prevotella* enterotype. However, it seems difficult to change the enterotype by diet alone, as it was reported that the microbial enterotypes remained stable during a 6-month randomized controlled diet intervention (Roager, Licht, Poulsen, Larsen, & Bahl, 2014).

On the other hand, short-term dietary changes can rapidly alter the gut microbiota. David *et al.* showed that short-term consumption of diets with entirely plant or animal products altered the human gut microbiota rapidly and reproducibly (David et al., 2014). The results were in line with

another study, which showed diets supplemented with resistant starch or non-starch polysaccharides affected the gut microbiota in a few days, while the gut microbiota could still be clustered at the level of the individual and no significant changes were found at the phyla level (Walker et al., 2011).

2.2.3 Specific foods

Specific foods affect the human gut microbiota differently. Among many examples, whole grain (corn, wheat, barley) breakfast increased the level of *Bifidobacteria* in the feces (Carvalho-Wells et al., 2010; Costabile et al., 2008; Martinez et al., 2013); consumption of wild blueberry drink for 6 weeks increased amount of *Bifidobacterium longum* and *Bifidobacterium adolescentis* (Guglielmetti et al., 2013; Vendrame et al., 2011); and the daily consumption of red wine polyphenols for 4 weeks significantly increased the level of *Enterococcus*, *Prevotella*, *Bacteroides*, *Bifidobacterium*, *Bacteroides uniformis*, *Eggerthella lenta*, and *Blautia coccoides–Eubacterium rectale* groups (Queipo-Ortuno et al., 2012). In another example, consumption of pistachio had better effect to favor the growth of butyrate producing bacteria than that of almond (Ukhanova et al., 2014).

2.2.4 Food constituents

Not only different specific foods, but also specific food constituents, impact the metabolism and composition of gut microbiota differently. Dietary fibers [e.g. resistant starch, inulin, frucooligosaccharides (FOS), galactooligosaccharides, arabinoxylans], are the main carbohydrate energy source for the gut bacteria and most affect community structure, though fat, protein, and phytochemicals also impact the microbiome. In this section, the impact of fat, protein and phytochemicals on gut microbiota will be discussed and the effect of dietary fiber will be discussed in the following one. In general, long term intake of a saturated fat diet is positively

correlated with *Bacteroides* enterotype (G. D. Wu et al., 2011). Fat affected gut microbiota through the stimulation of secretion of bile acids and increase deoxycholic acid, which had anti-microbial activity (David et al., 2014; Islam et al., 2011). High protein diets increase the branched SCFA content, and reduce butyrate and corresponding level of butyrogenic *Roseburia* and *Eubacterium* (David et al., 2014). Phytochemicals, such as phenolic acids and flavonoids, exhibited anti-microbial activity which alter gut microbiota composition.

2.3 Dietary fiber and the gut microbiome

2.3.1 Short chain fatty acids as key bacterial metabolites of dietary fiber fermentation

The undigested carbohydrates in the upper GI tract, referred to as dietary fiber, are the major dietary substrates for gut bacteria growth. The key microbial metabolites of the human colon fermentation process are short chain fatty acids (SCFAs), in particular acetate, propionate, and butyrate (typically ranging from 3:1:1 to 10:2:1 in molar ratios) (Cummings, Pomare, Branch, Naylor, & Macfarlane, 1987). SCFAs are important energy and signaling molecules, and have very different but important impacts on host physiology in various aspects (Koh, De Vadder, Kovatcheva-Datchary, & Backhed, 2016).

Butyrate is the preferred energy source for colonic epithelial cells and has been shown to lower inflammatory immune factors (Cushing, Alvarado, & Ciorba, 2015). It plays a protective role against colon cancer and colitis through inducing apoptosis of colon cancer cells and regulates gene expression by inhibiting histone deacetylases (Chriett et al., 2019). Moreover, it improves gut barrier function by stimulation of the formation of mucin, antimicrobial peptides, and tight-junction proteins (Riviere, Selak, Lantin, Leroy, & De Vuyst, 2016). It is increasingly accepted that butyrate producing bacteria and butyrate are beneficial to human health.

Propionate is also the energy source for epithelial cells, and recently has been considered as an important signaling molecule in satiety response. It plays a role in gluconeogenesis when transferred to liver, and interacts with fatty acids receptors FFAR2 and FFAR3 to activate intestinal IGN (Brown et al., 2003; De Vadder et al., 2014; Tazoe et al., 2008). Propionate is converted to glucose in intestinal gluconeogenesis and, therefore, promotes energy homeostasis through decreasing the production of hepatic glucose (De Vadder et al., 2014).

Acetate, as the most abundant SCFA of bacterial metabolites, is an essential substrate for cross-feeding species to produce butyrate (Riviere et al., 2016). For examples, *Faecalibacterium prausnitzii* cannot grow without acetate in pure culture (Duncan et al., 2004). Within the human body, after absorption, acetate is transferred to the portal vein and metabolized in various tissues (Riviere et al., 2016).

2.3.2 Fiber types and gut microbiota

Different types of dietary fibers are fermented by human gut bacteria differently. Resistant starch, including physically inaccessible starch (RS1), native granules (RS2), retrograded starch (RS3), and chemically modified starch (RS4) have been shown to favor different bacteria growths in the colon. Consumption of diets containing retrograded starch (RS3) for 10 weeks increased the level of *Ruminococcus bromii*, *Oscillibacter*, and *Eubacterium rectale* in most subjects (Walker et al., 2011). Another study investigated the impact of RS2 and RS4 on the gut microbiota showing that RS4 raised the abundance of *Bifidobacterium adolescentis* and *Parabacteroides distasonis*, while RS2 increased the amount of *R. bromii* and *E. rectale* (Martinez, Kim, Duffy, Schlegel, & Walter, 2010). Inulin and FOS have been investigated for their prebiotic effect to increase butyrate production and increase the abundance of *Bifidobacterium* (Benus et al., 2010; Costabile et al., 2010; Waitzberg et al., 2012).

2.3.3 Insoluble fiber and gut microbiota

While the role of soluble dietary fibers has garnered the most attention related to their role in gut health and contain the best known prebiotics (Slavin, 2013), the insoluble fermentable fiber matrices of plant cell walls also have an important role in supporting bacterial community structure (Flint, Scott, Duncan, Louis, & Forano, 2012). Relevant to butyrate production, these insoluble fibers seem to be preferentially fermented by the Clostridia bacteria groups locationally associated with the gut mucosa, and which contain some of the most prominent butyrate producers in the gut. These are also known by their *Clostridium* cluster designation and in the mammalian gut the main ones are *Clostridium* cluster IV, XIVa, and XIVb (Van den Abbeele et al., 2013). For example, *Clostridium* cluster XIVa has butyrogenic Eubacterium rectales and Roseburia intestinalis, among others, and has been shown to strongly attach to insoluble fermentable substrates such as brans and mucins (Leitch, Walker, Duncan, Holtrop, & Flint, 2007; Van den Abbeele et al., 2013). Recently, from a Brazilian group and ours, Cantu-Jungles *et al.* found that two insoluble β-D-glucans obtained from the fungi *Cookeina speciosai* were highly butyrate producing and *in vitro* specifically promoted *Clostridium* cluster XIVa butyrogentic *Anaerostipes*, and to a lesser extent *Bacteroides uniformis* and *Roseburia* (Cantu-Jungles et al., 2018). However, the insoluble property of these fibers limits their application in the food industry. It would be appealing to develop soluble fiber with similar butyrogenic effects, and fabricated soluble fiber matrices would be a potential way to achieve this target due to the matrix effect.

2.3.4 Fine fiber structure and gut microbiota

Dietary fiber-gut microbiota relationships have evolved to be highly specific due to substrate sensing and enzymatic adaptions that best equip certain species or strains to utilize varied fiber

structures (Hamaker & Tuncil, 2014; Larsbrink et al., 2014; Martens et al., 2014; E. D. Sonnenburg et al., 2010). For example, we recently reported on one *Anaerostipes spp.* that was highly specific to the fungus *Cookeina speciosa* β-glucans, and dramatically increased this one OTU from less than 0.5 to ~24% in a 24 h *in vitro* fecal fermentation (Cantu-Jungles et al., 2018). Specificity of fiber to gut function was also showed in a human study that investigated the impact of carbohydrate staple foods on the gut microbiota, revealing that intake of wheat and oats favored bifidobacteria, whereas rice suppressed bifidobacteria and wheat suppressed *Lactobaciilus, Ruminococcus*, and *Bacteroides* (J. Li et al., 2017). These results support the idea that the vast array of discrete structures of dietary fiber align to specific bacteria and favor their individual growth (Hamaker & Tuncil, 2014). From that point of view, it is highly beneficial to investigate the relation between response between gut microbiota and specific fine fiber structures rather than general structures. By adding such studies together, a framework can be built with information to manipulate the gut microbiota in a predictive way to improve human health.

2.4 Arabinoxylans

Arabinoxylan (AX), the main non-polysaccharide in cereals, is the major polymer in the cell wall of pericarp and endosperm cells, and the aleurone layer (Izydorczyk & Biliaderis, 1995). AXs have been widely used in the cereal industry, such as animal feeds, gluten-starch separation (Frederix, Van Hoeymissen, Courtin, & Delcour, 2004), bread making (Courtin & Delcour, 2002), and refrigerated dough (Simsek & Ohm, 2009). Moreover, AXs exhibited beneficial biological properties, including improving postprandial metabolic responses in patients with impaired glucose tolerance, and inhibiting the growth of tumor (Cao et al., 2011). Also, as an

important dietary fiber, the heterogenic structure of AX affects its utilization by human gut microbiota.

2.4.1 The molecular structure of AX

2.4.1.1 General structure of AX

AXs show different fine structures based on their botanical source, including cereals such as corn, rye, barley, oats, sorghum, wheat, rice, and other plants such as banana. AX can be extracted with various methods. For example, water, alkaline solubilization, enzyme extractions, physical treatments, and different combinations of these techniques, which can alter the structure of AX as well (Fadel et al., 2018; Izydorczyk & Biliaderis, 1995). The structure of AX differs in sugar composition, linkage pattern, and molecular weight, though the general structure of AX is similar (Izydorczyk & Biliaderis, 1995). AX consists of a linear backbone chain of β-D-1,4-linked xylopyranosyl residues with various compositions of branched structures. α-L-Arabino-furanosyl residues are attached to some or most of the Xylp residues at the O-2, O-3, and/or O-2,3 positions (Dornez, Gebruers, Delcour, & Courtin, 2009). AX can be neutral or acidic depending whether they contain 4-O-methyl-D-glucuronopyranosyl or D-glucuronopyranosyl substituents (Buchanan et al., 2003). Ferulic acid is commonly esterified on the O-5 position of arabinose branches (Izydorczyk & Biliaderis, 1995; Z. X. Zhang, Smith, & Li, 2014).

2.4.1.2 Solubility of AX

AXs are divided into water-extractable AX (WE-AX) and water-unextractable AX (WU-AX) fractions. WE-AX, which is loosely bound to the cell wall, accounts for 25-30% of AX in wheat flour (Izydorczyk & Biliaderis, 1994). The WU-AX that covalently and non-covalently interacted with lignin and cellulose are retained in the cell wall when exposed to water (Iiyama,

Lam, & Stone, 1994). WU-AX, however, is readily solubilized in alkali, which de-esterifies the diferulate crosslinks. Corn bran has higher alkali-soluble AX content than wheat or rice bran, as well as a higher portion of branches that contain both arabinose and xylose (Devin J. Rose, Patterson, & Hamaker, 2010). Wheat bran AX contains more unsubstituted backbone xylosyl regions, which can up to six repeating units (Schooneveld-Bergmans, Beldman, & Voragen, 1999).

2.4.1.3 Molecular weight of AX

The molecular weight of AX varies based on botanical source. Corn bran AX is essentially one molecular weight of ~500 kDa, while rice and wheat AXs mainly contain two fractions (~200 kDa and ~500 kDa) (Devin J. Rose et al., 2010). Rumpagaporn *et al*. compared alkali solubilized AX from corn, wheat, rice and sorghum bran and showed that sorghum bran AX (SAX) had highest weight-average molecular size of 540 kDa, followed by an endoxylanase-hydrolyzate of wheat alkali-extractable arabinoxylan (420 kDa), and corn bran arabinoxylan (360 kDa) (Rumpagaporn et al., 2015). CAX showed higher homogenous structure than AX from other botanical sources (Rumpagaporn et al., 2015).

2.4.1.4 Linkage pattern of AX

AX have various compositions of branched structures with α-L-arabino-furanosyl residues attached to some or most of the Xylp residues at O-2, O-3, and/or O-2,3 positions (Dornez et al., 2009). There are more arabinofuranosyl residues singly linked to the O-3 position of xylose than at the O-2 position (Izydorczyk & Biliaderis, 1994). CAX, wheat bran arabinoxylan, and sorghum bran arabinoxylan (SAX) are highly branched with at least 64% of substitution (Izydorczyk & Biliaderis, 1995; Rumpagaporn et al., 2015).

Some AXs have xylose units in branches and, in this case, terminal xylose could either be at the one xylose residual at the non-reducing end of the xylose backbone, singly branched at the O-3 position on the xylose backbone, or linked at O-2 or O-3 position of the branched arabinose (Saulnier, Marot, Chanliaud, & Thibault, 1995; Saulnier, Vigouroux, & Thibault, 1995). The content of terminal xylose linked directly to xylose backbone in CAX was 16%, and no terminal xylose was directly linked to xylose backbone in SAX (Rumpagaporn et al., 2015).

For the arabinose linkage, α-L-arabino-furanosyl residues are attached to some or most of the Xylp residues at O-2, O-3, and/or O-2,3 positions (Dornez et al., 2009). In addition, in the disaccharide chain linked to the xylose backbone, terminal xylose could be either (1, 2)- or (1, 3)-linked with arabinofuranosyl residues. The (1, 5)-linked arabinose residues may belong to the linking with another arabinose residual, terminal galactopyranosyl residue, or ferulic acid (Rumpagaporn et al., 2015).

2.4.2 Arabinoxylan and gut microbiota

2.4.2.1 Arabinoxylan and SCFAs

The major degrader of AXs in human gut is *Bacteroidetes*, which is the backbone xylan depolymerizing species. AX is degraded by the starch utilization system (Sus)-like system that is encoded in polysaccharide utilization loci in *Bacteroidetes* (Koropatkin, Cameron, & Martens, 2012). AX is first hydrolyzed to arabinoxylooligosaccharides (AXOS) by glycoside hydrolases and then further degraded to individual monosaccharides in the periplasm of Gram (-) bacteria. AXOS, along with AX, can also be further utilized by *Firmicutes* and *Actinobacteria,* to produce arabinose and xylose (Michlmayr et al., 2013; Sheridan et al., 2016). Arabinose and xylose ferments by *L. acidophilus, L. brevis, B. caterulatum, B. longum, B. dentium,* and *Roseburia spp.* to generate SCFA (Michlmayr et al., 2013; Ndeh & Gilbert, 2018; Riviere, Gagnon, Weckx,

Roy, & De Vuyst, 2015). Acetate is the most abundant SCFA in AX treatment, followed by propionate, and butyrate (Chen et al., 2017; Kaur, Rose, Rumpagaporn, Patterson, & Hamaker, 2011; Devin J. Rose et al., 2010; Rumpagaporn et al., 2015). AXOS showed butyrogenic effects and promoted the growth of *Bifidobacterium, Eubacterium, Faecalibacterium prausnitzii, Anaerostipes,* and *Roseburia* species (Riviere et al., 2016). In a humanized rat study, *Akkermansia muciniphila,* which is mucin-degrading bacteria, changed its predominant habit from caecum to distal region by long chain AX supplements, and converted mucin to propionate (Van den Abbeele et al., 2011).

2.4.2.2 AX structures affect gut microbiota composition

Emerging evidence shows that the various structures of AX affect fermentation rates, SCFA production, and gut microbiota composition differently (Chen et al., 2017; Kaur et al., 2011; Devin J. Rose et al., 2010; Rumpagaporn et al., 2015). Gut bacteria fermented AX from different botanical sources differently due to the structural variation of AX (Devin J. Rose et al., 2010). We previously found that alkaline-extracted soluble arabinoxylans from different botanical sources were fermented differently by human gut bacteria, and corn bran arabinoxylan exhibited highest SCFAs among corn, rice, and wheat bran arabinoxylan at 24 h human *in vitro* fecal fermentation (Devin J. Rose et al., 2010). This may because corn AX has less branched arabinose compared with rice AXs, and the bacteria were required to remove the arabinose branches until they use the xylose backbone. The results indicated a two-stage utilization, including an initial degradation of the unsubstituted regions followed by the highly branched arabinose being metabolized (Devin J. Rose et al., 2010). In another *in vitro* study, no correlation between AX molecular weight, arabinose/xylose ratio, or degree of substitution and fermentation rate was found (Rumpagaporn et al., 2015). Sorghum and rice bran AX were fermented faster

than corn bran AX (CAX), as they had a simple branched structure compared with CAX (Rumpagaporn et al., 2015). Similarly, Chen et al. also found sorghum bran AX was fermented more rapidly than CAX (Chen et al., 2017).

The degree of polymerization (DP) of AX showed different impacts on gut microbiota. AXs treated with xylanase had higher prebiotic index than AX without xylanase treatment (Vardakou et al., 2008). Lower DP of AXOS supplements had higher SCFA production than higher DP AXOS were also found by Geraylou *et al.* (Geraylou et al., 2013). These results were confirmed by many researchers (Gemen, de Vries, & Slavin, 2011; Pollet et al., 2012; Riviere et al., 2016). However, high DP AX also exhibited good prebiotic effects. High molecular WE-AX supplementation restored bacteria number that had been reduced by high-fat diet in mice (Neyrinck et al., 2011). Long chain AXs with high DP promoted propionate production in the distal region of the colon, as well as the growth of mucin degrader bacteria *Akkermansia muciniphila* (Van den Abbeele et al., 2011). Butyrate producing bacteria, including *Roseburia* and *E. rectale,* were promoted by a higher DP WU-AXs diet compared to WE-AX in a rat study (Damen et al., 2011). Taken together, AXs with higher DP or MW had positive prebiotic effect on gut microbiota as well as high SCFA production. Furthermore, FA esterified in the branched arabinose or free FA decreased the fermentability of AXOS, as bound FA inhibited enzyme activity by steric hindrance and free FA had anti-microbial activity (Snelders et al., 2014).

AXs have been shown to increase the abundance of *Bacteroides spp.*, *Roseburia, E. retale, Anaerostipes caccae, Clostridium clusters XIVa* and *Lactobacillus spp.* in several studies (Damen et al., 2011; Van den Abbeele et al., 2011). Bifidogenic effect of AX has rarely been reported (Broekaert et al., 2011). It is probably because the main enzyme that *Bifidobacterium* species produce are xylosidases and arabinofuranosidases (Van Den Broek & Voragen, 2008;

Zeng, Xue, Peng, & Shao, 2007). AXOS with lower DP, which are easier accessed by xylosidases and arabinofuranosidases, can be utilized by *Bifidobacterium* species. Jaskari *et al.* observed that *Bifidobacterium spp.* use xylooligomers as substrate (Jaskari et al., 1998). Sanchez *et al.* found that AXOS with average DP of 29 increased the level of *Bifidobacteria* in the ascending colon, and *Lactobacilli* in both ascending colon and transverse colon (Sanchez et al., 2009). It was also shown in an *in vitro* study that abundance of *Bifidobacteria*, *Lactobacilli*, and *Eubacterium rectale* was increased, while that of *Bacteroides* was decreased upon AXOS supplementation (Riviere et al., 2016; Snelders et al., 2014).

In conclusion, DP, DS, sugar composition, and linkage patterns of AX affect fermentation rate and production of SCFAs, as well as the composition of gut microbiota. It is well known that the SCFAs exhibit beneficial physiological functions. Therefore, it is possible that the structural variation of AX affects their health function through changing the fermentation pattern of gut microbiota.

2.5 Gelling properties of crosslinked AX

In addition to the beneficial health effect of AX as dietary fiber, ferulic acid that is esterified to the branched arabinose also exhibited antioxidant activity and has gained attention for its interesting functional and biological properties (Ayala-Soto, Serna-Saldivar, Garcia-Lara, & Perez-Carrillo, 2014; Mendez-Encinas, Carvajal-Millan, Rascon-Chu, Astiazaran-Garcia, & Valencia-Rivera, 2018). FA is the most abundant phenolic acid in AX with a content between 895 and 1174 μg/g dry matter of destarched bran (Dynkowska, Cyran, & Ceglinska, 2015). Content of FA depends on the origin of the tissue as well as extraction methods used to isolate AX (Mendez-Encinas et al., 2018). AX extracted from the pericarp or aleurone layer had higher FA content than endosperm (Snelders, Dornez, Delcour, & Courtin, 2013). FA content in AX

varied from 0.001 to 7 mg/g AX (Morales-Burgos et al., 2017). CAX had higher FA (6-7 mg/g AX) than millet bran and ispaghula seed (Iqbal, Akbar, Hussain, Saghir, & Sher, 2011; Morales-Burgos et al., 2017). AX showed a unique gelling property by the crosslinking of FA using oxidizing agents such as laccase or peroxidase/H_2O_2 (Figueroa-Espinoza & Rouau, 1998). The concentration of AX, Mw, and particularly the FA content significantly affects the gelling ability of AX (Mendez-Encinas et al., 2018).

2.5.1 Gelling mechanism of crosslinked AX

Crosslinked AX formed gels, through the formation of di-FA formation between the adjacent polysaccharide chains, leads to a three-dimensional gel network formation. During gelling, FA dimerization formed different structures dependent on the radical position at the benzol ring during the oxidation reaction (Mendez-Encinas et al., 2018). Five di-FAs, including 8-5′, 8-O-4′, 5-5′, 8-5’ benzo, and 8-8′ and one tri-FA (4-O-8′/5′-5′), have been detected in AX gels (Mendez-Encinas et al., 2018). Among these, di-FA and tri-FA, 8-5′ and 8-O-4′ were most abundant. However, decrease of FA monomers due to the oxidation of FA was not consistent with the amount of di-FA and tri-FA formed in gelation, which may be explained by the formation of larger FA oligomers, such as FA tetramers, FA pentamers or oligomers that are not yet identified (Carvajal-Millan, Landillon, et al., 2005; Vansteenkiste, Babot, Rouau, & Micard, 2004).

FA content is crucial for the gel formation. Kale *et al.* found that a strong gel was formed by the crosslinking action of laccase in CAX extracted with mild alkali that removes diferulate crosslinks, but retains much of the uncrosslinked bound ferulic acid (Kale, Hamaker, & Campanella, 2013). When treated with high concentration of alkali, no AX gel formed due to low ferulic acid content; and bound ferulic acid content was associated with the structural properties of the gel, including pore size and crosslinking density.

2.5.2 Structural parameter of AX gels

Crosslinking density (ρc), mesh size (ξ), and molecular weight between crosslinks (Mc), which are usually used to explain the structural characteristics of AX gels, are calculated by the examination of the swelling ratio of gels (Carvajal-Millan, Landillon, et al., 2005). The FA content is important for the gel structure, and it is reported that high FA content results in denser crosslinking, smaller mesh size and Mc, and more compact structures (Carvajal-Millan, Landillon, et al., 2005; Martinez-Lopez et al., 2016). Moreover, AX concentration had a high impact on the swelling ratio of AX gels. Martínez-López *et al.* found that swelling ratio increased from 9 to 18 g water/g AX, when the concentration of AX decreased from 6 to 4% (Martinez-Lopez et al., 2016). It is reasoned that higher concentration of AX would involve more FA to form the gel, and thus result in the formation of a more compact gel with limited the water absorption capacity. In contrast, when lower concentration of AX was used, longer un-crosslinked chain sections remained in the gel, which trapped more water and showed higher swelling ratio (Meyvis, De Smedt, Demeester, & Hennink, 2000; Rossmurphy & Shatwell, 1993).

2.5.3 Viscoelastic property of AX gels

Viscoelastic property of AX gels was examined by small-amplitude shear oscillatory rheology. The gelation ability of AX was associated with the AX concentration, Mw, the molecular structure of AX (e.g. degree of substitution), and FA content (Izydorczyk & Dexter, 2008). AX gels exhibited a typical characteristic of a solid-like material with a constant storage modulus (G') value independent of shear frequency, while the loss modulus (G'') was much smaller than G' and dependent of shear frequency (Carvajal-Millan, Landillon, et al., 2005; Martinez-Lopez, Carvajal-Millan, Rascon-Chu, Marquez-Escalante, & Martinez-Robinson, 2013). The kinetics of

AXs gelation showed a rapid increase of G' and reached a plateau (Izydorczyk & Dexter, 2008). The rapid increase of G' was due to covalent crosslinking formed between FA residues, and when enough di-FA formed, a gel was formed with limited the movement of AX chains, which prevented the formation of new crosslinking; thus a plateau was formed. In addition, higher FA content of AX formed stronger gels with higher G' (Carvajal-Millan, Landillon, et al., 2005; Mendez-Encinas et al., 2018).

2.5.4 Microstructure of AX gels

The microstructure of AX gels has been mostly examined by scanning electron microscopy (SEM). AX gels showed an imperfect honeycomb-like structure using cryo-SEM (Iravani, Fitchett, & Georget, 2011; Martinez-Lopez et al., 2013). AX from different botanical sources formed different gel structures. Martínez-López *et al.* observed that CAX gels exhibited an irregular honeycomb structure, while nejayote AX gels were a mix of sheets and rigid plates (Martinez-Lopez et al., 2013). Furthermore, the freezing rate prior to SEM examination also impacted gel results, and a fast freezing procedure had better persevered structure of AX gels (Mendez-Encinas et al., 2018).

2.6 Conclusion

This review highlights the importance of dietary fiber, particularly the fine structure, on gut microbiota composition which plays an important role in the host health. Structural variation, even within the same type of dietary fiber, differently affects fermentation rates and products, as well as the gut microbiota composition. This is probably because dietary fiber-gut microbiota relationships have evolved to be highly specific due to substrate sensing and enzymatic adaptions that best equip certain species or strains to utilize varied fiber structures (Hamaker & Tuncil,

2014; Larsbrink et al., 2014; Martens et al., 2014; E. D. Sonnenburg et al., 2010). AXs, as one important dietary fiber class, have attracted much attention, because of their biological activities. However, few studies have been done to investigate the specificities of structure to these functions, including at the level of plant genotype × environment. Furthermore, insoluble fermentable fibers could promote the butyrate production and butyrogenic *Clostridial cluster* XIVa. Identifying different structures of fiber substrates or fabricating a variety of substrates using enzyme treatments, and evaluating their fermentation profiles would likely lead to new ways to modulate the gut microbiota.

CHAPTER 3. FECAL MICROBIOTA RESPONDS TO CORN BRAN ARABINOXYLAN CHEMICAL STRUCTURES IN A GENOTYPE-SPECIFIC WAY

3.1 Abstract

As a major part of the dietary fiber classification, plant polysaccharides often have chemically complex structures which may differ by genotype and growing environment. Arabinoxylans from cereal cell walls are known to differently impact human gut microbiota composition and fermentation metabolites due to variability in structure, though specificities of structure to these functions are not known at the level of genotype × environment. Here, we compared corn bran arabinoxylan (CAX) extracted from 4 genotypes × 3 growing years at the Purdue Agronomy Farm in fecal fermentations to test the hypotheses that 1) CAXs extracted from different corn brans show distinct structures, and 2) these cause genotypic and environment-specific differences in fermentation by human gut microbiota. Monosaccharides and linkage analysis revealed that CAXs had different structures and the differences were genotype-specific, but not significantly due to environment. PCA analysis revealed that both short chain fatty acid production and microbial community shifted also in a genotype-specific way. Thus, small structural changes, in terms of sugar and linkage compositions, cause significant changes in fermentation response and show very high specificity of structure to gut microbiota function. It may possible that crop genotypes may one day be developed for an optimal targeted gut microbiota response.

3.2 Introduction

The human gut is inhabited with a large number of microorganisms, and they play an important role in maintaining human health. Essential functions of gut microbiome include fermenting indigestible food components into absorbable metabolites, synthesizing vitamins and producing

short chain fatty acids (SCFA), stimulating and regulating the immune system, increasing gut barrier function, and outcompeting pathogen colonization (Heintz-Buschart & Wilmes, 2018). A number of studies have revealed that dysbiosis of the gut microbiota ecosystem is associated with a multitude of chronic non-communicable diseases including irritable bowel disease, obesity, type 2 diabetes and cardiovascular disease (Everard & Cani, 2013; Louis et al., 2014; Patterson et al., 2016; Shreiner et al., 2015; Simren et al., 2013). The gut microbiome is influenced by many factors, and diet may be considered as the most important (De Filippis, Vitaglione, Cuomo, Canani, & Ercolini, 2018). Type, quality, and origin of the food shapes the gut microbiota composition, and affects the diversity, richness, function and impacts host-microbe interactions (Makki, Deehan, Walter, & Backhed, 2018).

The low intake of dietary fibers in the Western-style diet may contribute to depletion of specific bacterial taxa and result in dysfunctions contributing to increase in the development of chronic inflammatory diseases (E. D. Sonnenburg & Sonnenburg, 2014; J. L. Sonnenburg & Backhed, 2016). A recent study reviewed and analyzed 185 prospective studies and 58 clinical trials with 4634 adult participants, and found that higher daily intakes of dietary fiber (25-29 g) decreased 15-30% of all-cause and cardiovascular-related mortality, incidence of coronary heart disease, stroke incidence and mortality, type 2 diabetes, and colorectal cancer (Reynolds et al., 2019). While most of these studies are focused on the amount of daily fiber intake, limited data are available regarding the types of fiber consumed [i.e. fiber source (e.g. fruits, cereals, or vegetables) or subcategories (e.g. solubility, structure, extracted or whole grain) (Reynolds et al., 2019). Yet, it is well known that dietary fiber-gut microbiota relationships have evolved to be highly specific due to substrate sensing and enzymatic adaptions that best equip certain species or strains to utilize varied fiber structures (Hamaker & Tuncil, 2014; Larsbrink et al., 2014;

Martens et al., 2014; E. D. Sonnenburg et al., 2010). For example, we have recently reported on one *Anaerostipes spp.* was highly specific to *Cookeina speciosa* β-glucans, and dramatically increased from less than 0.5% to ~24% in a 24 h *in vitro* fecal fermentation (Cantu-Jungles et al., 2018). Specificity of fiber to gut function was also showed in a human study that investigated the impact of carbohydrate staple foods on gut microbiota, revealing that intake of wheat and oats favor bifidobacteria, whereas rice suppressed bifidobacteria and wheat suppressed *Lactobaciilus, Ruminococcus* and *Bacteroides* (J. Li et al., 2017).

Arabinoxylans, the main non-starch polysaccharide in cereals, are heteroglycans composed of β-1,4-linked xylan backbone with single arabinose branches or containing more complex branched structures with arabinose, galactose, glucuronic acid, and xylose. In bran cell walls, they are usually highly crosslinked with ferulic acid. Over sources, they widely vary in structure, which has been shown to differentially affect immunomodulation (Mendis, Leclerc, & Simsek, 2016). Arabinoxylans have demonstrated effects on the gut bacterial community, as it was reported that an arabinoxylan supplement effectively restored back to normal a microbial shift induced by a high-fat diet in mice (Neyrinck et al., 2011), and arabinoxylan-oligosaccharides (AXOS) with high degree of polymerization (DP) of 61 significantly decreased branched SCFA concentration while AXOS with low avDP (≤ 3) increased acetate and butyrate production as well as the level of *bifidobacteria* in rats (Van Craeyveld et al., 2008). We previously found that alkaline-extracted soluble arabinoxylans from different botanical sources were fermented differently by human gut bacteria, and maize bran arabinoxylan exhibited highest SCFAs among maize, rice and wheat bran arabinoxylan at 24 h human *in vitro* fecal fermentation, and structural differences also drove differences in fermentation rate (Devin J. Rose et al., 2010; Rumpagaporn et al., 2015). Recently, we reported that solubilized maize and sorghum arabinoxylans supported

different bacteria in *in vitro* fecal fermentation (Chen et al., 2017). Thus, variations in arabinoxylan chemical structures impact the way they are utilized by the gut bacteria.

We hypothesized that there is genotypic variation in arabinoxylan structures that impact the gut microbiota, as determined by fermentation metabolites and bacteria abundance. Moreover, structures of dietary fiber might be affected by growing environment and have similar different functional outcomes. As an example of a model dietary fiber, which we have used before, we chose to test this hypothesis using corn bran arabinoxylan and to examine differences in structure and gut microbiota function in different genotypes grown over different years. We felt this would put a focus on evaluation of gut functional effects of arabinoxylan on its specific fine structural variations instead of considering, as many do, of arabinoxylan as a generalized structure. Supporting this idea is that fine structure of arabinoxylans has been shown to be vary by genotype in wheat (Ordaz-Ortiz, Devaux, & Saulnier, 2005; Skendi, Biliaderis, Izydorczyk, Zervou, & Zoumpoulakis, 2011).

In the present study, we selected four corn genotypes, including MS71, CML103, B73 and OH43, which were grown in plots at the Agronomy Farm near West Lafayette, IN and harvested in 2013, 2015 and 2016, respectively. Corn bran arabinoxylan (CAX) solubilized with alkaline was then fermented with fecal microbiota obtained from three healthy donors. To our knowledge, this is the first study to provide scientific insight on how fiber structures impact gut microbial communities at the level of genotype × environment of a crop.

3.3 Material and Methods

3.3.1 Materials

Four genotypes of corns MS71, CML013, B73 and OH43 were grown in plots at the Agronomy Farm near West Lafayette, IN and harvested in 2013, 2015 and 2016, and were gifted from Dr.

Mitchell R. Tuinstra. Thermostable α-amylase, proteinase, human salivary α-amylase, pepsin, and pancreatin were obtained from Sigma-Aldrich (St. Louis, MO, USA). Fructooligosaccharide (FOS) was gifted from Ingredion (Ingredion Incorporated, Westchester, IL, USA). All chemicals used were of analytical grade.

3.3.2 Arabinoxylan extraction

Corns were soaked in warm water for 4 h and brans were separated by hands. Arabinoxylans were extracted followed by a protocol as described before (Kale et al., 2013). CAXs were named with their genotypes, growing place, and growing year. The samples were: MS71-WL13, MS71-WL15, MS71-WL16, CML103-WL13, CML103-WL15, CML103-WL16, B73-WL13, B73-WL15, B73-WL16, OH43-WL13, OH43-WL15, and OH43-WL16.

3.3.3 Neutral and acidic monosaccharides composition, and linkage pattern of CAXs

Neutral and acidic monosaccharides composition of CAXs were determined as their trimethylsilyl derivatives following the protocol described before (Doco, O'Neill, & Pellerin, 2001). The derivatives were analyzed with an Agilent 7890A gas chromatograph (Agilent Technologies, Santa Clara, CA, USA) equipped with an Agilent DB-5 capillary column. Helium was used as carrier gas at a flow rate of 1 mL/min. Injection volume was 0.2 μL at a split ratio of 50/1. Oven temperature was set at 140 °C initially, held for 2 min, and increased to 180 °C by 2 °C/ min, held for 1 min, and increased by 30 °C/min to 235 °C where it was held for 15 min. The glycosidic linkage composition of CAXs was measured by GC-MS after methylation, hydrolysis, reduction and acetylation according to Pettolino et. al. (Pettolino, Walsh, Fincher, & Bacic, 2012). An Agilent 7890A gas chromatograph and 5975C inert MSD with a triple-axis detector (Agilent Technologies, Santa Clara, CA, USA) equipped with an Agilent BPX70 column was used to analyze samples. Helium was used as the carrier gas at a flow rate of 1

mL/min. Injection volume was 1 μL at a split ratio of 10/1. Oven temperature was initially set at 170 °C, held for 2 min, and increased by 3 °C/min to 260 °C where it was held for 3 min. For the MS setup, MS quad and MS source were maintained at 106 °C and 230 °C, respectively. The data was collected in a scan mode from 100 to 350 m/z at 2.14 scans/s and with a solvent delay of 3 min.

3.3.4 *In vitro* human fecal fermentation of CAXs

CAXs were first treated with upper gastrointestinal tract digestion following a protocol as described previously (Lebet, Arrigoni, & Amado, 1998). The samples were then freeze dried and conducted with *in vitro* fecal fermentation as described by Chen *et al*. (Chen et al., 2017). Briefly, fresh stool samples were collected from three healthy participants who had no previous history of gastrointestinal disorders and had not taken any antibiotic for at least 3 months. Stool samples were transferred to an anaerobic chamber immediately and dispersed with basic culture medium (1:3, *w/v*), followed by filtration through four layers of cheesecloth. Then 50 mg of CAXs and fructooligosaccharides (FOS) were added to a mixture of 4 mL of culture medium and 1 mL of fecal inocula. The mixtures were incubated at 37 °C, collected and centrifuged at 0, 4, 8, 12, and 24 h. Supernatants were used for SCFA analysis, and the pellets were stored at -80 °C for DNA extraction. All experiments involving stool samples were conducted following a protocol approved by the Institutional Review Board of Purdue University (IRB protocol 1510016635).

3.3.5 SCFA analysis

Supernatants were filtered through a 0.22 μm polyethersulfone membrane and analyzed with gas chromatograph (Agilent 7890A GC, Agilent Technologies, Santa Clara, CA, USA) equipped with a fused silica capillary column (Nukol, Supelco nr 40369-03A, 30 m × 0.25 mm, id 0.25 μm, Palo Alto, CA, USA) following the protocol as described by Kaur *et al*. (Kaur et al., 2011).

3.3.6 DNA extraction and sequencing

DNA was extracted following a protocol as described by Zhang *et al.* (C. H. Zhang et al., 2012). DNA was extracted using the MP FastDNA spin kit (MP Biomedicals, Santa Ana, CA, USA) according to the manufacturer's instruction. Then, the V1-V3 region of the 16S rRNA gene was amplified by PCR with primers 5′-CGTATCGCCTCCCTCGCGCCATCAGACGAGTGCGTAGAGTTTGATYMTGGCTCAG-3′ and 5′-CTATGCGCCTTGCCAGCCCGCTCAGNNNNNNNNNNATTACCGCGGCTGCTGG-3′ with a sample-unique 10-mer oligonucleotide barcode. Analyses were performed at the DNA Services Facility at University of Illinois at Chicago (Chicago, IL, USA). The Illumina-generated sequencing data were analyzed by the QIIME platform (Caporaso et al., 2010). Operational taxonomic units (OTUs) were generated using the UCLUST method with a 97% similarity threshold in QIIME, and taxonomic annotations were assigned to each OTU by comparing to the Greengenes (version 13_8) database (McDonald et al., 2012). Singleton OTUs and samples with abnormally low number of reads were eliminated. Principal components analysis (PCA) and construction of the heatmap were carried out in R software.

3.3.7 Statistical analysis

Data were reported as mean ± SD for triplicate determinations. One-way ANOVA and Tukey's test were employed to identify differences in means. Statistics were analyzed using SPSS for Windows (version rel. 10.0.5, 1999, SPSS Inc., Chicago, IL, USA), Origin for Windows (version Srl b9.3.1.273, OriginLab Corp., Northampton, MA, USA) and RStudio software.

3.4 Results and Discussion

Arabinoxylans from cereal cell walls are known to differently impact human gut microbiota composition and fermentation metabolites due to variability in structure. However, specificities of structure to these functions is not known at the level of genotype × environment. Therefore, we investigated the impact of CAXs extracted from different genotypes and grown in different years on the gut microbial community. This is the first study to show that microbiota and its fermentation metabolites respond to CAX in a genotype-specific way, but not due to the environment.

3.4.1 CAXs extracted from different corn genotypes showed distinct chemical structures

3.4.1.1 CAXs exhibited different neutral and acidic sugar composition

Emerging evidence shows that discrete chemical structures, including monosaccharide composition and linkage patterns of the dietary fibers, affect fecal microbiota composition and their metabolites (Chen et al., 2017; Hamaker & Tuncil, 2014; Rumpagaporn et al., 2015; E. D. Sonnenburg et al., 2010). Here, the neutral and acidic sugar composition of CAXs extract from different corn bran samples were analyzed to investigate structural basis for genotype x environment effect on microbiota composition and metabolic products. As shown in **Table 3.1,** CAXs were composed of arabinose, xylose, galactose, and glucuronic acids [note that glucose was detected in minor amount, though removed from the table as CAX does not contain glucose; glucose likely was from a minor amount of residual starch in the corn bran that was solubilized by the alkali extraction solvent]. B73-WL13 had significantly ($P < 0.05$) higher xylose content (571.97 mg/g CAX) than other samples, while no significant differences in arabinose content were found among the 12 CAXs. Accordingly, B73-WL13, along with B73-WL15, had the lowest arabinose/xylose (A/X) ratios (0.46 and 0.47) (**Table 3.1**). The 12 CAX samples

exhibited a wider range of galactose (58.05-101.21 mg/g CAX) and glucuronic acid (18.23-23.35 mg/g CAX) contents. The A/X ratios of the CAXs are consistent with a typical ratio of ~0.5 (Devin J. Rose et al., 2010). It is noteworthy that B73-WL13 showed highest galactose and lowest glucuronic acid and A/X ratio (**Table 3.1**).

3.4.1.2 Corn genotypes affect CAX compositions

CAXs extracted from different corn genotypes had different galactose, glucuronic acid, and A/X ratios, while arabinose and xylose contents did not show significant differences (**Table 3.1**). As shown in **Figure 3.1,** B73 had significantly higher galactose content than MS71, CML103, and OH43 (**Figure 3.1**). CML103 and OH43 had significantly higher glucuronic acid than MS71 and B73 (**Figure 3.1**). OH43 had highest A/X ratio, while B73 had lowest A/X ratio (**Figure 3.1**). Thus, corn genotypes affect the chemical composition of CAXs.

Principle component analysis (PCA) was conducted to further examine how growing time and genotypes affected the monosaccharide composition of CAXs. Different colors and shapes of the dots represent different corn genotypes and growing year, respectively (**Figure 3.2**). No clear separation among the growing years was observed (**Figure 3.2**). For genotypes, B73 and MS71 exhibited clear separation from CML103 and OH43, though no clear cluster separation was found between CML103 and OH43. This is likely related to close similarity in CAX composition between CML103 and OH43. Taken together, the neutral and acidic sugar composition as well as the PCA analysis indicate that CAXs extracted from different genotypes had different structures, while CAXs from same genotype grown over different years tend to have similar structure.

3.4.1.3 CAXs exhibited different linkage patterns

The general structure of CAX contained a linear β-(1,4)-linked xylose backbone with arabinose mono- or di-substituted through O-2 or/and O-3 to xylose residues. As shown in **Table 3.2,** the

side chain of arabinofuranosyl residues was singled linked at O-3 position in all CAXs, this probably due to the retention time of alditol acetates of 2-O- and 3-O-methylxylose was too close to separate (Izydorczyk & Biliaderis, 1994). Different CAXs had different linkage patterns as expressed by different contents of each linkage (**Table 3.2**). Assuming that (1,4)-, (1,3,4)- and (1,2,3,4)-linked xylose residues all belong to the xylose backbone, the percentage of un-, mono-, and di-substituted xylose were calculated in **Table 3.3.** CAXs were highly branched with at least 66% of substitution, which was similar with we reported before (Rumpagaporn et al., 2015). MS71-WL13 and MS71-WL15 had lowest disubstitution and highest monosubstitution (**Table 3.3**).

3.4.2 SCFA production of CAXs in *in vitro* fecal fermentation

3.4.2.1 CAXs were slow fermented propiogenic fibers

Total SCFAs, acetate, propionate and butyrate production of each CAX in *in vitro* fecal fermentation are shown in **Table 3.4.** All CAXs were fermented slower with less than 60% of total SCFAs production at 4 h compared to FOS, the fast fermenting, butyrate-producing positive control (**Table 3.4**). CML103-WL15 and CML103-WL16 produced adequate amount of total SCFAs with FOS and significantly higher than other CAXs at 8 h. At 24 h, all CAXs showed similar amount of total SCFAs with FOS except MS71-WL13 and MS71-WL15, which were significantly lower ($P < 0.05$) (**Table 3.4**). A similar trend was found in the acetate production. For propionate, all CAXs were fermented with substantially higher levels than FOS at 24 h, confirming that CAXs are generally propiogenic (Chen et al., 2017; Devin J. Rose et al., 2010; Rumpagaporn et al., 2015). Among the CAXs, B73-WL15 produced the highest amount (44.28 mM) of propionate and CML103-WL16 the lowest amount (34.84 mM), accounting for ~78% of propionate produced by the former **(Table 3.4)**. FOS had higher butyrate than all CAXs at 24 h

(**Table 3.4**). For the CAXs, OH43-WL13 showed highest and MS71-WL13 lowest butyrate production (**Table 3.4**). When the absolute SCFAs amount at 24 h was calculated proportionally to a molar ratio value, CML103 and FOS showed relatively higher acetate and lower propionate proportions ($P < 0.05$). B73-WL16 had highest butyrate proportion of all CAXs (**Figure 3.5)**.

3.4.2.2 CAXs extracted from different corn genotypes exhibited distinct SCFAs profile

PCA analysis of SCFA production of *in vitro* fecal fermentation of CAX samples at 24 h was employed to examine how corn genotypes and growing year affected gut microbiota metabolites. As shown in **Figure 3.3,** SCFAs fermented from CAXs of different corn genotypes by fecal microbiota clustered separately, while no clear separation was found among growing years. The result was in accordance to the structural characterization of CAXs, where CAXs extracted from same genotype presented similar chemical structures over years. Moreover, gut microbiota fermented CAXs from different genotypes to acetate, propionate and butyrate at different rates. For example, CML103 fermented fastest with significantly higher total SCFAs and acetate production at 8 h (**Figure 3.4A** and **B**), while MS71 fermented slowest with lowest total SCFAs at all time points among the four genotypes (**Figure 3.4A**). In contrast, for propionate, CML103 produced the lowest amount, while B73 and OH43 had the highest amounts at 24 h among four corn genotypes (**Figure 3.4C**). CML103 had higher butyrate at 4 and 8 h fermentation, though at 24 h had lowest butyrate production. OH43 produced the highest butyrate amount among four corn genotypes ($P < 0.05$) (**Figure 3.4D**). The faster fermenting property of CML103 might related to its lower amount of terminal xylose in the branches, as terminal xylose has been reported to correlate to slower fermentation rate (Rumpagaporn et al., 2015). The results suggest that OH43 and B73 could be better propiogenic and butyrogenic genotypes, and that these differences in SCFAs production are likely due to structural differences of CAXs. Previously,

our laboratory found that different cereal arabinoxylan fibers and brans showed arabinoxylan-specific and cereal-specific differences in fermentation by fecal microbiota (Devin J. Rose et al., 2010; Rumpagaporn et al., 2015; Tuncil, Thakkar, Arioglu-Tuncil, Hamaker, & Lindemann, 2018). Here, the results indicate that even within the same cereal, CAXs extracted from different corn genotypes showed distinct chemical structures, resulting in them being fermented differently by human gut bacteria.

3.4.3 Microbiota shift of CAXs in *in vitro* fecal fermentation

3.4.3.1 Corn genotypes influenced α and β diversity of fermenting microbial communities

To examine whether corn genotypes alter the relative abundance of microbial species, microbiota compositions at 24 h fermentation were determined by 16S rRNA gene sequencing. The α and β diversities were calculated based on 97% identity level of operational taxonomic units (OTUs). The overall structures of the microbial community with different substrates were compared using the Bray-Curtis dissimilarity metric based on the relative abundance of OTUs at 24 h fermentation. As shown in **Figure 3.6**, microbiota fermenting the CAXs from different genotypes clustered separately, except for CML103-WL13 which was clustered with MS71 genotype. Permutational Multivariate Analysis of Variance Using Distance Matrices was conducted by Adonis function, and confirmed that CAXs from different genotypes resulted in significantly different communities ($P < 0.001$). Around 92% of the variation in distances could be explained by the genotype effects. The results indicate that fecal microbiota respond to CAXs in a genotype-specific way. As the chemical compositions of CAXs were distinct (**Figure 3.2**), the it is reasonable that structural differences were the basis for the rise in divergent microbial populations during the 24 h fermentation.

In general, α-diversity of CAX treatments significantly decreased after 24 h fermentation ($P < 0.05$), which included assessment by number of species observed, inverse Simpson, Chao1, Shannon, Simpson evenness indices, ACE, and Fisher (**Figure 3.7A-G**). Community richness did not significantly vary among CAXs of different genotypes, except for MS71, which showed significantly lower inverse Simpson, Shannon index, and Simpson values ($P < 0.05$). The overall reduction of α-diversity for CAX treatments was likely due to particular bacteria being preferentially increased in relative abundance at the expense of other species (Tuncil et al., 2018). FOS treatment resulted in higher α-diversity than CAX treatments. The low richness of CAXs treatment found in our results was likely due to the large expansion of the genera *Bacteroides* (**Figure 3.9 and 3.10**) and probably related to the fact that relatively few bacteria can utilize CAX due to its complex structure.

3.4.3.2 Corn genotypes differentially impacted the microbial community

The microbial composition of CAX treatments at 24 h of fermentation was compared to elucidate how different corn genotypes affect the gut microbial community (**Figure 3.9**). CAXs from different genotypes drove strong clustering in the microbial community structure (**Figure 3.8**). Although *Bacteroides* are generally good arabinoxylan degraders (Chassard, Goumy, Leclerc, Del'homme, & Bernalier-Donadille, 2007; Koropatkin et al., 2012; Martens et al., 2011), the magnitude of increase in the relative abundance of different *Bacteroides* species was genotype-dependent (**Figure 3.10**). For example, the most dominant bacteria for CAXs treatment was Unassigned *Bacteroides*, which increased in relative abundance after 24 h fermentation to ~37% in MS71 genotype that was significantly higher ($P < 0.05$) than the ~32% relative abundance for B73 and OH43 genotypes. In contrast, while not statistically significant, OH43 CAX treatment trended higher in relative abundance for *Bacteroides eggerthii*, followed by MS71 and CML103;

and, for *Bacteroides ovatus*, the highest increase in the relative abundance was observed for MS71, followed by B73, CML103 and OH43. These results suggested that though *Bacteroides* genera showed high ability to utilize CAXs, individual species exhibited different genotype preferences and affected the overall competition dynamics of the community.

Other bacteria OTUs also showed different response to different corn genotypes. For example, for Unassigned *Ruminococcus*, OH43 had a 2-fold increase relative abundance over MS71 ($P < 0.05$) (**Figure 3.10**). These results could explain the lower butyrate production in MS71, as *Ruminococcus* is associated with crossfeeding of butyrogenic bacteria that belong to the same *Clostridium* cluster XIVa. Significant increase in B73 in the relative abundance of Unassigned *Clostridiales*, which contains butyrogenic members may also explain variation in butyrate production. Statistically different bacterial relative abundances of *Parabacteroides distasonis* and Unassigned *Fusobacterium* were also observed among genotypes. Overall, differences in the varied CAX fine structures is speculated to have caused the bacterial growth differences.

3.4.3.3 SCFAs production is correlated with bacteria

To examine whether a correlation exists between SCFAs and gut bacteria, a feature ranking with recursive feature elimination model was used to identify OTUs responsible for individual and total SCFA production. As shown in **Table 3.5**, with data including all treatments and time points processed, Unassigned *Phascolarctobacterium* was identified as the most important OTU for acetate and propionate production. *Phascolarctobacterium*, known to be a substantial acetate/propionate producer, was reported in a human study to increase 3.62-fold by psyllium husk, which contains arabinoxylan (Jalanka et al., 2019; F. F. Wu et al., 2017). *Faecalibacterium prausnitzii* was the most important OTU related to butyrate production, followed by Unassigned *Blautia* and *Eubacterium dolichum. F. prausnitzii* (belong to *Clostridial* cluster IV), Unassigned

Blautia and *E. dolichum*, all belonging to *Clostridium* cluster XIVa, are known butyrogenic bacteria and expected to have a significant contribution to butyrate production (Louis & Flint, 2009; Riviere et al., 2016). Therefore, the results indicated the model is a good fit to examine correlations between individual and total SCFAs and corresponding bacteria. The model was further applied to single genotypes to examine the important OTU that responsible for individual SCFA production. As shown in **Table 3.5**, the important OTU ranking varied for the different corn genotypes, further confirming that gut bacteria responded to CAX treatments in a genotype-specific way. Moreover, the model was run for individual samples and found that, even within the same genotype, different samples also showed different important OTU rankings (data not shown).

3.5 Conclusion

In conclusion, this is the first paper to show that gut microbiota responds to fiber treatment in a genotype-specific way. CAXs extracted from different corn genotypes showed distinct chemical structures and, when fermented by human gut microbiota, they exhibited different SCFA profiles, as well as induced different gut microbiota community shifts. The results from this study indicate that not only fiber type or source should be considered for modulating gut microbiota composition, but also genotypic differences were another good indicator. The study highlights a level of difference that exists in dietary fibers at the chemical structure level that impact the gut microbiota community.

Table 3.1 Neutral and acidic monosaccharides composition of 12 CAXs extracted from corn with different genotypes and growing years[a].

Samples	Arabinose (mg/g)	Xylose (mg/g)	Galactose (mg/g)	Glucose (mg/g)	Glucuronic acid (mg/g)	A/X ratio
MS71-WL13	250.55 ± 18.90a	487.82 ± 32.51b	58.05 ± 3.03d	70.06 ± 4.23c	18.23 ± 2.16e	0.51 ± 0.01abc
MS71-WL15	242.75 ± 19.14a	480.74 ± 14.11b	58.67 ± 2.95cd	70.38 ± 3.09c	26.55 ± 2.01abcd	0.50 ± 0.03bcd
MS71-WL16	241.71 ± 27.52a	504.40 ± 54.64b	61.35 ± 8.23bcd	72.89 ± 11.13bc	22.75 ± 1.52bcde	0.48 ± 0.00de
CML103-WL13	242.28 ± 5.17a	498.65 ± 9.28b	77.58 ± 12.67abcd	84.03 ± 15.79abc	23.02 ± 2.52bcde	0.49 ± 0.01cde
CML103-WL15	263.40 ± 11.13a	519.40 ± 24.57b	66.98 ± 3.58bcd	74.17 ± 4.88bc	27.59 ± 1.30abc	0.51 ± 0.00bcd
CML103-WL16	249.46 ± 0.42a	488.42 ± 8.54b	60.70 ± 2.06bcd	68.59 ± 7.70c	32.35 ± 3.28a	0.51 ± 0.01bcd
B73-WL13	263.79 ± 2.76a	571.97 ± 7.45a	101.21 ± 8.96a	108.25 ± 3.23a	19.22 ± 1.12de	0.46 ± 0.00e
B73-WL15	243.55 ± 2.80a	517.84 ± 4.14b	84.85 ± 6.43abc	98.19 ± 11.48ab	16.89 ± 0.90e	0.47 ± 0.00e
B73-WL16	242.41 ± 3.14a	498.63 ± 13.70b	85.78 ± 18.02ab	88.40 ± 10.74abc	21.09 ± 5.07cde	0.49 ± 0.01cde
OH43-WL13	254.57 ± 5.46a	467.41 ± 11.79b	63.90 ± 1.28bcd	70.58 ± 4.84c	29.18 ± 0.23ab	0.54 ± 0.00a
OH43-WL15	267.67 ± 8.61a	519.37 ± 20.90b	68.01 ± 4.27bcd	70.65 ± 3.79c	28.16 ± 0.99abc	0.52 ± 0.01abc
OH43-WL16	257.12 ± 8.01a	493.82 ± 15.98b	63.25 ± 3.73bcd	69.80 ± 1.53c	27.39 ± 1.86abc	0.52 ± 0.00ab

[a] A/X was arabinose to xylose ratio. Data are expressed as mean ± SD (n = 3). Sample values marked by the different letters are significant different ($P < 0.05$).

Table 3.2 Glycosidic linkage composition (mol%) of 12 CAXs extracted from corn with different genotypes and growing years.[b]

Component	Linkage indicated	MS71-WL13	MS71-WL15	MS71-WL16	CML103-WL13	CML103-WL15	CML103-WL16	B73-WL13	B73-WL15	B73-WL16	OH43-WL13	OH43-WL15	OH43-WL16
2,3,5-Me_3-Ara	(Ara*f*)1→	15.69 ± 1.21	14.92 ± 0.18	13.99 ± 0.27	15.96 ± 0.35	18.79 ± 2.13	15.90 ± 0.22	13.87 ± 0.69	13.31 ± 0.61	13.29 ± 0.96	16.28 ± 0.37	17.09 ± 0.73	16.64 ± 0.57
3,5-Me_2-Ara	→2(Ara*f*)1→	4.38 ± 1.05	4.67 ± 0.07	5.51 ± 0.18	4.13 ± 0.16	2.58 ± 0.88	4.13 ± 0.27	6.22 ± 0.57	5.71 ± 0.21	5.11 ± 0.72	4.09 ± 0.15	4.51 ± 0.53	4.35 ± 0.60
2,5-Me_2-Ara	→3(Ara*f*)1→	3.68 ± 0.15	3.42 ± 0.17	3.43 ± 0.07	2.62 ± 0.22	3.24 ± 0.83	3.40 ± 0.04	4.33 ± 0.01	3.30 ± 0.66	3.79 ± 0.27	3.28 ± 0.22	3.58 ± 0.17	3.34 ± 0.04
2,3-Me_2-Ara	→5(Ara*f*)1→	1.30 ± 0.09	1.26 ± 0.04	1.25 ± 0.03	1.51 ± 0.06	1.73 ± 0.43	1.51 ± 0.09	1.96 ± 0.16	2.03 ± 0.32	2.04 ± 0.06	1.81 ± 0.11	1.58 ± 0.06	1.38 ± 0.07
2,3,4-Me_3-Xyl	(Xyl*p*)1→	14.59 ± 1.27	13.04 ± 0.99	9.12 ± 0.29	11.84 ± 0.61	12.21 ± 2.75	10.99 ± 0.86	11.14 ± 0.58	13.21 ± 0.56	11.97 ± 2.04	10.33 ± 2.90	13.24 ± 1.70	13.67 ± 0.93
2,3-Me_2-Xyl	→4(Xylp)1→	10.80 ± 0.30	10.06 ± 0.52	7.23 ± 0.29	9.50 ± 0.77	9.04 ± 1.82	8.10 ± 0.91	7.70 ± 0.22	9.74 ± 0.70	8.56 ± 0.17	6.88 ± 0.86	9.82 ± 0.31	9.59 ± 0.75
2-Me_1-Xyl	→4(Xylp)1→3↑	19.31 ± 1.30	18.72 ± 1.36	12.65 ± 0.38	17.86 ± 0.96	17.96 ± 2.33	17.82 ± 3.19	14.44 ± 1.00	16.28 ± 1.48	16.73 ± 2.15	12.52 ± 1.71	17.02 ± 1.03	17.70 ± 0.40
Xyl	→4(Xylp)1→2↑,3↑	2.09 ± 0.52	3.15 ± 1.29	10.28 ± 0.41	5.18 ± 0.21	6.46 ± 1.24	6.09 ± 2.23	11.03 ± 0.65	5.90 ± 0.78	6.13 ± 1.05	9.26 ± 2.98	6.11 ± 1.70	4.38 ± 0.93
2,3,6-Me_3-Glc	→4(Glc*p*)1→	1.14 ± 0.34	0.68 ± 0.43	0.65 ± 0.44	0.56 ± 0.24	1.34 ± 1.34	0.56 ± 0.23	0.50 ± 0.25	0.66 ± 0.25	0.37 ± 0.24	0.38 ± 0.04	0.81 ± 0.08	0.66 ± 0.29
2,3-Me_2-Glc	→4(Glc*p*)1→6↑	5.86 ± 0.34	6.35 ± 0.43	6.64 ± 0.44	7.84 ± 0.24	6.08 ± 1.34	6.29 ± 0.23	10.32 ± 0.25	9.16 ± 0.25	8.47 ± 0.24	6.68 ± 0.04	6.25 ± 0.08	6.32 ± 0.29
2,3,4,6-Me_4-Gal	(Gal*p*)1→	5.27 ± 0.05	5.26 ± 0.99	5.59 ± 0.29	7.22 ± 0.14	6.33 ± 0.05	5.66 ± 0.02	9.23 ± 0.06	7.62 ± 0.19	7.84 ± 0.10	5.56 ± 0.35	6.02 ± 0.09	5.80 ± 0.09
2,4,6-Me_3-Gal	→3(Gal*p*)1→	0.54 ± 0.05	0.61 ± 0.99	0.55 ± 0.29	0.54 ± 0.14	0.36 ± 0.05	0.41 ± 0.02	0.89 ± 0.06	0.86 ± 0.19	0.74 ± 0.10	0.83 ± 0.35	0.78 ± 0.09	0.52 ± 0.09

[b]Glycosidic linkage was determined by gas chromatography of alditol acetates of partially methylated polysaccharides. Molar ratio was converted by peak areas using molar response factor. Values were expressed as proportion of all partially methylated alditol acetates detected.

Table 3.3 Percent substitution of xylopyranosyl residues in the xylan backbone.

Type of substitution	Unsubstituted xylose	Monosubstituted xylose	Disubstituted xylose
MS71-WL13	33.54	59.97	6.49
MS71-WL15	31.51	58.63	9.87
MS71-WL16	23.97	41.94	34.08
CML103-WL13	29.19	54.89	15.92
CML103-WL15	27.02	53.68	19.31
CML103-WL16	25.30	55.67	19.03
B73-WL13	23.21	43.53	33.25
B73-WL15	30.51	51.00	18.48
B73-WL16	27.24	53.25	19.51
OH43-WL13	24.01	43.68	32.31
OH43-WL15	29.80	51.65	18.54
OH43-WL16	30.28	55.89	13.83

Table 3.4 Short chain fatty acid production of 12 CAXs compared with blank and FOS by fecal microbiota from *in vitro* fermentation.

SCFA	Blank	MS71-WL13	MS71-WL15	MS71-WL16	CML103-WL13	CML103-WL15	CML103-WL16	B73-WL13	B73-WL15	B73-WL16	OH43-WL13	OH43-WL15	OH43-WL16	FOS
Total SCFA														
4 h	11.31 ± 0.47f	36.78 ± 4.43e	36.17 ± 2.37e	40.66 ± 0.32de	47.95 ± 3.28bc	48.38 ± 2.95bc	52.14 ± 1.61b	44.50 ± 3.74cd	47.19 ± 1.63bcd	47.35 ± 1.88bcd	51.03 ± 2.36bc	51.26 ± 2.33bc	46.10 ± 0.34bcd	93.22 ± 1.39a
8 h	13.39 ± 0.69f	77.08 ± 2.33e	81.58 ± 2.06de	82.92 ± 1.78de	94.95 ± 5.11bc	101.92 ± 3.40ab	105.29 ± 5.94a	80.11 ± 1.27e	78.49 ± 1.85e	82.61 ± 2.04de	89.99 ± 3.07cd	85.43 ± 4.62cde	80.85 ± 1.37de	105.87 ± 4.39a
12 h	12.05 ± 0.41h	95.30 ± 3.58g	92.88 ± 3.84efg	94.09 ± 2.51fg	102.74 ± 1.31cdef	107.55 ± 3.32bcd	111.18 ± 1.09bc	100.91 ± 2.47defg	102.97 ± 5.15cdef	104.72 ± 3.92bcde	105.99 ± 3.19bcd	112.89 ± 2.05b	108.87 ± 5.92bcd	125.63 ± 2.28a
24 h	15.34 ± 1.70c	117.45 ± 4.43b	119.34 ± 6.17b	121.06 ± 9.12ab	121.89 ± 5.12ab	128.78 ± 6.10ab	122.63 ± 6.60ab	131.22 ± 4.85ab	134.18 ± 5.66ab	122.18 ± 4.70ab	132.96 ± 6.91ab	137.08 ± 7.97a	129.82 ± 2.44ab	132.72 ± 5.93a
Acetate														
4 h	7.73 ± 0.35h	24.75 ± 3.64g	25.87 ± 0.68fg	28.07 ± 2.48efg	34.08 ± 1.45bcd	34.46 ± 1.45bcd	37.64 ± 1.47b	30.57 ± 1.13def	33.29 ± 1.23bcd	33.48 ± 1.13bcd	35.52 ± 2.03bc	36.46 ± 1.37bc	32.29 ± 0.57cde	72.20 ± 1.59a
8 h	9.30 ± 0.47f	50.41 ± 1.00e	52.87 ± 1.80de	54.06 ± 3.84de	65.28 ± 3.04bc	70.17 ± 3.04ab	72.52 ± 4.25a	51.62 ± 0.98e	50.47 ± 1.23e	53.95 ± 1.06de	58.76 ± 1.26cd	56.09 ± 2.51de	52.63 ± 0.88de	74.45 ± 3.42a
12 h	8.34 ± 0.18f	58.86 ± 2.29de	57.14 ± 2.41e	58.15 ± 0.13de	67.27 ± 1.70bc	70.04 ± 1.70b	72.37 ± 0.75b	62.14 ± 0.93cde	62.68 ± 3.44cde	63.63 ± 2.62cd	66.14 ± 1.84bc	71.11 ± 0.88b	67.74 ± 4.43bc	83.14 ± 0.80a
24 h	10.97 ± 1.35c	70.91 ± 2.66b	72.28 ± 4.09b	73.28 ± 3.52b	78.76 ± 4.68ab	83.19 ± 4.68ab	79.25 ± 4.69ab	79.05 ± 3.48ab	80.71 ± 4.06ab	72.23 ± 3.10b	81.29 ± 5.01ab	86.22 ± 7.13a	80.15 ± 3.00ab	87.95 ± 4.32a
Propionate														
4 h	2.61 ± 0.07d	9.79 ± 0.59bc	7.93 ± 1.31c	10.11 ± 0.17bc	10.94 ± 0.48bc	10.54 ± 0.96bc	11.17 ± 0.44b	11.21 ± 2.88b	11.04 ± 0.46b	10.69 ± 0.52bc	11.87 ± 0.33ab	11.39 ± 0.72b	10.74 ± 0.34bc	14.58 ± 1.23a
8 h	2.96 ± 0.28d	23.76 ± 1.35bc	25.10 ± 0.41abc	25.37 ± 0.40abc	25.53 ± 1.11abc	27.03 ± 1.00ab	27.68 ± 0.93a	24.73 ± 0.52abc	24.28 ± 0.40abc	24.87 ± 2.58abc	26.66 ± 2.04abc	24.73 ± 1.93abc	24.11 ± 0.43abc	23.05 ± 1.50c
12 h	2.63 ± 0.23e	31.89 ± 1.12abcd	30.72 ± 1.36bcd	30.80 ± 0.66bcd	29.38 ± 1.25cd	31.37 ± 1.38abcd	32.46 ± 2.12abc	33.57 ± 1.73ab	34.02 ± 1.57ab	35.45 ± 1.07a	33.40 ± 1.37abc	34.63 ± 1.08ab	34.64 ± 1.16ab	27.84 ± 1.97d
24 h	3.12 ± 0.24g	39.45 ± 1.07bcd	39.15 ± 1.46bcde	39.90 ± 2.70bc	35.53 ± 1.49de	37.20 ± 1.40cde	34.83 ± 1.87e	43.29 ± 0.56ab	44.28 ± 1.80a	41.78 ± 1.28ab	41.50 ± 1.53abc	41.39 ± 1.64abc	40.67 ± 0.70abc	29.04 ± 0.91f
Butyrate														
4 h	0.97 ± 0.06d	2.23 ± 0.25cd	2.37 ± 0.50bc	2.49 ± 0.19bc	2.93 ± 0.40bc	3.38 ± 0.57bc	3.34 ± 0.48bc	2.72 ± 0.64bc	2.86 ± 0.20bc	3.18 ± 0.25bc	3.63 ± 0.67b	3.41 ± 0.51bc	3.07 ± 0.08bc	6.44 ± 0.55a
8 h	1.13 ± 0.23g	2.91 ± 0.05f	3.61 ± 0.17def	3.48 ± 0.16ef	4.14 ± 0.38bcde	4.72 ± 0.27bc	5.09 ± 0.77b	3.75 ± 0.16cdef	3.73 ± 0.40cdef	3.78 ± 0.28cdef	4.57 ± 0.15bcd	4.61 ± 0.18bcd	4.11 ± 0.08bcde	8.36 ± 0.61a
12 h	1.07 ± 0.02g	4.55 ± 0.32f	5.02 ± 0.08ef	5.13 ± 0.36def	6.09 ± 0.10bcd	6.14 ± 0.42bcd	6.34 ± 0.43	5.20 ± 0.18def	6.27 ± 0.32bc	5.64 ± 0.48cde	6.46 ± 0.10bc	7.15 ± 0.47b	6.49 ± 0.38bc	14.66 ± 0.56a
24 h	1.25 ± 0.26e	7.09 ± 0.84d	7.92 ± 0.68cd	7.88 ± 0.70cd	7.60 ± 0.57cd	8.40 ± 0.28bcd	8.55 ± 0.58bcd	8.88 ± 0.92bcd	9.19 ± 0.25bc	8.17 ± 0.33cd	10.17 ± 0.93b	9.47 ± 0.64bc	9.00 ± 0.31bc	15.73 ± 0.82a

[a]Data are expressed as mean ± SD (n = 3). Sample values marked by the different letters are significant different ($P < 0.05$).

Table 3.5 Important OTU that associated with short chain fatty acid analyzed by Linear support vector machine methods (SVM) based Recursive Feature Elimination (RFE).

	Important OTU Rank	Acetate	Propionate	Butyrate	Total SCFA
All data	1	Unassigned *Phascolarctobaterium*	Unassigned *Phascolarctobaterium*	*Faecalibacterium prausnitzii*	Unassigned *Megamonas*
	2	Unassigned *Coprococcus*	Unassigned *Coprococcus*	Unassigned *Blautia*	Unassigned *Coprococcus*
	3	Unassigned *Ruminococcaceae*	*Ruminococcus gnavus*	*Eubacterium dolichum*	Unassigned *Phascolarctobaterium*
	4	Unassigned *Ruminococcus*	Unassigned *Ruminococcus*	Unassigned *Erysipelotrichaceae*	*Faecalibacterium prausnitzii*
Genotypes					
MS71	1	Unassigned *Erysipelotrichaceae*	*Eubacterium biforme*	*Eubacterium biforme*	*Eubacterium biforme*
	2	Unassigned Other	Unassigned Other	Unassigned *Bifidobacterium*	Unassigned *Bifidobacterium*
	3	Unassigned *Ruminococcaceae*	Unassigned *Oscillospira*	Unassigned *Phascolarctobaterium*	Unassigned *Peptostreptococcaceae*
	4	Unassigned *Lachnospiraceae*	Unassigned *Lachnospiraceae*	Unassigned *Oscillospira*	Unassigned Other
CML103	1	Unassigned *Erysipelotrichaceae*	*Eubacterium biforme*	Unassigned *Ruminococcus*	Unassigned *Phascolarctobaterium*
	2	Unassigned *Peptostreptococcaceae*	Unassigned *Oscillospira*	Unassigned *Clostridiales*	*Eubacterium biforme*
	3	Eubacterium D*olichum*	*Eubacterium Dolichum*	Unassigned *Erysipelotrichaceae*	*Eubacterium dolichum*
	4	Unassigned *Clostridiales*	Unassigned *Clostridiales*	*Faecalibacterium prausnitzii*	Unassigned *Clostridiales*
B73	1	Unassigned *Phascolarctobaterium*	*Eubacterium dolichum*	Unassigned *Ruminococcus*	Unassigned *Phascolarctobaterium*
	2	Unassigned *Coprococcus*	*Bacteroides ovatus*	*Parabacteroides distasonis*	Unassigned *Bacteroides*
	3	Unassigned *Megamonas*	*Eubacterium biforme*	Unassigned *Erysipelotrichaceae*	Unassigned *Erysipelotrichaceae*
	4	*Collinsella aerofaciens*	*Collinsella aerofaciens*	Unassigned *Phascolarctobaterium*	Unassigned Other
OH43	1	Unassigned *Megamonas*	Unassigned *Oscillospira*	Unassigned *Clostridiales*	Unassigned *Erysipelotrichaceae*
	2	Unassigned *Blautia*	Unassigned *Clostridiales*	*Eubacterium dolichum*	Unassigned *Blautia*
	3	*Eubacterium biforme*	Unassigned *Phascolarctobaterium*	Unassigned *Erysipelotrichaceae*	*Eubacterium biforme*
	4	Unassigned Other	*Bacteroides eggerthii*	*Eubacterium biforme*	Unassigned Other

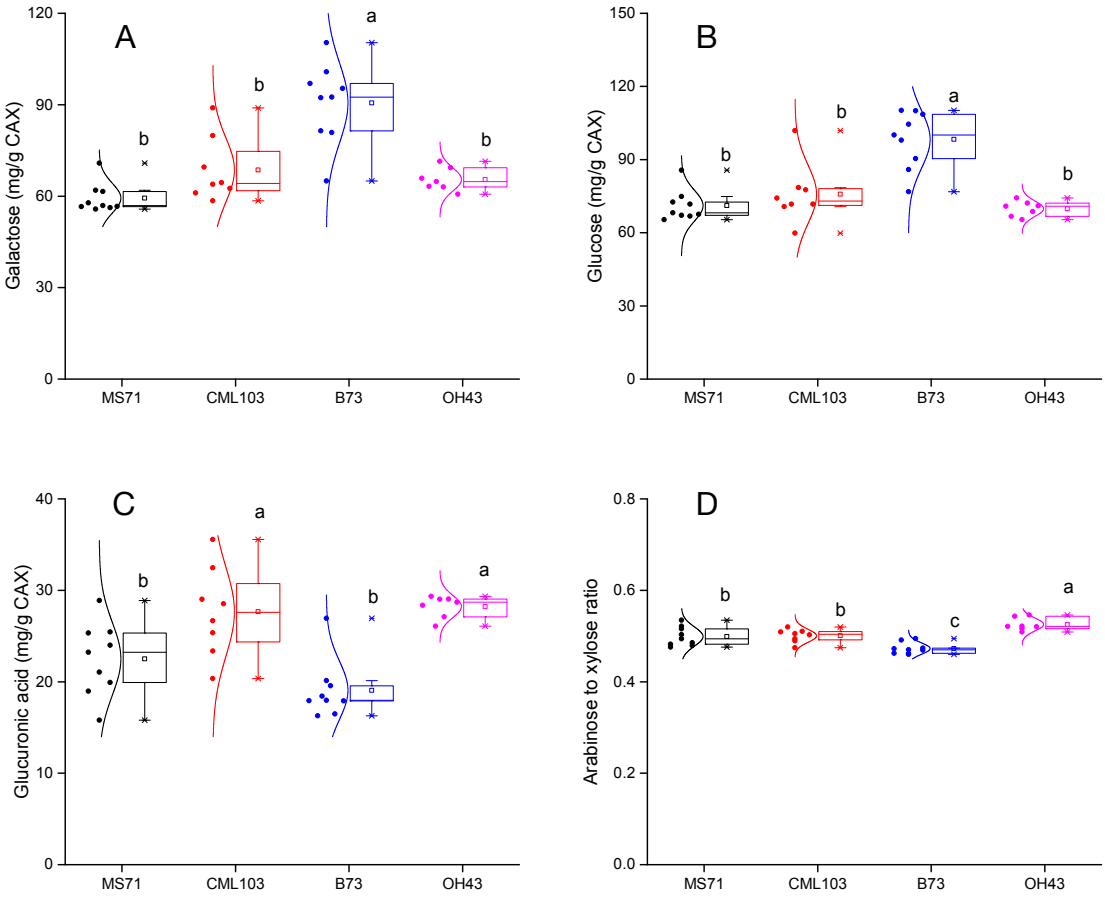

Figure 3.1 Boxplot of A) galactose; B) glucose; C) glucuronic acid; and D) arabinose to xylose ratio of CAX extracted from different corn genotypes.

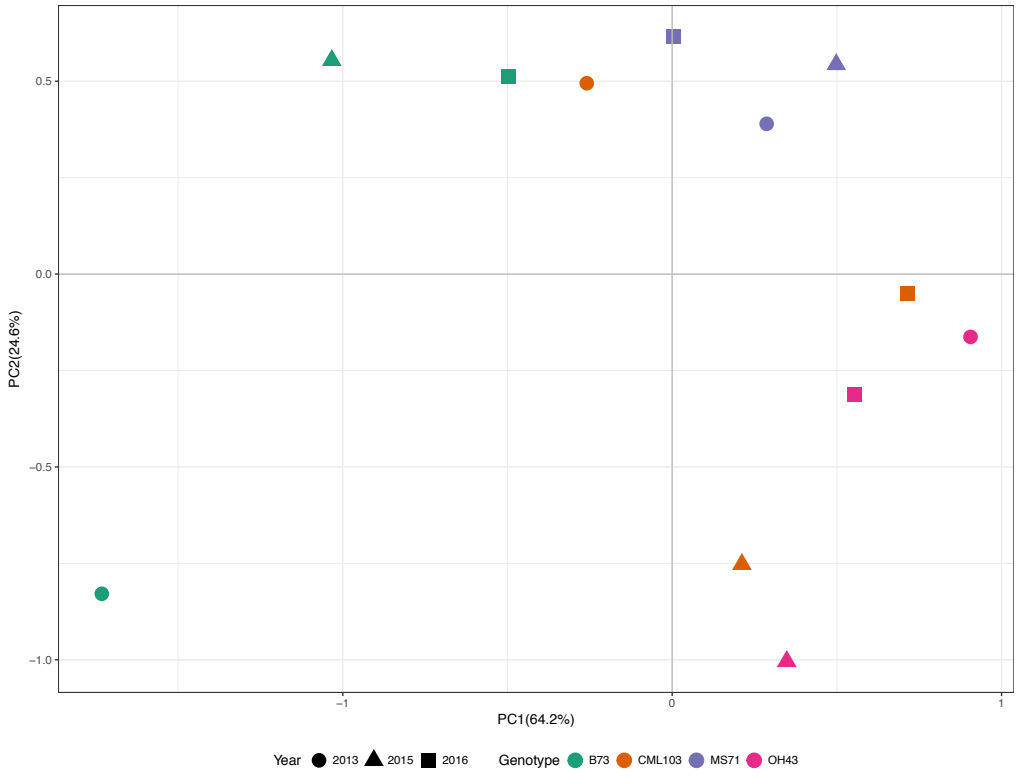

Figure 3.2 Principle component analysis (PCA) of neutral and acidic monosaccharides composition of arabinoxylan extracted from different corn genotypes.

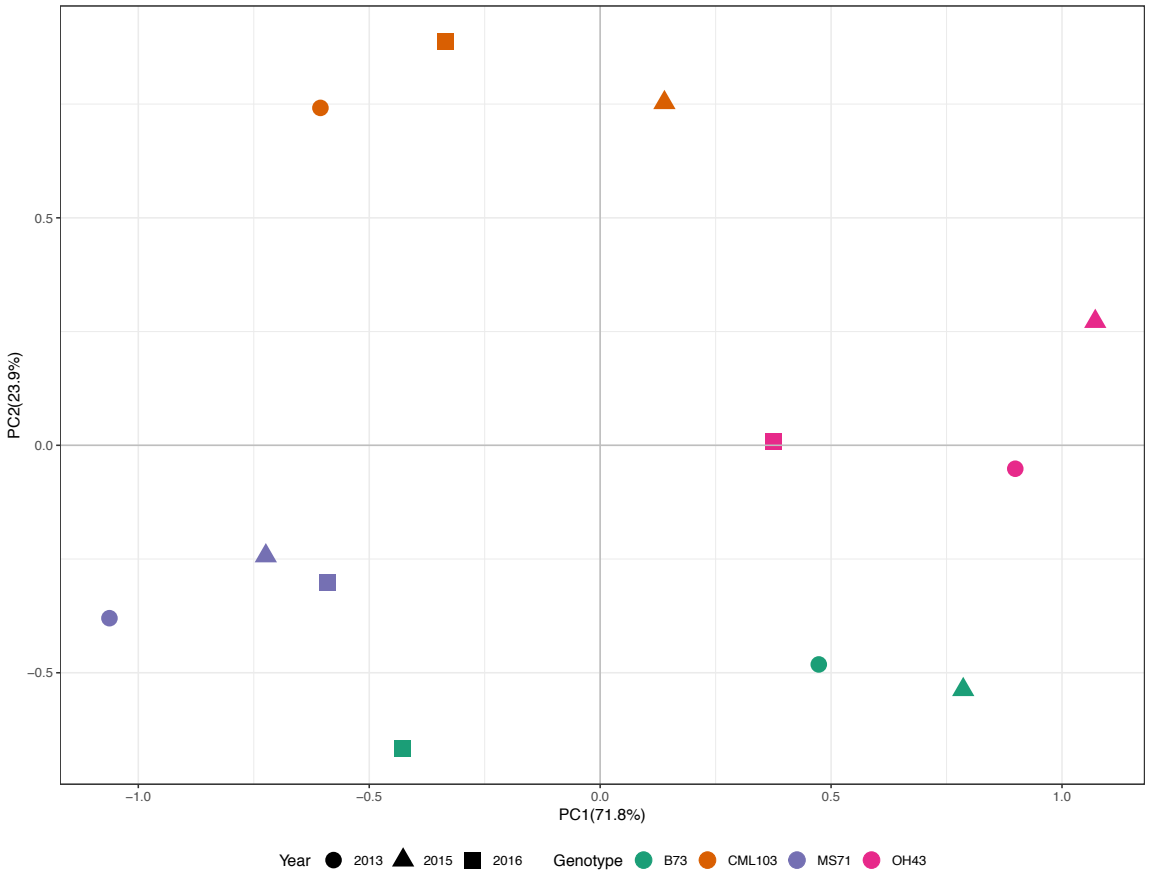

Figure 3.3 Principle component analysis (PCA) of short chain fatty acid production of arabinoxylan extracted from different corn genotypes in *in vitro* human fecal fermentation at 24 h.

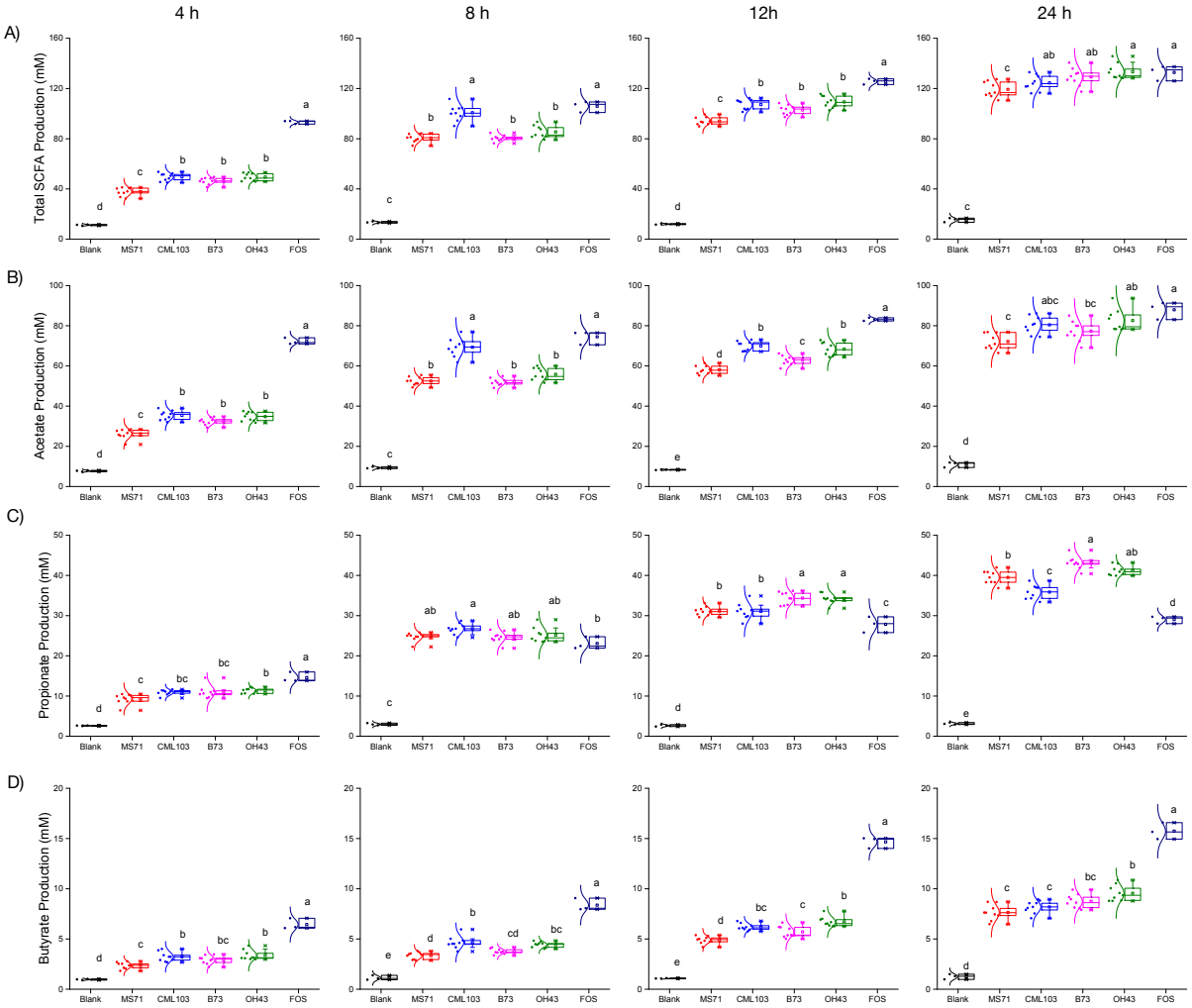

Figure 3.4 A) Total short chain fatty acids B) acetate, C) propionate, and D) butyrate production of blank, CAX extracted from different genotypes and FOS at 4, 8, 12, and 24 h in *in vitro* fecal fermentation. Different letters represent statistically significant differences ($P < 0.05$).

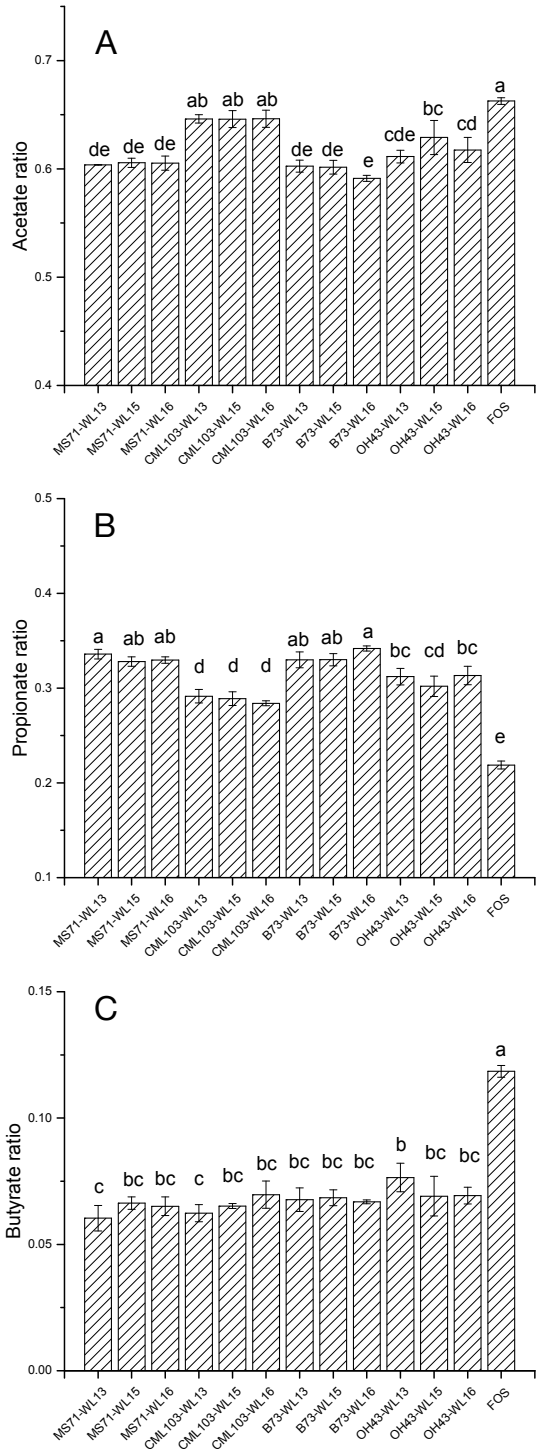

Figure 3.5 A) Acetate; B) propionate; C) butyrate proportion of 12 CAXs compared with blank and FOS by fecal microbiota from *in vitro* fermentation. Different letters represent statistically significant differences ($P < 0.05$).

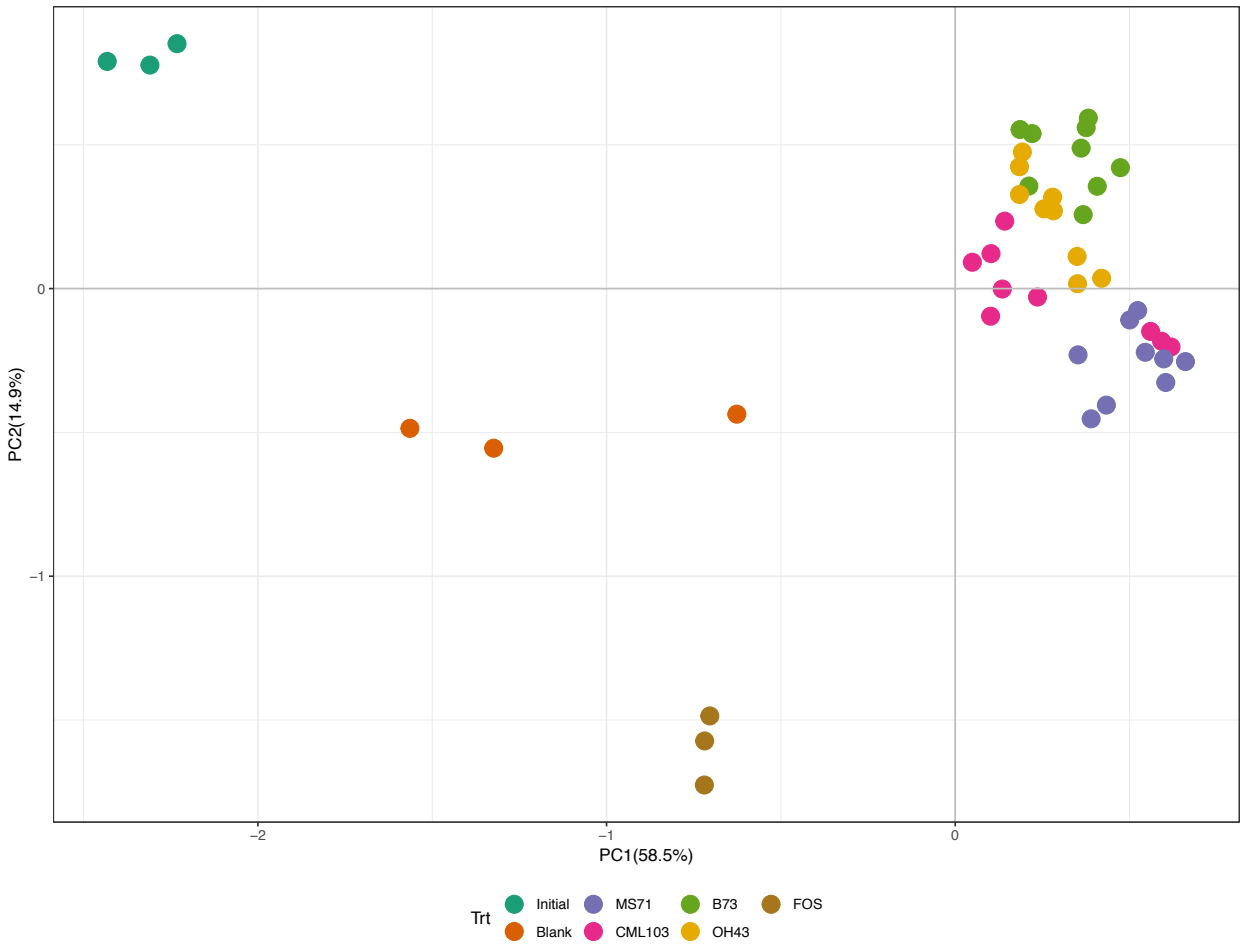

Figure 3.6 PCA analysis of microbiota composition treated with CAXs, blank and FOS by Bray-Curtis dissimilarity after *in vitro* fecal fermentation for 24 h .

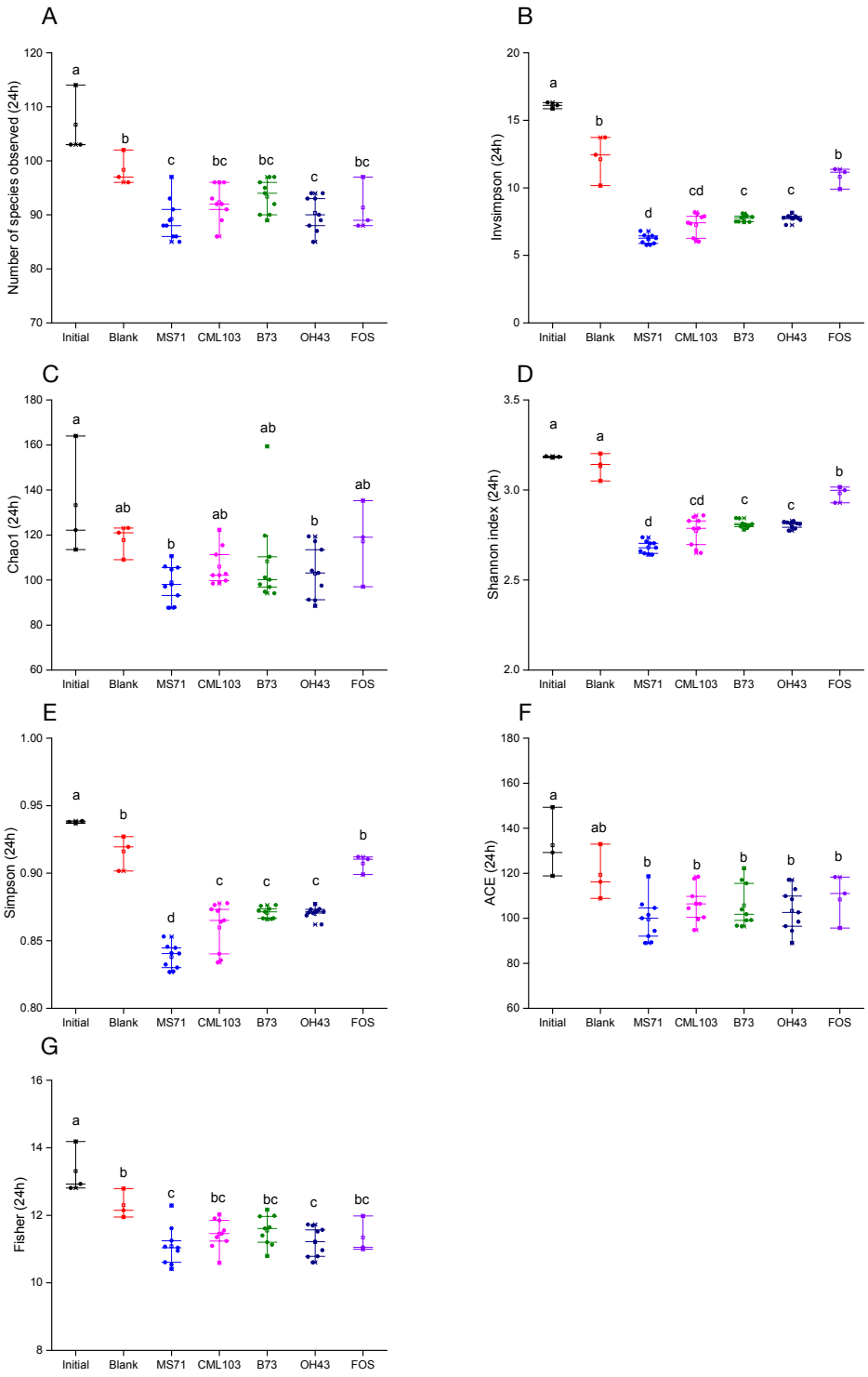

Figure 3.7 Alpha diversity analysis of fecal microbial communities after *in vitro* fecal fermentation for 24 h: A) number of species observed; B) inverse Simpson index; C) Chao estimated of richness; D) Shannon index; E) Simpson evenness index; F) ACE index; and G) Fisher index. Different letters represent statistically significant differences ($P < 0.05$).

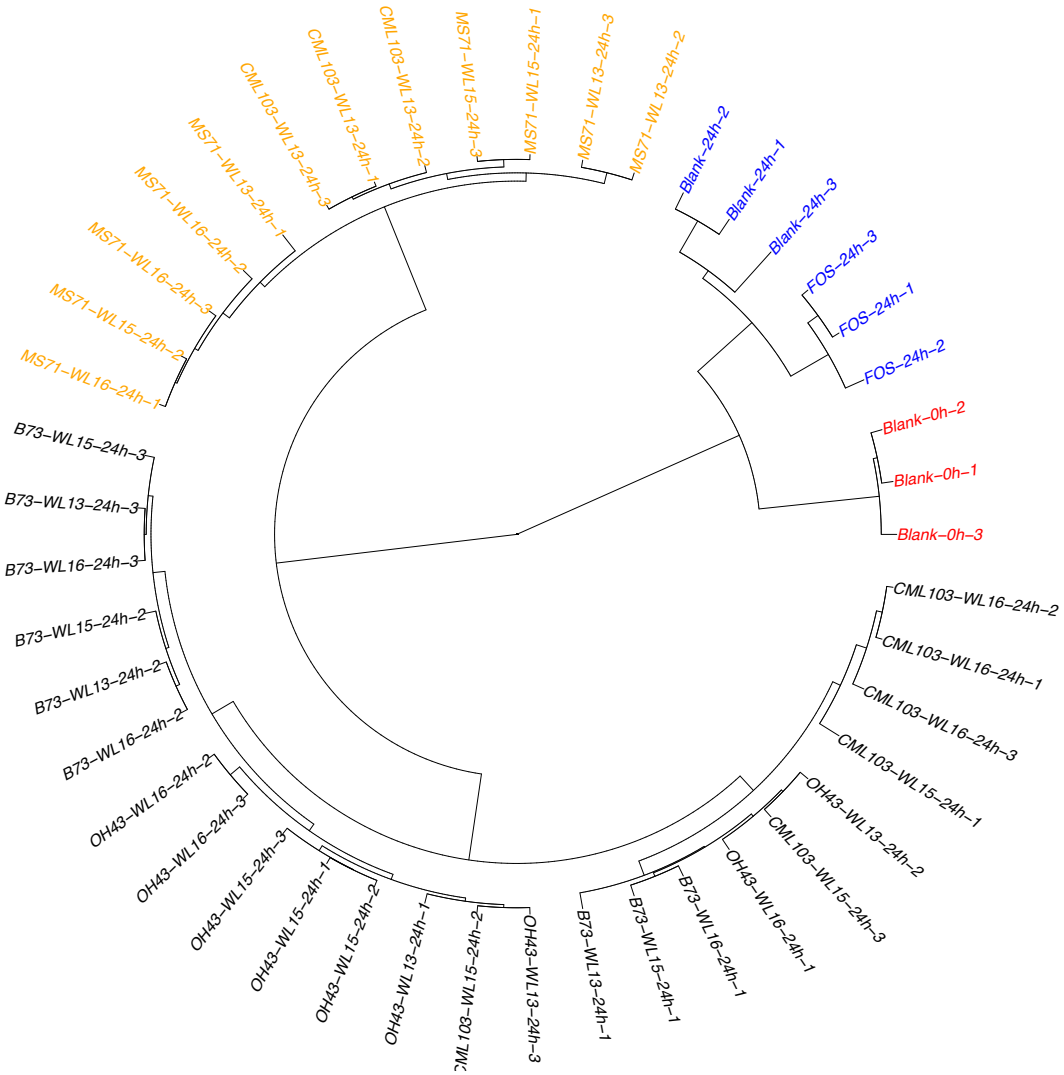

Figure 3.8 Dissimilarity of microbiota after 24 h fermentation with each fiber. Samples were clustered using the Ward agglomerative algorithm on Euclidean distances.

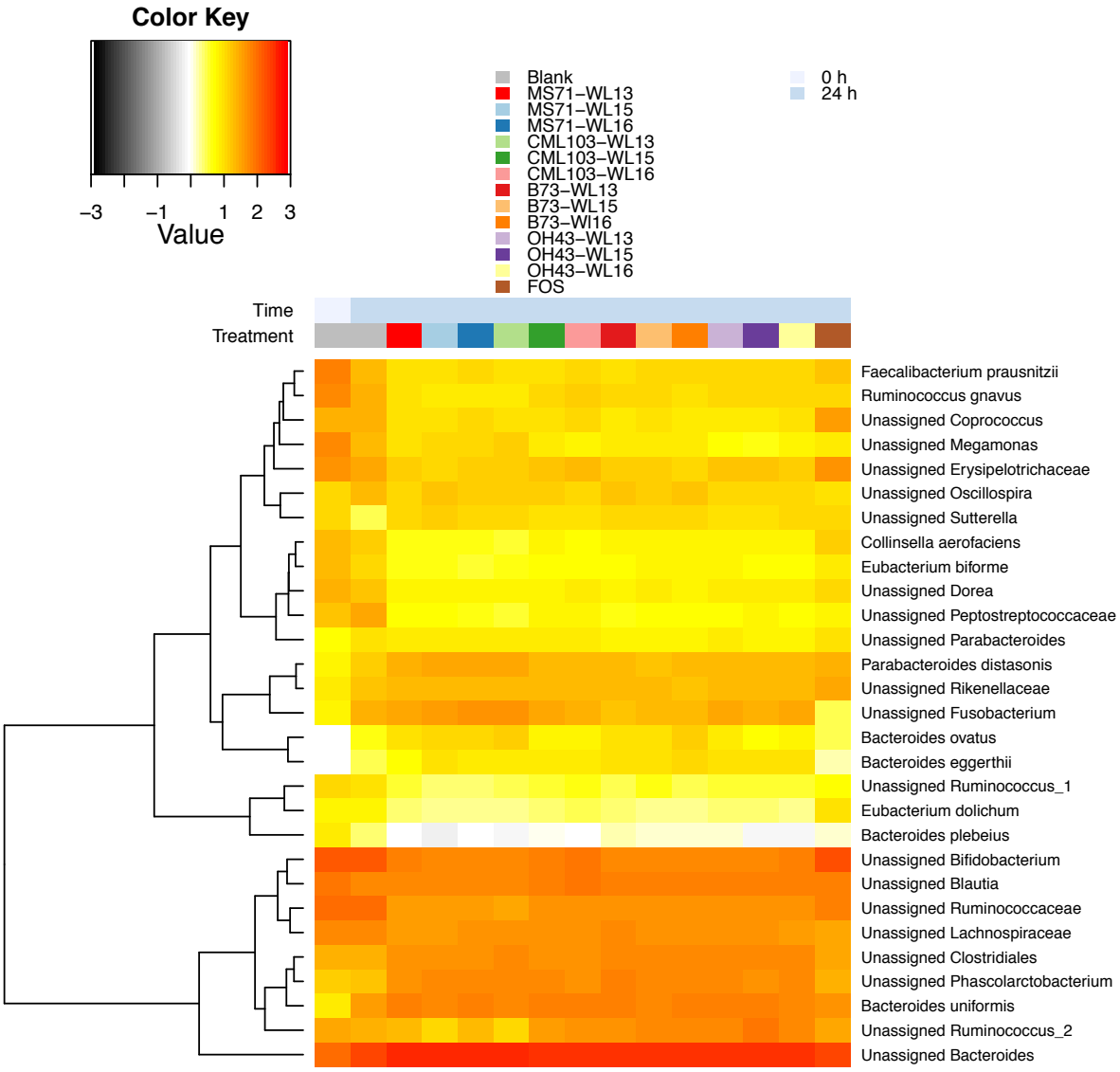

Figure 3.9 Heatmap of the microbial taxa after *in vitro* fermentation for 24 h.

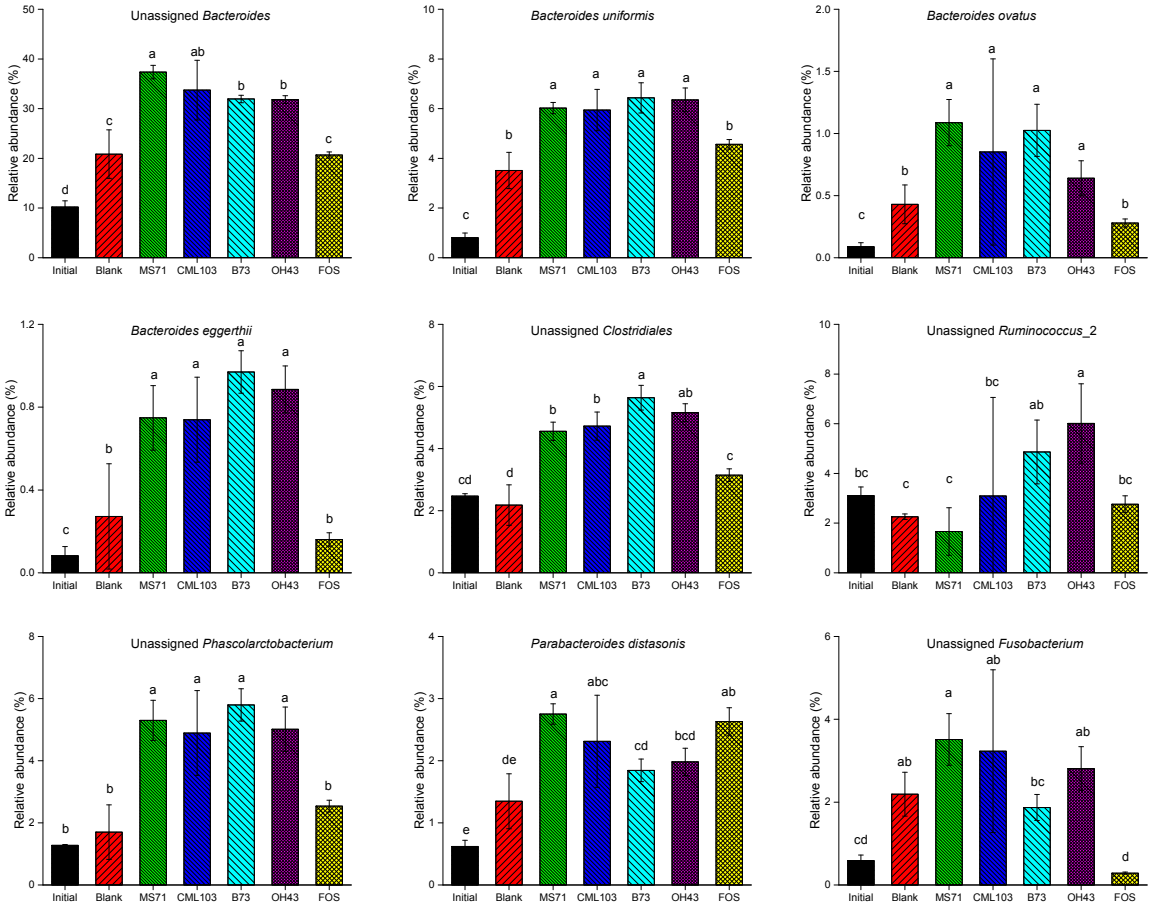

Figure 3.10 Bar graphs of relative abundances of most represented microbial taxa after *in vitro* fecal fermentation for 24 h. Different letters represent statistically significant differences ($P < 0.05$).

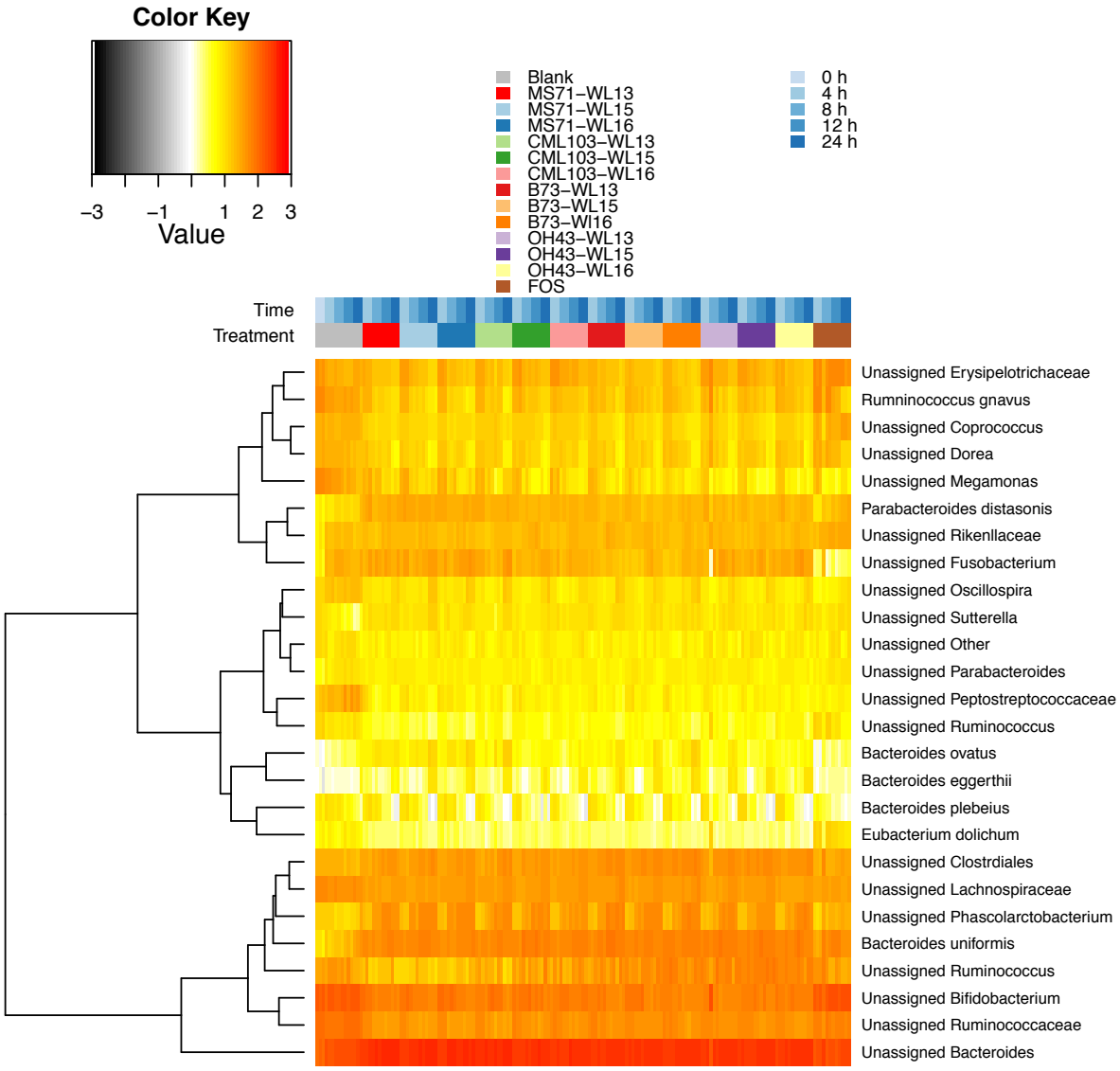

Figure 3.11 Heatmap of the shift of in key OTUs during fermentation.

CHAPTER 4. FABRICATION OF A SOLUBLE CROSSLINKED CORN BRAN ARABINOXYLAN MATRIX SUPPORTS A SHIFT TO BUTYROGENIC GUT BACTERIA

4.1 Abstract

Insoluble fermentable cell wall matrix fibers have been shown to support beneficial butyrogenic gut *Clostridia*, but have restricted use in food products. Here, a soluble fiber matrix was developed that exhibited a similar effect. Two concentrations of sodium hydroxide, 0.25 M and 1.5 M, were used to extract corn arabinoxylan (CAX) with different residual levels [high (H) and low (L)] of bound ferulic acid (FA) to make CAX-HFA and CAX-LFA. After laccase treatment to make diferulate crosslinks, soluble matrices were formed with average mer levels of 3.5 to 4.5. *In vitro* human fecal fermentation of CAX-LFA, CAX-HFA, soluble crosslinked 3.5 mer CAX-LFA (SCCAX-LFA), and 4.5 mer SCCAX-HFA revealed that the SCCAX matrices had somewhat slower fermentation property as measured by gas production, total short chain fatty acids, and carbohydrate disappearance, with proportionally higher butyrate levels. 16S rRNA gene sequencing showed that SCCAX fibers promoted OTUs associated with butyrate production including *Unassigned Ruminococcaceae*, *Unassigned Blautia*, *Fecalibacterium prausnitzii,* and Unassigned *Clostridium*. Thus, when the physical form of an individual soluble polysaccharide was changed to a soluble crosslinked matrix, *in vitro* fermentation was shifted to Clostridial butyrate producers. The study shows that fiber physical form influences gut bacteria competition towards substrate. Crosslinking of soluble fibers may be a strategy for developing soluble matrices with good physical functionality for beverages and other foods to improve gut health.

4.2 Introduction

The metabolites of the human gut microbiota, especially short chain fatty acids (SCFAs) such as acetate, propionate, and butyrate, are important in maintaining intestinal homeostasis, along with low inflammation and good barrier function (Louis et al., 2014; Riviere et al., 2016; Sharon et al., 2014). Butyrate, in particular, is the preferred energy source for colonic epithelial cells and has been shown to lower inflammatory immune factors (Cushing et al., 2015), play a protective role against colon cancer and colitis, and improve gut barrier function by stimulation of the formation of mucin, antimicrobial peptides, and tight-junction proteins (Riviere et al., 2016). Using dietary modulation to promote butyrogenic bacteria and butyrate production has become a strategy for the treatment or prevention of a growing list of gut microbiome-associated chronic diseases, such as metabolic syndrome and colon cancer (Canani et al., 2011; Hand, Vujkovic-Cvijin, Ridaura, & Belkaid, 2016; Neyrinck et al., 2012; Patterson et al., 2016). However, the dietary conditions resulting in an increased butyrate production in the gut are not yet fully understood.

While the role of soluble dietary fibers has gained the most attention related to their role in gut health (Slavin, 2013), the insoluble fermentable fiber matrices of plant cell walls also have an important role in supporting bacterial community structure (Flint et al., 2012; Hamaker & Tuncil, 2014). Relevant to butyrate production, these insoluble fibers seem to be preferentially fermented by the Clostridia groups locationally associated with the gut mucosa, and which contain some of the most prominent butyrate producers in the gut. These are also known by their *Clostridium* cluster designations and, in the mammalian gut, the main ones are *Clostridium* clusters IV, XIVa, and XIVb.(Van den Abbeele et al., 2013) For example, butyrogenic *Eubacterium rectales* (*Clostridium* cluster XIVa) and *Roseburia intestinalis* (*Clostridium* cluster IV) have been shown to strongly attach to insoluble fermentable substrates such as brans and mucins (Leitch et al.,

2007; Van den Abbeele et al., 2013). Recently, we found that two insoluble β-D-glucans obtained from the fungi *Cookeina speciosai* were highly butyrogenic *in vitro* and specifically promoted *Clostridium* cluster XIVa *Anaerostipes*, and to a lesser extent *Roseburia* (Cantu-Jungles et al., 2018). However, the insoluble property of these fibers limits their application in the food industry. It would be desirable to develop soluble fibers with similar butyrogenic effects, and we thought fabricating of soluble fiber matrices might be a way to achieve this target.

Arabinoxylans are non-starch polysaccharides found in cereal brans, consisting of arabinose, xylose, galactose, glucuronic acid as well as varying amounts of bound ferulic acid (Izydorczyk & Biliaderis, 1995; Neacsu et al., 2013; Z. X. Zhang et al., 2014). With the treatment of laccase (EC1.10.3.2), which is an oxidase that forms dimers and trimers of phenolic compounds, alkali-solubilized arabinoxylans that are rich in esterified ferulic acid become crosslinked (Baldrian, 2006; Kale et al., 2013). When enough crosslinks are formed, a gel is generated (Kale et al., 2013). Martinez-Lopez *et al.* investigated *in vitro* degradation of crosslinked arabinoxylan gels by bifidobacteria and found higher crosslinking density resulted in slower degradation of the three-dimensional structure by fermentation (Martinez-Lopez et al., 2016). We recently found that, instead of forming a gel with laccase, low arabinose/xylose ratio arabinoxylans form soluble crosslinked complexes (average 3.5-4.5 mer) that have a special acid gelation property (Chapter 5). Here, we hypothesized that such soluble fiber matrices might favor butyrogenic Clostridia. In the present study, we investigated whether arabinoxylans in their soluble crosslinked matrix form versus uncrosslinked form support butyrogenic Clostridia bacteria and increase butyrate production.

4.3 Experimental

4.3.1 Materials

Corn bran was gifted from Agricor (Marion, IN, USA). Thermostable α-amylase, proteinase, laccase from *Trametes versicolor*, human salivary α-amylase, pepsin, pancreatin, and sodium hydroxide were obtained from Sigma-Aldrich (St. Louis, MO, USA). Hexane, ethanol, and concentrated hydrochloric acid were obtained from Mallinckrodt Chemicals (Phillipsburg, NJ, USA). Fructooligosaccharide (FOS) was gifted from Ingredion (Ingredion Incorporated, Westchester, IL, USA).

4.3.2 Arabinoxylan extraction from corn bran

Corn bran was defatted with hexane following removal of starch and protein by thermostable α-amylase and proteinase, respectively. Then, arabinoxylan was solubilized with two concentrations of sodium hydroxide solution (0.25 and 1.5 M) and precipitated with four volumes of absolute ethanol. The precipitate was dried at 45 °C in a hot air oven, re-dissolved in water, and freeze-dried. Two samples [CAX-low ferulic acid (CAX-LFA) and CAX-high ferulic acid (CAX-HFA)] were obtained from 1.5 M and 0.25 M sodium hydroxide extraction, respectively.

4.3.3 Arabinoxylan crosslinking

Crosslinking of CAX-LFA and CAX-HFA was done following a protocol previously described in our laboratory (Kale et al., 2013). Briefly, 2% (*w/v*) of CAX-LFA and CAX-HFA was prepared, followed by addition of laccase (1.675 nkat/mg arabinoxylan). The reaction was kept at room temperature for 24 h and boiled for 10 min to deactivate the enzyme. After crosslinking, samples were freeze-dried. Two samples, soluble crosslinked CAX (SCCAX)-LFA and SCCAX-

HFA, the products of laccase treatment of CAX-LFA and CAX-HFA, were obtained. All samples were stored in a vacuum desiccator for further use.

4.3.4 Structural features of arabinoxylan

The molecular weight and size of arabinoxylan was determined using an Agilent 1100 high pressure size exclusion chromatograph (HPSEC) equipped with refractive index (RI) and multiangle light scattering (MALS) detectors (Agilent Technologies, Santa Clara, CA, USA), and polymers were separated with Superdex 200 and 30 columns connected in series (GE Healthcare Bio-Sciences, Pittsburgh, PA, USA). The mobile phase was purified water, injection volume was 100 μL, and flow rate was 0.4 mL/min.

Monosaccharide composition of arabinoxylans was measured according to Pettolino *et. al.* (Pettolino et al., 2012). Neutral sugar composition was determined by gas chromatography (GC) after hydrolysis, reduction, and acetylation. An Agilent 7890A gas chromatograph and 5975C inert MSD with a triple-axis detector (Agilent Technologies, Santa Clara, CA, USA) was used to analyze samples. Helium was used as the carrier gas at a flow rate of 1 mL/min through an Agilent BPX70 column. Injection volume was 1 μL at a split ratio of 10/1. Oven temperature was initially 170 °C, held for 2 min, and increased by 3 °C/min to 260 °C where it was held for 3 min.

4.3.5 *In vitro* fecal fermentation

In vitro fecal fermentation studies were conducted as described by Chen *et al.* (Chen et al., 2017). Briefly, fresh stool samples were obtained from healthy participants who had no previous history of gastrointestinal disorders and had not taken any antibiotic or probiotic for at least three months. Stool samples were transferred immediately to an anaerobic chamber and dispersed with basic culture medium (1:3, *w/v*), followed by filtration through four layers of cheesecloth. Then

50 mg of CAX-LFA, CAX-HFA, SCCAX-LFA, SCCAX-HFA, and FOS were added to a mixture of 4 mL of culture medium and 1 mL of fecal inocula. The mixtures were incubated at 37 °C. At 0, 4, 8, 12, and 24 h, gas production was measured with a graduated syringe. Then, culture samples were collected and centrifuged. Supernatants were used for SCFA and carbohydrate disappearance analyses, and the pellets were saved at -80 °C for DNA extraction. All experiments involving fecal samples were conducted following a protocol approved by the Institutional Review Board of Purdue University (IRB protocol #1510016635).

4.3.6 SCFA analysis

Supernatants were filtered through a 0.22 μm polyethersulfone membrane. SCFA analysis was conducted using a gas chromatograph (Agilent 7890A GC, Agilent Technologies, Santa Clara, CA, USA) equipped with a fused silica capillary column (Nukol, Supelco nr 40369-03A, 30 m × 0.25 mm, id 0.25 μm, Palo Alto, CA, USA) as described by Kaur *et al*. (Kaur et al., 2011).

4.3.7 DNA extraction and sequencing

The pellet was used for DNA extraction as described by Zhang *et al.* (C. H. Zhang et al., 2012). DNA was extracted using the MP FastDNA spin kit (MP Biomedicals, Santa Ana, CA, USA) according to the manufacturer's instruction. Then, the V1-V3 region of the 16s rRNA gene was amplified by PCR with primers 5′-CGTATCGCCTCCCTCGCGCCATCAGACGAGTGCGTAGAGTTTGATYMTGGCTCAG-3′ and 5′-CTATGCGCCTTGCCAGCCCGCTCAGNNNNNNNNNNATTACCGCGGCTGCTGG-3′ with a sample-unique 10-mer oligonucleotide barcode. Analyses were performed at the DNA Services Facility at University of Illinois at Chicago (Chicago, IL, USA).

4.3.8 Bioinformatics

The Illumina-generated sequencing data were analyzed by the QIIME platform (Caporaso et al., 2010). Operational taxonomic units (OTUs) were generated using the UCLUST method

with a 97% similarity threshold in QIIME, and taxonomic annotations were assigned to each OTU by comparing to the Greengenes (version 13_8) database (McDonald et al., 2012). Singleton OTUs and samples with abnormally low number of reads were removed. Principal components analysis (PCA) and construction of the heatmap were carried out in R software.

4.3.9 Statistical analysis

Data were reported as mean ± SD for triplicate determinations. One-way ANOVA and Tukey's test were employed to identify differences in means. Statistics were analyzed using SPSS for Windows (version rel. 10.0.5, 1999, SPSS Inc., Chicago, IL, USA), Origin for Windows (version Srl b9.3.1.273, OriginLab Corp., Northampton, MA, USA) and RStudio software.

4.4 Results and discussion

There is good evidence that fermentable insoluble plant cell wall fiber matrices support and favor Clostridia butyrate-producing bacteria (Cantu-Jungles et al., 2018; Flint et al., 2012). However, insoluble fibers are not always accessible to gut bacteria and may not be well fermented and do not function well in processed foods. Therefore, we investigated soluble fiber matrix entities that might favor butyrate-producing bacteria, as well as have broader application for the food industry. This is the first study to show that unique soluble matrix entities can be used to increase butyrate production and favor butyrate-producing bacteria.

4.4.1 Structural characterization of CAX and SCCAX

Previously, we found that the CAX in this study had an unusually low arabinose/xylose ratio (0.20 – 0.24), compared to a typical ratio of ~0.5, and consequently a relatively low ferulic acid

content (Devin J. Rose et al., 2010). It was for this reason that we were able to fabricate the SCCAX matrices with the laccase treatment. In contrast, the commonly-found higher arabinose/xylose ratio CAX, with a high degree of feruloylation, forms gels when treated with laccase (Kale et al., 2013). Different concentrations of alkali were used to generate relatively low and high ferulic acid CAX (CAX-LFA, CAX-HFA). As shown in **Table 4.1**, M_w of CAX-LFA and CAX-HFA was 1.56×10^5 and 3.17×10^5, respectively. CAX-HFA had higher polydispersity (1.82) than CAX-LFA (1.30). After laccase treatment, M_w of SCCAX-LFA and SCCAX-HFA was approximately 3.5 and 4.5 fold higher than CAX-LFA and CAX-HFA, respectively, and M_n of SCCAX-LFA and SCCAX-HFA increased around 3.1 and 4.6 fold of CAX-LFA and CAX-HFA, respectively. However, the polydispersity of CAX and SCCAX remained similar after laccase treatment. Therefore, soluble fiber matrices were fabricated with averages of 3.5 and 4.5 polymers per unit.

Arabinoxylans consist a linear β-1,4 linked D-xylopyranose backbone with arabinofuranose residues mono- or di- attached to xylose residues at O-2, O-3 and/or O-2,3 positions (**Table 4.2)**. Assuming that (1,4)-, (1,3,4)-, and (1,2,3,4)-linked xylose residues were all on the xylan backbone, percent of un-, mono- and di-substituted xylose units of CAX and SCCAX were calculated (**Table 4.3**). CAX had over 50% unsubstituted, ~17% monosubstituted, and ~30% disubstituted backbone xylose. No significant differences in glycosidic linkage patterns were found between CAX and SCCAX, indicating the oxidizing action of laccase had no effect on glycosidic linkages.

4.4.2 In vitro fecal fermentation of CAX and SCCAX

4.4.2.1 Carbohydrate disappearance of CAX and SCCAX during in vitro fecal fermentation

The utilization of CAX and SCCAX by gut microbiota during *in vitro* fecal fermentation was directly investigated by residual carbohydrate depletion over time. As shown in **Table 4.3**, there was more undigested arabinoxylan in the ferments of SCCAX-HFA and SCCAX-LFA at 4, 8, and 12 h, compared with CAX-HFA and CAX-LFA, indicating that the crosslinked soluble arabinoxylan matrices somewhat impede utilization of arabinoxylan by gut bacteria.

4.4.2.2 Gas production of CAX and SCCAX

Gas production of CAX and SCCAX during *in vitro* fecal fermentation is shown in **Figure 4.1.** FOS, as the fast fermenting control, was rapidly utilized by the bacteria generating a high gas volume at 4 h. In comparison, CAX and SCCAX were slowly fermented as shown by small amounts of gas produced at 4 h, which is consistent with our previous findings (Rumpagaporn et al., 2015). Fermentation of SCCAX-HFA and SCCAX-LFA generated moderately, but significantly ($P < 0.05$), less gas than CAX-HFA and CAX-LFA, respectively, also showing that SCCAX was fermented slower than CAX.

4.4.2.3 SCFA production of CAX and SCCAX

SCFA profiles were also different for SCCAX compared to CAX, with butyrate proportion (of total SCFAs) being significantly higher in SCCAX than CAX (**Figure 4.2** and **4.3**). Highest butyrate proportion was found in SCCAX-HFA (~ 7.1%), while CAX-LFA showed lowest butyrate proportion (~5.9%). In addition, Fecal microbiota fermented all five fibers to near completion in 24 h, with slightly lower total SCFA production for SCCAX-HFA (**Figure 4.2**). At 24 h, the four CAX and SCCAX samples produced higher levels of propionate, lower levels of butyrate, and same levels of acetate compared to FOS. The higher level of propionate

production could increase the appetite-regulating hormones peptide YY and glucagon-like peptide 1 and prevent weight gain of overweight adults (Chambers et al., 2015). Additionally, CAX-HFA and CAX-LFA showed higher acetate, propionate, and total SCFA production than SCCAX-HFA and SCCAX-LFA at different fermentation time points. Thus, we concluded that the utilization of SCCAX by human fecal microbiota was delayed while the proportion of butyrate to total SCFAs was increased due to the matrix effect of the SCCAX. Thus, less carbohydrate disappearance, lower gas production, and lower total SCFA production of SCCAX show that soluble crosslinked arabinoxylan matrices slow down utilization of the arabinoxylan polymers by gut microbiota. The property of slow dietary fiber fermentation in the colon is indeed desirable, as most severe chronic colonic diseases such as colon cancer predominantly originate in the distal colon (D. J. Rose, Demeo, Keshavarzian, & Hamaker, 2007; Sharma, Vasudeva, & Howden, 2000).

4.4.3 Influence of CAX and SCCAX on human gut microbiota

4.4.3.1 Influence of CAX and SCCAX on human gut microbiota community structure

As shown in **Figure 4.4A**, the structure of the microbiota shifted significantly after 24 h fermentation for the five fiber treatments based on principal component analysis (PCA). Principle component 1 (PC1) explained 54.2% of the total variation while PC2 explained 22.6% of the total variation. SCCAX-HFA showed significantly higher PC1 score than other fiber treatments (**Figure 4.4B**), indicating distinct gut bacteria composition compared to CAX-LFA, CAX-HFA and SCCAX-LFA in the 24 h fermentation.

4.4.3.2 Phyla and genera level changes due to fiber treatments

Accumulating studies have showed that changes in gut microbiota composition are related to the development of obesity (J. L. Sonnenburg & Backhed, 2016). The gram-positive *Firmicutes* and the gram-negative *Bacteroidetes* are the two most common phyla present in human colon (Eckburg et al., 2005). In general, CAX, SCCAX and FOS treatments significantly decreased the *Firmicutes*/*Bacteroidetes* (F/B) ratio compared to the blank (**Figure 4.5**). Furthermore, CAX and SCCAX treatments exhibited better ability to decrease F/B ratio than FOS treatment (**Figure 4.5**).

Although no significant difference in F/B ratio was found between SCCAX-LFA and CAX-LFA, SCCAX-HFA showed lower F/B ratio than CAX-HFA, suggesting that SCCAX could decrease the *Firmicutes* level while increase *Bacteroidetes* level when enough crosslinks between ferulic acid were formed (**Figure 4.5**). Laccase treatment could be a good strategy to improve the functional characteristic of CAX in regard to modulating human gut microbiota. For CAX and SCCAX treatment, the increase of relative abundance of *Bacteroidetes* phylum at 24 h was mainly contributed by the genus *Prevotella* and *Bacteroides*, which both were good at degradation of dietary fibers (**Figure 4.6A**) (Koropatkin et al., 2012; Martens et al., 2011). In the strain level, CAX and SCCAX fermentation resulted in approximately 3.3 folds and 3.8 folds increase in the relative abundance of *Prevotella copri* and one *Unassigned Bacteroides* after 24 h, respectively (**Figure 4.6A**). The increase was likely reflective of effective use soluble arabinoxylans by them.

4.4.3.3 SCCAX promotes the relative abundance of butyrate-producing bacteria

Fermentable insoluble plant cell wall matrix fibers tend to promote butyrate-producing Clostridia, particularly the gut mucosal-associated *Clostridium* clusters IV and XIVa (Cantu-

Jungles et al., 2018; Louis & Flint, 2009). These bacteria appear to have a competitive advantage towards degrading and utilizing these type of fibers. Although the SCCAX fabricated in this study is not insoluble, it is a small matrix form of the individual CAX polymer. Therefore, it seems reasonable that these same butyrogenic bacteria become somewhat more competitive on SCCAX than on CAX, as was evidenced by the slightly higher butyrate levels.

Unassigned Ruminococcaceae, *Unassigned Blautia, Faecalibacterium prausnitzii,* and *Unassigned Clostridium* were identified as the butyrate-producing OTUs that increased in SCCAX compared to CAX (**Figure 4.6B**). SCCAX-HFA treatment showed significantly higher relative abundance of the summation of these four bacteria than CAX-HFA, though no significant difference was detected between SCCAX-LFA and CAX-LFA. *Unassigned Blautia* species belongs to the *Lachnospiraceae* family and *Clostridium* cluster *XIVa* bacteria, which showed highest relative abundance (~11.1%) in SCCAX-HFA treatment, followed by CAX-HFA, SCCAX-LFA and CAX-LFA. Emerging evidence points to butyrate-producing bacteria as a functional group that, with other key bacteria, form an ecological "guild" rather than a monophyletic group to create a stable, healthy gut (Riviere et al., 2016; Zhao et al., 2018). These functional groups may co-respond when adapting to changed environments to maintain gut homeostasis (Velasquez-Manoff, 2015). Here, the results suggest that these four butyrate-producing bacteria respond as a group to the structural difference between CAX and SCCAX, resulting in the increase of butyrate proportion.

The relationship between butyrate proportion and the butyrate-producing bacteria was further examined by *Pearson* correlation analysis. As shown in **Table 4.5**, butyrate proportion showed a sum of the four bacteria correlation ($R = 0.984$, $P < 0.05$), further support that these bacteria respond together to utilize SCCAX to increase the overall butyrate proportion.

Our thinking is that the matrix structures of SCCAX provide a competitive environment for these butyrate-producing bacteria (**Figure 4.7)**, and as well as support *Prevotella/Bacteroides* that are good at degrading arabinoxylans (**Figure 4.6A**). SCCAX-HFA, versus SCCAX-LFA, significantly increased butyrate proportion likely due to its comparably larger and denser matrix structure, which would better support the butyrate-producing bacteria. Perhaps with a further increased size and density of the soluble matrix structures, one could achieve a greater butyrogenic effect. Thus, future work will focus on amplifying the butyrogenic effects of these complexes.

4.5 Conclusion

In conclusion, laccase treatment of low arabinose/xylose ratio CAXs led to the formation of SCCAXs, which was soluble fiber matrix, which for the SCCAX-HFA showed significantly higher butyrate production by human gut bacteria. SCCAX versus CAX exhibited a gut microbiota composition shift with an increase in a group of butyrate-producing bacteria (Unassigned *Ruminococcaceae*, Unassigned *Blautia*., F. *prausnitzii*, and Unassigned *Clostridium*). In sum, forming soluble fiber matrix could be a good strategy to favor the growth of butyrate-producing bacteria to improve human gut health.

Table 4.1 The molecular weight of CAX and SCCAX.[a]

Samples	Mw (g/mol)	Mn (g/mol)	Mw/Mn
CAX-LFA	1.56×10^5	1.20×10^5	1.30
SCCAX-LFA	5.47×10^5	3.75×10^5	1.46
CAX-HFA	3.17×10^5	1.74×10^5	1.82
SCCAX-HFA	1.45×10^6	8.04×10^5	1.80

[a]Mw stands for weight average molecular weight; Mn stands for number average molecular weight; CAX-LFA and CAX-HFA stand for arabinoxylan extracted by 1.5 and 0.25 M NaOH, respectively. SCCAX-LFA and SCCAX-HFA stand for crosslinked CAX-LFA and CAX-HFA, respectively.

Table 4.2 Glycosidic linkage composition (mol%) of CAX and SCCAX.[b]

Component	Linkage indicated	CAX-LFA	SCCAX-LFA	CAX-HFA	SCCAX-HFA
2,3,5-Me_3-Ara	(Ara*f*)1→	10.37 ± 0.35	11.21 ± 0.62	10.31 ± 0.18	10.76 ± 0.21
3,5-Me_2-Ara	→2(Ara*f*)1→	3.44 ± 0.33	3.17 ± 0.22	3.47 ± 0.13	3.49 ± 0.15
2,5-Me_2-Ara	→3(Ara*f*)1→	2.19 ± 0.02	1.62 ± 0.48	3.35 ± 0.07	2.78 ± 0.07
2,3,4-Me_3-Xyl	(Xyl*p*)1→	14.56 ±2.87	14.02 ± 0.51	14.15 ± 1.22	12.93 ± 0.34
2,3-Me_2-Xyl	→4(Xylp)1→	30.81 ± 2.78	30.78 ± 0.49	31.95 ± 1.14	31.63 ± 0.50
2-Me_1-Xyl	→4(Xylp)1→3↑	9.51 ± 0.12	9.96 ± 0.27	10.61 ± 0.37	10.70 ± 0.27
Xyl	→4(Xylp)1→2↑,3↑	17.04 ± 2.22	18.84 ± 0.51	18.88 ± 1.07	20.23 ± 1.09
2,3,4,6-Me_4-Glc	(Glc*p*)1→	nd	nd	1.01 ± 0.11	0.51 ± 0.12
2,3,6-Me_3-Glc	→4(Glc*p*)1→	3.41 ± 0.37	2.68 ± 0.18	1.45 ± 0.01	2.12 ± 0.03
Glc	→4(Glc*p*)1→2↑,3↑,6↑	3.69± 0.36	3.62 ± 0.18	0.05 ± 0.01	0.14 ± 0.03
2,3,4,6-Me_4-Gal	(Gal*p*)1→	4.38 ± 0.74	3.54 ± 0.24	5.11 ± 0.12	5.19 ± 0.26
Gal	→4(Gal*p*)1→2↑,3↑,6↑	1.52 ± 0.23	1.56 ± 0.24	0.15 ± 0.03	0.30 ± 0.26

[b]Glycosidic linkage was determined by gas chromatography of alditol acetates of partially methylated polysaccharides. Molar ratio was converted by peak areas using molar response factor. Values were expressed as proportion of all partially methylated alditol acetates detected.

Table 4.3 Percent substitution of xylopyranosyl residues in the xylan backbone of CAX and SCCAX.

Type of substitution	CAX-LFA (%)	SCCAX-LFA (%)	CAX-HFA (%)	SCCAX-HFA (%)
Unsubstituted xylose	53.7	51.7	52.0	50.6
Monosubstituted xylose	16.6	16.7	17.3	17.1
Disubstituted xylose	29.7	31.6	30.7	32.3

Table 4.4 Carbohydrate disappearance of CAX-LFA, SCCAX-LFA, CAX-HFA and CAX-HFA after 0, 4, 8, and 12 h of *in vitro* fecal fermentation.[c]

Samples	Time (h)	Ara (mg/mL)	Xyl (mg/mL)	Gal (mg/mL)	Glc (mg/mL)
CAX-LFA	0	1.62 ± 0.01	7.49 ± 0.10	0.49 ± 0.06	0.51 ± 0.04
	4	0.72 ± 0.17	3.76 ± 0.79	0.24 ± 0.06	0.15 ± 0.00
	8	0.22 ± 0.06	1.50 ± 0.32	0.15 ± 0.02	0.13 ± 0.02
	12	0.02 ± 0.01	0.40 ± 0.07	0.05 ± 0.01	0.13 ± 0.02
SCCAX-LFA	0	1.61 ± 0.04	7.36 ± 0.01	0.51 ± 0.03	0.63 ± 0.04
	4	0.76 ± 0.15	4.03 ± 0.67	0.27 ± 0.07	0.17 ± 0.00
	8	0.25 ± 0.03	1.67 ± 0.21	0.15 ± 0.03	0.13 ± 0.06
	12	0.10 ± 0.01	0.79 ± 0.04	0.09 ± 0.00	0.12 ± 0.02
CAX-HFA	0	1.77 ± 0.02	7.61 ± 0.05	0.55 ± 0.02	0.18 ± 0.01
	4	0.61 ± 0.08	3.25 ± 0.44	0.18 ± 0.02	0.15 ± 0.01
	8	0.24 ± 0.01	1.56 ± 0.06	0.15 ± 0.00	0.14 ± 0.00
	12	0.05 ± 0.04	0.48 ± 0.03	0.07 ± 0.01	0.13 ± 0.05
SCCAX-HFA	0	1.72 ± 0.02	7.55 ± 0.03	0.55 ± 0.02	0.28 ± 0.01
	4	0.69 ± 0.14	3.62 ± 0.71	0.20 ± 0.04	0.15 ± 0.01
	8	0.35 ± 0.03	2.21 ± 0.15	0.18 ± 0.01	0.13 ± 0.01
	12	0.19 ± 0.03	1.34 ± 0.26	0.07 ± 0.06	0.08 ± 0.07

[c] Ara, Xyl, Gal and Glc stand for arabinose, xylose, galactose, and glucose, respectively.

Table 4.5 Pearson correlation coefficients between butyrate proportion in total short chain fatty acid and the relative abundance of butyrate-producing bacteria after 24 h *in vitro* fecal fermentation.[d]

	Unassigned Ruminococcaceae	*Unassigned Blautia*	*Faecalibacterium prausnitzii*	*Unassigned Clostridium*	Total
Butyrate proportion	0.915	0.881	0.064	0.922	0.984
p-value	0.085	0.119	0.936	0.078	0.016

[d] Total represents the sum of relative abundance of *Unassigned Ruminococcaceae*, *Unassigned Blautia, Faecalibacterium prausnitzii,* and *Unassigned Clostridium.* Butyrate proportion means the ratio of butyrate in total short chain fatty acid production.

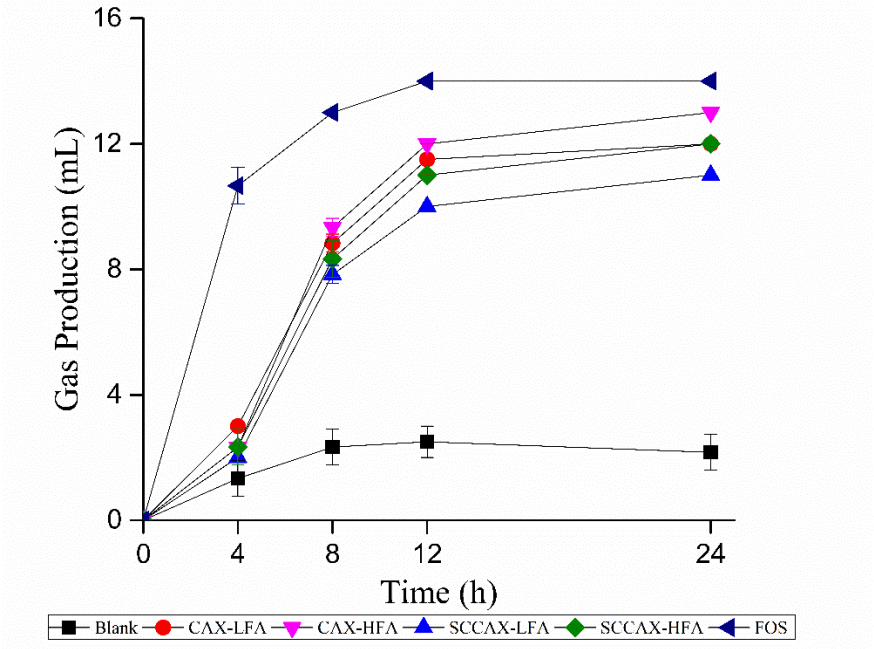

Figure 4.1 Gas production of CAX-LFA, CAX-HFA, SCCAX-LFA, and SCCAX-HFA compared to Blank and FOS (positive fast fermenting comparator) by fecal microbiota from *in vitro* fermentation.

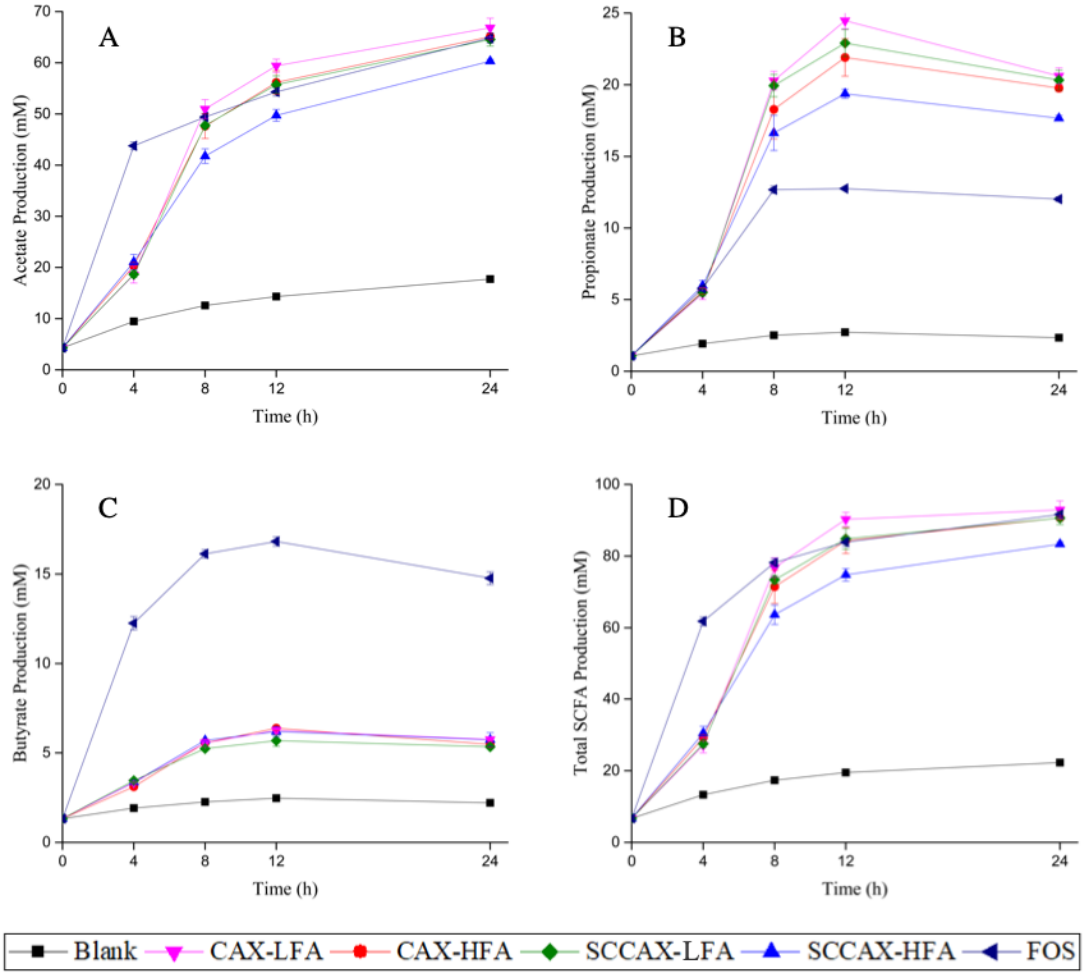

Figure 4.2 A) Acetate, B) propionate, C) butyrate, and D) total short chain fatty acid (SCFA) production of CAX-LFA, CAX-HFA, SCCAX-LFA and SCCAX-HFA compared to Blank and FOS (positive fast fermenting comparator) by fecal microbiota from *in vitro* fermentation.

.

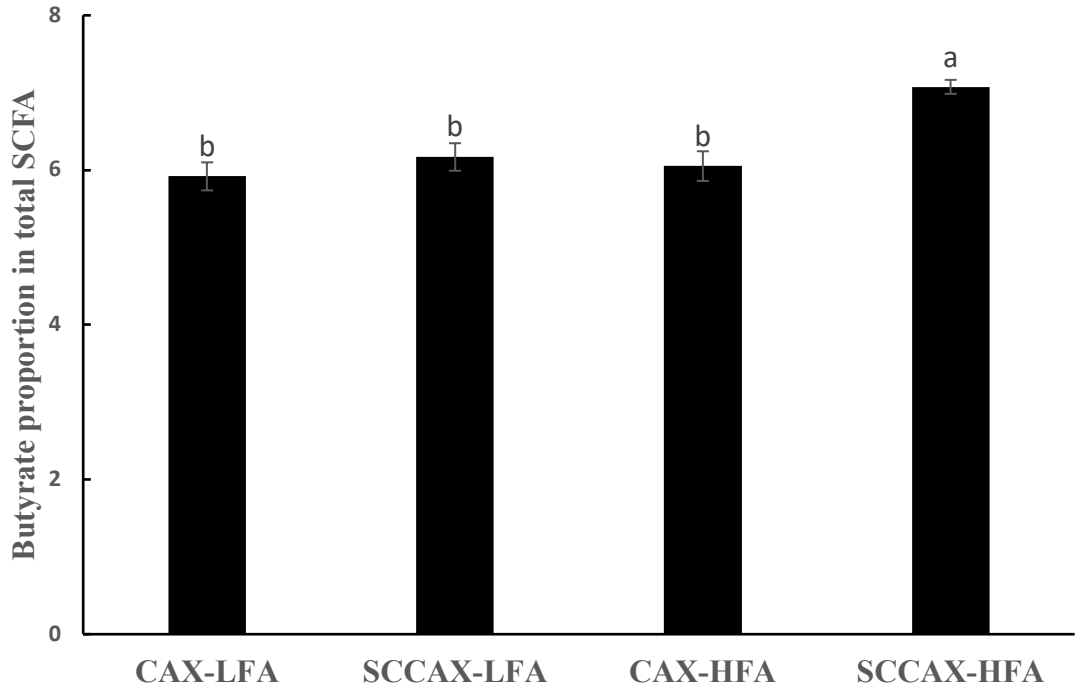

Figure 4.3 Butyrate proportion in total short chain fatty acid (SCFA) production of CAX-LFA, SCCAX-LFA, CAX-HFA, and SCCAX-HFA after 24 h of *in vitro* fecal fermentation.

A)

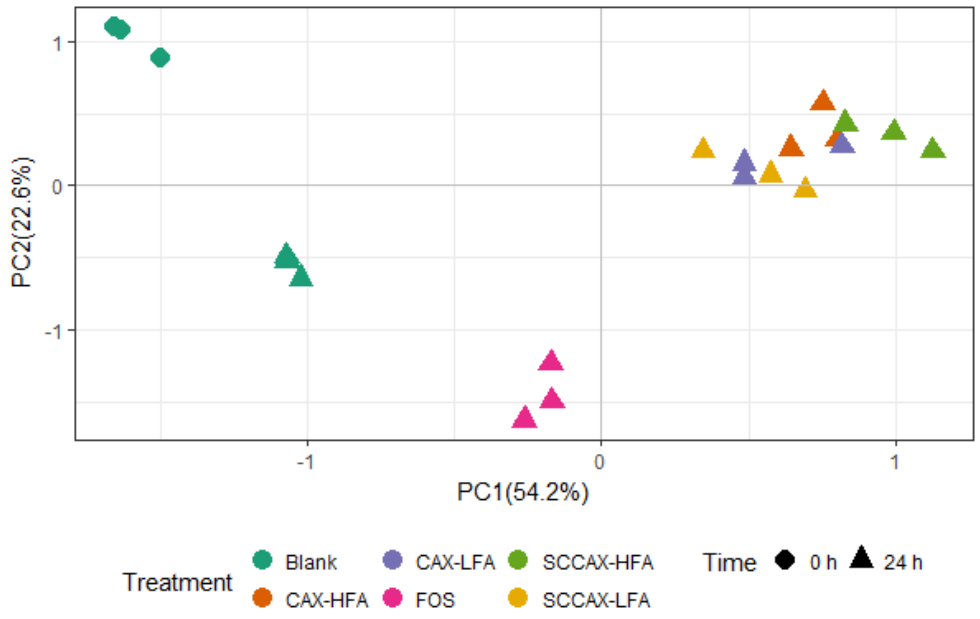

B)

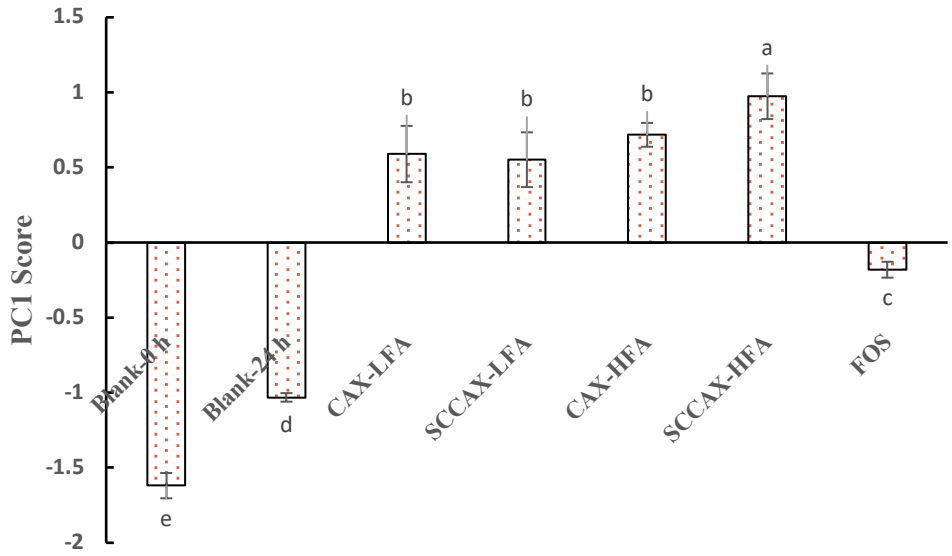

Figure 4.4 **A)** Principle component analysis (PCA) of fecal microbial communities based on relative abundances of OTUs at 97% similarity level, and **B)** Bar chart showing the scores of the primary principle component (PC1) after 24 h *in vitro* fermentation with Blank, CAX-LFA, CAX-HFA, SCCAX-LFA, SCCAX-HFA and FOS treatments.

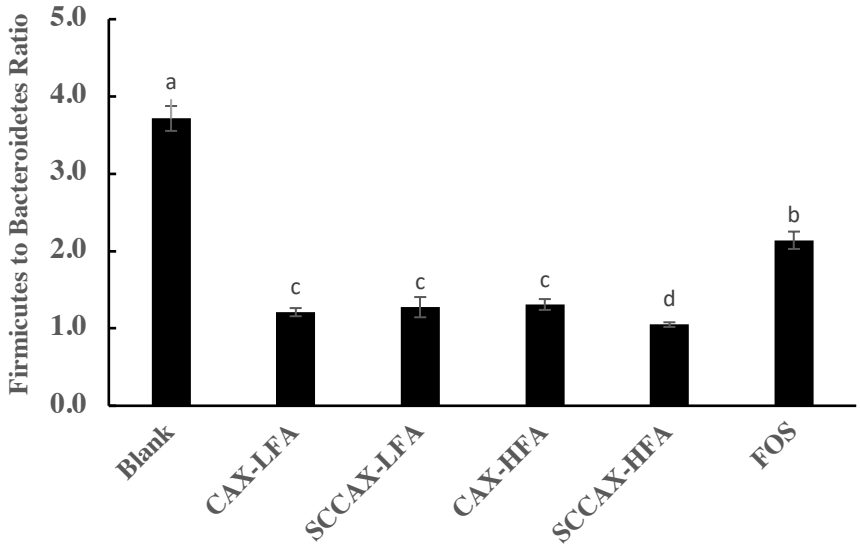

Figure 4.5 Firmicutes to Bacteroidetes ratio of CAX-LFA, SCCAX-LFA, CAX-HFA and SCCAX-HFA after 24 h of *in vitro* fecal fermentation.

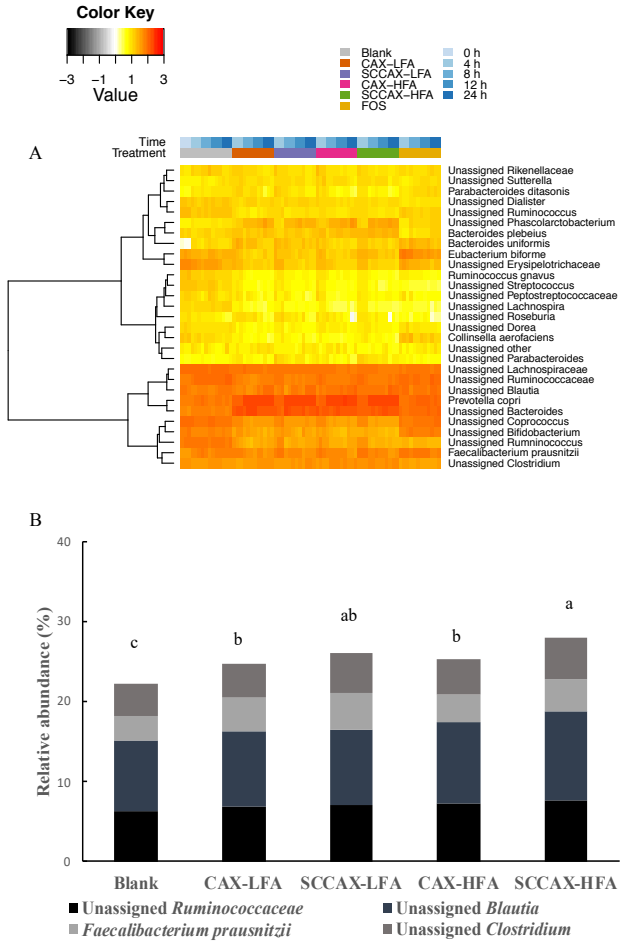

Figure 4.6 Heatmap of the shift in key OTUs during fermentation; **B)** Relative abundance of butyrate-producing bacteria, Unassigned *Ruminococcaceae,* Unassigned *Blautia, Faecalibacterium prausnitzii,* and Unassigned *Clostridium* of CAX-LFA, SCCAX-LFA, CAX-HFA and SCCAX-HFA treatments after 24 h of *in vitro* human fecal fermentation. Different letters represent significant differences ($P < 0.05$).

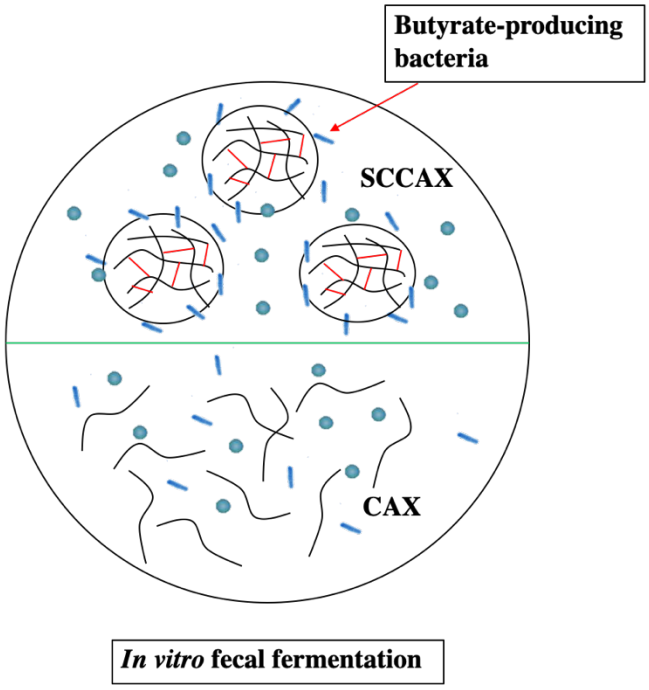

Figure 4.7 Schematic of proposed idea that the SCCAX matrix provides a competitive environment for butyrate-producing Clostridia during *in vitro* human fecal fermentation. SCCAX = soluble crosslinked corn bran arabinoxylan.

CHAPTER 5. ACID GELATION OF SOLUBLE LACCASE-CROSSLINKED CORN BRAN ARABINOXYLAN AND POSSIBLE GEL FORMATION MECHANISM

5.1 Abstract

Here, we reveal a new food gel formed on simple pH reduction of a water-soluble crosslinked corn bran arabinoxylan complex. This is different from low pH gelling high-methoxyl pectin that requires high sugar content, and it is similar in gelling property to low acyl gellan gum though is readily soluble in water. Alkaline-solubilized corn bran arabinoxylan (CAX) with two levels of residual bound ferulic acid was treated with laccase, a crosslinking enzyme, to produce two soluble, crosslinked CAX (SCCAX) complexes of different sizes (avg. 3.5 and 4.5-mer). Both of the SCCAXs formed gels at pH 2, with the larger, more heavily feruloylated SCCAX forming the stronger gel. Gels showed shear-thinning behavior and a thermal and pH reversible property. A gel forming mechanism was proposed to occur through noncovalent crosslinking including hydrogen bonds and hydrophobic interaction among the SCCAX complexes. This mechanism was supported by structural characterization of crosslinked CAX complexes using a Zeta-sizer and FT-IR spectroscopy. Applications of SCCAX gels might be where low pH low sugar gels are desired or a beverage containing SCCAX might be taken with gelling occurring in the low pH environment of the stomach, as well as in other food gels and as a drug delivery matrix.

5.2 Introduction

Hydrogels are three dimensional hydrophilic or amphiphilic polymer networks that are capable of retaining large amounts of water or biological fluids (Singh & Lee, 2014). Polymer interactions that lead to the formation of hydrogels include hydrogen and ionic bonding, hydrophobic interactions, and covalent crosslinks (Akhtar, Hanif, & Ranjha, 2016; Nishinari,

Zhang, & Ikeda, 2000). For example, high-methoxyl pectin forms a gel when sufficient sugar and acid are present to reduce hydration and negative charge, and promote hydrophobic interactions. In gelling of sodium alginate, addition of calcium ions create ionic bridges with acid groups to form an irreversible gel (Whistler & BeMiller, 2008). Chitosan-polyvinyl alcohol form gels in the presence of glutaraldehyde as the covalent crosslinking agent (Zu et al., 2012).

Food polysaccharides are non-toxic, biocompatible, biodegradable, either water-soluble or extractable in food-grade solvents, and generally have high swelling ability. These are properties that make them well suited for food uses, as well as for biomedical, pharmaceutical, and cosmetic applications. Arabinoxylan is a type of plant polysaccharide found in cell walls of endosperm and bran tissues of cereals and other monocot seeds. They are either soluble in water or extractable in dilute alkali (Neacsu et al., 2013). Arabinoxylans consist of a linear backbone chain of β-D-xylopyranosyl residues linked through (1,4) glycosidic bonds with various compositions of branched structures. α-L-Arabinofuranosyl residues are attached to some or most of the *Xylp* residues at O-2, O-3, and/or O-2,3 positions. Arabinoxylans can be neutral or acidic depending whether they contain 4-O-methyl-D-glucuronopyranosyl or D-glucuronopyranosyl substituents (Buchanan et al., 2003). Ferulic acid is commonly esterified on the O-5 position of arabinose branches (Izydorczyk & Biliaderis, 1995; Z. X. Zhang et al., 2014). It was reported that there are about 75 ferulic acid residues esterified to one corn bran arabinoxylan (CAX) polymer that has a degree of polymerization of about 2000 (Saulnier & Thibault, 1999), with many of the residues participating in diferulate crosslinks that makes CAX largely insoluble in the cell wall matrix. De-esterification using alkali (e.g., sodium hydroxide) to remove crosslinks brings these polymers into solution, and residual bound ferulic acid plays an important role in the functionality of CAX (Kale et al., 2013). CAX solutions can form gels

through oxidative crosslinking of bound ferulic acid moieties (Vansteenkiste et al., 2004), and gel strength is associated with the ferulic acid content of arabinoxylan (Carvajal-Millan, Landillon, et al., 2005). A strong gel was formed by the crosslinking action of laccase in CAX extracted with mild alkali that removes diferulate crosslinks, but retains much of the uncrosslinked bound ferulic acid (Kale et al., 2013). When treated with high concentration of alkali, no arabinoxylan gel formed due to low ferulic acid content; and bound ferulic acid content was associated with the structural properties of the gel, including pore size and crosslinking density.

Here, we show a novel type of gel formation, where a soluble laccase-crosslinked CAX (SCCAX) complex forms a gel simply by lowering pH. Differently, high-methoxyl pectin requires high sugar content to gel at low pH, however low acyl gellan gum similarly demonstrates acid gelation though is different in its solubility characteristics (requires either a chelating agent or heat to solubilize) (Valli & Clark, 2010; Norton, Cox, & Spyropoulos, 2011). The overall scheme of formation of the low pH SCCAX gel is shown in **Figure 5.1**.

Potential applications of this kind of low pH gelling polysaccharide are low sugar low pH gels or a beverage containing SCCAX that might be taken with gelling occurring in the low pH environment of the stomach for the purpose of providing a satiating effect and lowering glycemic response due to slow gastric emptying. Moreover, arabinoxylan is an important cereal fiber that possesses health-promoting effects in the gut due to colonic fermentation (Duncan et al., 2016; Rumpagaporn et al., 2015). This new gel type based on CAX treatment could also have broader applications as food gels and drug delivery matrices.

5.3 Materials and methods

5.3.1 Materials

Corn bran was obtained from Agricor (Marion, IN, USA). Thermostable α-amylase, proteinase, laccase from *Trametes versicolor*, ferulic acid, 3,4,5-trimethoxy-cinnamic acid (TMCA), methanolic-HCl, and sodium hydroxide were obtained from Sigma-Aldrich (St. Louis, MO, USA). Hexane, ethanol, and concentrated hydrochloric acid were bought from Mallinckrodt Chemicals (Phillipsburg, NJ, USA). Tri-Sil and acetonitrile was obtained from Fisher Scientific (Thermo Fisher Scientific, Suwanee, GA, USA). Ultrapure water was prepared by a Millipore Ultra-Genetic polishing system with $< 5 \times 10^{-9}$ TOC and resistivity of 18.2 mΩ (Millipore, Billerica, MA, USA) and used for all experiments.

5.3.2 Arabinoxylan extraction from corn bran

Corn bran was defatted by suspending in hexane (solid to liquid ratio 1:10) and stirring for 30 - 45 min. The slurry was filtered and repeated once. The final residue was dried in a hot air oven at 45 °C. The defatted bran was then suspended in water and pH was adjusted to 7.0 using sodium hydroxide. The slurry was boiled with constant stirring for 5 min to gelatinize the starch. Thermostable α-amylase (4 mL per 100 g bran) was added after cooling the suspension to 90 °C and kept for 60 min to hydrolyze starch. The pH was adjusted to 6 with HCl after cooling the solution. Proteinase (5 mL per 100 g bran) was added and incubated for 4 h at 50 °C. The enzyme was inactivated by boiling the mixture for 5 min. The slurry was centrifuged at 10,000g for 20 min and washed with purified water twice. The final pellet was dried in a hot air oven at 45 °C to obtain de-starched bran (DSB). DSB (50 g) was suspended in 500 mL of sodium hydroxide solution (0.25 M and 1.5 M). After stirring for 24 h at room temperature, the suspension was centrifuged at 10,000g for 10 min. The supernatant pH was adjusted to 4 - 5

using concentrated hydrochloric acid. The arabinoxylan was precipitated from the supernatant with 4 volumes of absolute ethanol. The precipitate was dried in a hot air oven at 45 °C, re-dissolved in water and freeze-dried. Thus, two samples CAX-low ferulic acid (LFA) and CAX-high ferulic acid (HFA), extracted from 1.5 M and 0.25 M sodium hydroxide, respectively, were obtained.

5.3.3 Arabinoxylan crosslinking and gel formation

Arabinoxylan preparations (2%, *w/v*) were dissolved in purified water by stirring at room temperature. Then, laccase (1.675 nkat/mg arabinoxylan) was added (Kale et al., 2013). The reaction was kept for 24 h at room temperature and laccase was deactivated by boiling the samples for 10 min. Residual laccase activity was measured by using 0.0216 mM syringaldazine in methanol as substrate (Figueroa-Espinoza & Rouau, 1998), and no laccase activity was found. After crosslinking, samples were freeze-dried. Two samples, soluble crosslinked CAX (SCCAX)-LFA and SCCAX-HFA, the product of laccase treatment of CAX-LFA and CAX-HFA, respectively, were obtained. Samples were stored in a vacuum desiccator until further use. Arabinoxylan gels were prepared by dissolving SCCAX-LFA and SCCAX-HFA in hydrochloric acid solution (pH 2). SCCAX-LFA (3% and 5%, *w/v*) and SCCAX-HFA (3% and 5%, *w/v*) were mixed at 150 rpm in an Eppendorf ThermoMixer C (Eppendorf, Hauppauge, NY, USA) at 37 °C until samples were dissolved. Preliminary experiments showed that SCCAX-HFA and SCCAX-LFA did not form gel mixed at pH 3, 4, and 5, while gel formed immediately when pH was reduced to 2.

5.3.4 Ferulic acid and diferulic acid content of arabinoxylan

The determination of ferulic acid and diferulic acid (DFA) content of arabinoxylan followed a protocol previously described with minor modification (Pedersen et al., 2015; Vansteenkiste et

al., 2004). Briefly, 5 mL of 2 M NaOH was added to 50 mg of CAX-LFA, CAX-HFA, SCCAX-LFA and SCCAX-HFA. The mixtures were allowed to react for 18 h under nitrogen, were protected from light, and continuously stirred. After adding 25 μg of 3,4,5-trimethoxy-cinnamic acid (TMCA) as an internal standard, 0.95 mL of concentrated HCl was added to adjust pH to 2. Phenolics were extracted three times with 4 mL of diethyl ether, and dried under nitrogen. The dried extracts were re-dissolved in 1 mL of methanol, filtered through a 0.22 μm nylon membrane (Agilent Technologies, Santa Clara, CA, USA) for HPLC (Agilent 1100, Agilent Technologies, Santa Clara, CA, USA) analysis.

HPLC was performed using an Agilent Eclipse XDB-C18 column (250 × 9.4 mm, i.d. 5 μm; Agilent Technologies, Santa Clara, CA, USA) monitored at 320 nm. Temperature of the column oven was set at 35 °C. The elution gradient (mobile phase A: acetonitrile; mobile phase B: sodium acetate buffer 0.05 M, pH 4.0) used was: 15-35% A in 30 min, 35-60% A in 0.5 min, 60-15% A in 4.5 min, and 15% A for 5 min. Flow rate was 1 mL/min and the injection volume was 20 μL.

5.3.5 Structural features of arabinoxylan

Protein content of arabinoxylan was measured by the Micro BCA™ Protein Assay Kit according to manufacturer's instructions (Thermo Fisher Scientific, Waltham, MA, USA). The molecular weight and size of arabinoxylan was analyzed by an Agilent 1100 high pressure size exclusion chromatography (HPSEC) equipped with refractive index (RI) and multiangle light scattering (MALS) detector (Agilent Technologies, Santa Clara, CA, USA). Superdex 200 and 30 columns (GE Healthcare Bio-Sciences, Pittsburgh, PA, USA) was used to separate the polymers. The HPSEC conditions were: mobile phase was purified water, injection volume was 100 μL, flow rate was 0.4 mL/min. Neutral and acidic monosaccharide composition of the arabinoxylan

samples was determined as their trimethylsilyl (TMS) derivatives according to Doco *et al.* (Doco, O'Neill & Pellerin, 2001). An Agilent 7890A gas chromatograph and 5975C insert MSD with a triple-axis detector (Agilent Technologies, Santa Clara, CA, USA) was used. Helium was the carrier gas at a flow rate of 1 mL/min through an Agilent DB-5 capillary column. Injection volume was 0.2 μL at a split ratio of 50/1. Oven temperature was initially 140 °C, held for 2 min, and increased by 2 °C/min to 180 °C, held for 1 min, and increased at 30 °C/min to 235 °C where it was held for 15 min.

5.3.6 Solution shear rheology

Solutions (3% *w/v*) of arabinoxylans were prepared in hydrochloric acid solution (pH 5 and pH 2). Storage and loss moduli under small amplitude oscillatory shear and viscosity was measured using a TA ARES-G2 rotational rheometer (TA Instruments, Newcastle, DE, USA) with a 40 mm 1.999° cone plate and using a 55 μm gap at 37 °C. Flow curves were obtained over a shear rate range from 0.1 to 100 s^{-1}. Viscoelastic properties of the gels were measured by a frequency sweep test in a range of frequencies from 0.06 to 15.78 rad/s and a 3% strain, which was determined to be within the linear viscoelastic region.

Measurements were performed in triplicate and rheological parameters were calculated using the manufacturer's supplied computer software (TRIOS v4.0, TA Instruments, Newcastle, DE, USA). The viscosity of arabinoxylan solution samples was described by the power law model given by the equation below:

$$\eta = K\dot{\gamma}^{n-1}$$

Where η is apparent viscosity (Pa s), K is the consistency coefficient (Pa s^n), $\dot{\gamma}$ is the shear rate (s^{-1}) and n is flow behavior index.

5.3.7 Small amplitude oscillatory shear rheometry, temperature sweep test

The effect of temperature on gel storage was studied by loading the gel onto a TA ARES-G2 rotational rheometer (TA Instruments, Newcastle, DE, USA) with a 40 mm 1.999° cone plate. The storage and loss modulus were measured from 25 to 95 °C and temperature step was set at 5 °C. A 3% strain and a 1 Hz frequency were applied. Measurements were performed in triplicate and rheological parameters were calculated using the manufacturer's supplied computer software (TRIOS v4.0, TA Instruments, Newcastle, DE, USA).

5.3.8 Cryogenic scanning electron microscopy (Cryo-SEM) of gels

SCCAX gels (3% w/v) were prepared by dissolving SCCAX-LFA and SCCAX-HFA in hydrochloric acid solution (pH 2). After gelling, gels were put into slit holders in the cryo-holder, secured in place with a set screw, and plunged into a liquid nitrogen slush. A vacuum was pulled and the samples were transferred to a Gatan Alto 2500 pre-chamber (cooled to -170 °C). After fracturing the samples with a cooled scalpel to produce a free-break surface, samples were sublimated at -90 °C for 10 min followed by sputter coating for 120 s with platinum. Then, the samples were transferred to the microscope cryo-stage (-120 °C) for imaging. The samples were imaged with a FEI NOVA nanoSEM field emission SEM (FEI Company, Hillsboro, Oregon, USA) using the ET (Everhart-Thornley) detector operating at 5 kV accelerating voltage, ~4.5 mm working distance, spot 3, and 30 μm aperture. Magnifications were 1,000× - 5,000× for images.

5.3.9 Surface charge of arabinoxylan

CAX-LFA, CAX-HFA, SCCAX-LFA and SCCAX-HFA (3%, *w/v*) were dispersed in purified water and mixed until dissolved with an Eppendorf ThermoMixer C (Eppendorf, Hauppauge, NY, USA) at 37 °C. The ζ-potential of the samples were measured using a Zetasizer Nano ZS90

(Malvern Instruments, Malvern, UK). All measurements were carried out at 25 °C and performed in triplicate.

5.3.10 FT-IR spectra of arabinoxylan at different pH's

Solutions (3%, *w/v*) of SCCAX-HFA and SCCAX-LFA were prepared in pH 2 and pH 5 hydrochloric acid solution and then analyzed using Fourier-transform infrared (FT-IR) spectroscopy. Spectra were obtained with a Nexus 670 FT-IR spectrometer (ThermoNicolet, Madison, WI, USA) equipped with a deuterated triglycine sulfate (DTGS) detector and diamond attenuated total reflectance (ATR) crystal. Data were analyzed using OMNIC software (ThermoElectron Corp., Madison, WI, USA).

5.3.11 Statistical analysis

Data were reported as mean ± SD for triplicate determinations. One-way ANOVA and Tukey's test were employed to identify differences in means. Statistics were analyzed using SPSS for Windows (version rel. 10.0.5, 1999, SPSS Inc., Chicago, IL, USA) and Origin for Windows (version Srl b9.3.1.273, OriginLab Corp., Northampton, MA, USA).

5.4 Results and discussion

Arabinoxylan gels have been made by others using laccase treatment to crosslink the ferulic acid residues of the soluble polysaccharide (Carvajal-Millan, Guigliarelli, Belle, Rouau, & Micard, 2005; Carvajal-Millan, Landillon, et al., 2005; Kale et al., 2013), however they form at about pH 5 and subsequent to the addition of laccase. The mechanism of this gel formation is the covalent diferulate crosslink, which forms a polymer network that traps water. Here, a different kind of arabinoxylan gel was formed. The illustration in **Figure 5.1** shows that laccase treatment of CAX mediated the formation of a soluble crosslinked corn arabinoxylan (SCCAX) intermediate, which

formed a gel on pH reduction. We believe the soluble intermediate formed with laccase, rather than a gel, because the arabinoxylan used had a low arabinose/xylose ratio with coinciding lower feruloylated arabinose branches. To our knowledge, this is a new polysaccharide-based gel type, in which the soluble arabinoxylan in water alone forms a gel at low pH. It is differentiated from the low pH gel-forming property of high-methoxyl pectin that requires high sugar content to restrict water availability to the pectin, though is similar in gelling properties to low acyl gellan gum (Norton, Cox, & Spyropoulos, 2011). However, gellan gum is different from SCCAX in that it is not readily soluble in water requiring either heat or addition of a chelator. From a practical standpoint, SCCAX gels could be used in applications where low sugar low pH gels are desired or where a beverage containing SCCAX might be taken with gelling occurring in the low pH environment of the stomach.

Two soluble arabinoxylan samples were produced with alkali treatments, CAX-high ferulic acid (CAX-HFA) and CAX-low ferulic acid (CAX-LFA, **Figure 5.1**). Laccase-treated CAX-HFA and CAX-LFA formed SCCAX-HFA and SCCAX-LFA, respectively, which were soluble crosslinked CAX complexes of limited polymerization. Weak and strong gels were formed by lowering pH of solutions of SCCAX-LFA and SCCAX-HFA, while no gels were formed at low pH for uncrosslinked CAX-HFA and CAX-LFA. Gel structure dissipated when pH was increased to 5, showing it to be a pH-reversible gel type. Structural features, rheological properties, and parameters related to a possible formation mechanism are shown below.

5.4.1 Monosaccharide, ferulic acid and diferulic acid content of arabinoxylan samples

As shown in **Table 5.1**, CAX was composed of arabinose (~15%), xylose (~68%), glucose (~5%), galactose (~5%), and glucuronic acid (~1.5%). CAX had a low arabinose/xylose ratio of about 22% compared to a typical CAX value of ~50% (Devin J. Rose et al., 2010) (**Table 5.1**).

Low concentration of sodium hydroxide to extract CAX led to high residual ferulic acid; and high concentration of alkali resulted in greater ferulic acid depletion, which is in accordance with our previous results (Kale et al., 2013). We reported ferulic acid contents ranging from 2.1 to 15.0 mg/g when extracted with 0.5 – 1.5 M sodium hydroxide for 24 h, which was significantly higher than that of the present study of 0.61 and 1.15 mg/g (**Table 5.2**). The lower content of ferulic acid was associated with less arabinose branching in our CAX starting material and is likely the reason that no direct gels were formed by laccase treatment. Corn genotype and environment causes variation in ferulic acid contents ("Handbook of Hydrocolloids, 2nd Edition," 2009), and likely explains the low content of ferulic acid in our study.

After laccase treatment, remaining uncrosslinked ferulic acid decreased (**Table 5.2**). In CAX-HFA, 0.85 mg/g ferulic acid formed crosslinks in SCCAX-HFA, and a lesser 0.51 mg/g of ferulic acid of CAX-LFA was involved in crosslinking of SCCAX-LFA. Diferulic acids (DFA), including 8,8-DFA and 5,5-DFA, were found in both CAX and SCCAX. No significant change of 8,8-DFA was observed after laccase treatment while 5,5-DFA content of SCCAX was markedly lower than CAX. 8,5(benzofuran)-DFA was only found in CAX, while 8,5(decarboxylated)-DFA was only found in SCCAX (**Table 5.2**). Taken together, the DFA contents were not increased after laccase treatment, but rather it stayed at the same level. This phenomenon was previously reported and explained to be due to undetected DFA species (Castillo et al., 2009; Figueroa-Espinoza & Rouau, 1998; Lapierre et al., 2001).

5.4.2 Molecular size of arabinoxylan samples

To examine whether SCCAX complexes formed after laccase treatment, HPSEC was used to determine the molecular size of arabinoxylan samples. As shown in **Figure 5.2**, SCCAX-HFA had the largest hydrodynamic radius (Rh), followed by CAX-HFA, SCCAX-LFA, and CAX-

LFA. CAX-HFA showed larger Rh than CAX-LFA as higher alkali treatment removed more ferulic acid residues, resulting in fewer crosslinks formed during laccase treatment of arabinoxylan polymers (Kale et al., 2013). Also, SCCAX-HFA and SCCAX-LFA had larger Rh than CAX-HFA and CAX-LFA, respectively. Thus, instead of gel formation, laccase treatment of CAX induced the crosslinking of arabinoxylan and produced SCCAX complexes, which was in agreement with the ferulic acid content change of between CAX and SCCAX (**Table 5.2**). The Mw of arabinoxylan from the MALS detector showed that CAX-LFA and CAX-HFA formed average 3.5-mer and 4.5-mer SCCAX complexes after laccase treatment, respectively (**Figure 5.2**).

5.4.3 Rheological characterization of arabinoxylans at different pHs

Shear viscosity versus shear rate profiles of 3% solutions of CAX-LFA, CAX-HFA, SCCAX-LFA and SCCAX-HFA at different pH values are shown in **Figure 5.3**. All samples at pH 5, and CAX-LFA and CAX-HFA at pH 2, showed shear thinning behavior at low shear rates followed by Newtonian behavior at higher shear rate. Shear-thinning behavior was observed in SCCAX-HFA and SCCAX-LFA at pH 2. Both SCCAX-HFA and SCCAX-LFA at pH 2 revealed significantly higher solution viscosity than at pH 5, indicating that decrease the pH of SCCAX samples increased viscosity. This property was only found for the SCCAX samples, while no significant viscosity change was observed in the uncrosslinked CAX samples (**Figure 5.3**). Overall, all samples showed a pseudo-plastic behavior, which was confirmed by the flow behavior indices ($n < 1$) as shown in **Table 5.2.**

Within the linear region, flow curves of arabinoxylan were fitted to the Power-Law model in order to describe the apparent viscosity as a function of shear rate (**Table 5.3**). All data fitted well within the model, as R^2 values remained above 0.997. Higher flow consistency indices (K)

were shown by SCCAX-LFA and SCCAX-HFA at pH 2. In addition, lower flow behavior index (n), and therefore higher pseudo-plastic behaviors were displayed by SCCAX-LFA and SCCAX-HFA. Thus, pH decrease of SCCAX complex increased the viscosity of the solution and the behavior of the solution changed to shear-thinning from Newtonian behavior. Moreover, all samples at pH 5, and CAX-LFA and CAX-HFA at pH 2, showed low viscosity (lower K) and displayed Newtonian behavior (n near 1, **Table 5.3**).

Viscoelasticity measurements were performed to determine the gelation property of SCCAX-HFA and SCCAX-LFA at pH 2 and 5. As shown in **Figure 5.4,** at pH 5, no gel was formed for SCCAX-HFA and SCCAX-LFA and they exhibited the characteristic of a solution. When the pH was decreased to 2, G' of both SCCAX-HFA and SCCAX-LFA was greater than G'', and G' was independent of frequency, indicating that a strong gel was formed.

5.4.4 Effect of temperature on storage and loss moduli of arabinoxylans

To understand whether covalent bonds were involved in SCCAX gel formation at low pH, temperature sweeps of 3% and 5% of SCCAX-HFA and SCCAX-LFA at pH 2 were conducted. As shown in **Figure 5.5A** and **B**, SCCAX samples showed a clear decrease in storage and loss moduli, indicating that the forming of gels was not caused by covalent bonds, but the contribution of thermally reversible interactions. In addition, 5% SCCAX gels showed higher storage and loss moduli than 3% SCCAX gels, showing that higher concentration of SCCAX forms stronger gels. It was noteworthy that 3% SCCAX-HFA gels had higher storage and loss moduli than 5% SCCAX-LFA gels, showing that SCCAX-HFA forms much stronger gels than SCCAX-LFA.

5.4.5 Cryogenic scanning electron microscopy (Cryo-SEM) of arabinoxylan gels

Cryo-SEM images of 3% SCCAX-HFA and SCCAX-LFA gels made at different magnification levels are shown in **Figure 5.6**. The structure of the gels was honeycomb-like. The diameter of the pores in SCCAX-LFA gel was around 10 – 20 μm, and SCCAX-HFA pores were less than 10 μm. The pore size of the SCCAX-HFA gel were clearly smaller than the SCCAX-LFA gel, which was in accordance with the rheological results. Overall, the SCCAX-HFA gel showed a more dense structure and was a stronger gel compared to the SCCAX-LFA gel.

5.4.6 Proposed mechanism of SCCAX gel forming at low pH

To our knowledge, this is the first report of arabinoxylan in aqueous solution forming a strong gel simply by lowering of pH to 2. Apparently, the critical step is the formation of soluble laccase-mediated polymeric complexes of diferulate-crosslinked arabinoxylan, which is the entity that participates in the gel formation at low pH. The data shows that noncovalent crosslinking was involved in the gel formation, because the gels were both pH and thermally reversible. Gellan gum also has similar acid gelling property to SCCAX, though the polymers are quite different in structure with gellan gum having linear mainchain repeating units with acyl substituents and arabinoxylan being branched polysaccharide. Thus, the mechanisms of gel formation may be different.

Our proposed mechanism of formation of SCCAX to a gel is as follows. When pH decreases to 2, which is lower than the pKa of the glucuronic acid (pKa 3.21), the carboxylate groups (see **Table 5.1**) are protonated and became uncharged. As the result, the repulsive force between the polymer chains within the SCCAX complex decreases, giving polymer chains more of the characteristic of long neutral molecules. This, combined with the diferulate crosslinks found within the SCCAX complex, draws the polymers within the complex in close proximity with

each other, allowing for hydrogen bonding between chains to develop. We showed that 5'5-DFA was decreased and 8,5(decarboxylated)-DFA was increased, which may favor the gel formation as the intrachain bonds might be favored by 5'5-DFA which lead to reduction of elastic effectivity of arabinoxylan network (Hatfield & Ralph, 1999). Moreover, higher protein content in SCCAX-LFA may have contributed to its lower gel strength (**Table 5.1**), perhaps due to hindrance by residual protein molecules to the non-covalent interactions that likely occur among CAX chains during gelation (Vansteenkiste et al., 2004). In addition, the low arabinose to xylose ratio of the SCCAX could favor the aggregation of arabinoxylan chains (Peng et al., 2012), and enhanced hydrogen bonding to drive a physical interaction between arabinoxylan chains (Marquez-Escalante et al., 2018). In turn, the neutral SCCAX complexes in solution aggregate to form gels at pH 2, which may be explained by a combination of hydrophobic interaction and hydrogen bond forces.

5.4.7 Surface charges of arabinoxylan

The surface charges of CAX-LFA, CAX-HFA, SCCAX-LFA, and SCCAX-HFA solutions were measured using a zeta-potential analyzer. As shown in **Table 5.4**, all the arabinoxylan samples were negatively charged, which was caused by the dissociation of carboxyl groups of branched uronic acid. The ζ-potentials of CAX-LFA, SCCAX-LFA, CAX-HFA, and SCCAX-HFA were -11.1, -13.4, -11.6, and -15.2 mV, respectively. No significantly different surface charge density was found between CAX-LFA and CAX-HFA. After crosslinking, the surface negative charge was significantly increased, indicating the success in crosslinking of arabinoxylan under laccase treatment. Moreover, SCCAX-HFA showed highest negative charge, confirming that higher crosslinking density was formed in SCCAX-HFA. Taken together, dense soluble structures formed with laccase (denser in the SCCAX-HFA) and, when protonated (ferulic and glucuronic

acid residues) at low pH, the resulting uncharged, neutral polymeric structures presumably formed gel aggregates through hydrophobic and hydrogen bond interactions.

5.4.8 FT-IR spectra of SCCAX complex at different pH

To further understand the gel forming mechanism of SCCAX complexes, FT-IR was used to determine their structure at different pH's. **Figure 5.7** shows the FT-IR spectrum of SCCAX-HFA and SCCAX-LFA at pH 2 and pH 5 in the 600 – 4000 cm^{-1} region. The characteristic absorption bands at 3200 – 3550 cm^{-1} (broad) represents the hydroxyl-stretching vibrations of polysaccharides and water involved in hydrogen bonds (Fringant, Tvaroska, Mazeau, Rinaudo & Desbrieres, 1995). As shown in **Figure 5.7**, the absorption intensity of SCCAX-HFA and SCCAX-LFA at pH 2 was significantly higher than that at pH 5, suggesting that the decrease of pH increased intermolecular hydrogen bond interaction. The results indicate that intermolecular hydrogen bonds play an important role in the gel forming of SCCAX at low pH. In addition, the characteristic absorption region between 800-1500^{-1} cm represents C-C, C-O, C-OH and C-O-C stretch of arabinoxylan backbone (Nandini & Salimath, 2001), and 1500-1700^{-1} cm region represents the absorption bands of ferulic acid and protein (Kačuráková, et al., 1999). Notably, the absorbance band at 1035-1047 cm^{-1} represents the β (1-4) linked xylose backbone (Kačuráková, et al., 1999; Barron & Rouau, 2008), whereas the intense in our samples was relatively low. This might due to the low concentration of SCCAX (3%) used in the FT-IR analysis. Taken together, the surface charges of arabinoxylan samples, structural features including ferulic acid contents, molecular size and FT-IR data of arabinoxylans supported our proposed gel forming mechanism of SCCAX at low pH.

5.5 Conclusions

In summary, this report describes a new polysaccharide-based gel, where a stable solution of 3.5 to 4.5-mer arabinoxylan complexes readily forms a gel simply by lowering pH. It was previously reported that arabinoxylan extracted with low alkali concentration (0.25 or 0.5 M NaOH) formed gels at pH 5 when treated with laccase (Carvajal-Millan, Guigliarelli, et al., 2005; Carvajal-Millan, Landillon, et al., 2005; Kale et al., 2013). However, in the current study, no gel was formed at pH 5 for either SCCAX-LFA and SCCAX-HFA. We believe this was caused by the unusually low arabinose/xylose ratio of the CAX used (~ 0.22), and the coinciding low ferulic acid content of arabinoxylan in our study. Results support a view that the laccase-crosslinked SCCAX formed low pH gels due to hydrogen bond and hydrophobic interactions. Some applications may be obtained from SCCAX-formed gels, such as low sugar, low pH gels and a beverage, when consumed, that may gel in the low pH environment of the stomach to delay gastric emptying and increase satiety, as well as for other food gels and nutraceutical or drug delivery.

Table 5.1 Neutral and acidic monosaccharides composition and protein content of arabinoxylan[a].

Samples	Arabinose (%)	Xylose (%)	Galactose (%)	Glucose (%)	Glucuronic acid (%)	Protein (mg/g)
CAX-LFA	15.21a ± 3.07	68.11a ± 1.03	5.99a ± 1.03	5.65a ± 0.43	1.44a ± 0.06	57.78c ± 2.57
SCCAX-LFA	15.41a ± 1.13	67.46a ± 0.56	4.84a ± 0.56	4.92a ± 0.50	1.53a ± 0.16	113.38a ± 2.57
CAX-HFA	16.76a ± 1.71	67.58a ± 0.50	5.60a ± 0.49	5.86a ± 0.81	1.56a ± 0.54	22.89d ± 4.11
SCCAX-HFA	16.11a ± 0.68	68.89a ± 0.89	4.78a ± 0.48	5.09a ± 0.48	1.56a ± 0.16	75.04b ± 1.80

[a]CAX-LFA and CAX-HFA stand for corn bran arabinoxylan extracted by 1.5 M and 0.25 M NaOH, respectively; SCCAX-LFA and SCCAX-HFA stand for crosslinked CAX-LFA and CAX-HFA, respectively.

Table 5.2 Ferulic acid and diferulic acid (DFA) content in CAX and SCCAX[b]

Samples	Ferulic acid (mg/g)	8,8-DFA (mg/g)	5,5-DFA (mg/g)	8,5(benzofuran)-DFA (mg/g)	8,5(decarboxylated)-DFA (mg/g)	Total DFA (mg/g)
CAX-LFA	0.61b ± 0.06	0.47a ± 0.08	0.18ab ± 0.01	0.38b ± 0.07	nd	1.04b ± 0.05
CAX-HFA	1.15a ± 0.06	0.69a ± 0.10	0.36a ± 0.05	1.05a ± 0.15	nd	2.09a ± 0.20
SCCAX-LFA	0.10c ± 0.02	0.49a ± 0.09	0.02c ± 0.00	nd	0.51a ± 0.11	1.02b ± 0.31
SCCAX-HFA	0.30c ± 0.09	0.65a ± 0.14	0.04b ± 0.00	nd	0.66a ± 0.14	1.34ab ± 0.01

[b]CAX-LFA and CAX-HFA stand for corn bran arabinoxylan extracted by 1.5 M and 0.25 M NaOH, respectively; SCCAX-LFA and SCCAX-HFA stand for crosslinked CAX-LFA and CAX-HFA, respectively. nd stands for not detected. Data are expressed as mean ± SD (n = 3). Sample values marked by the different letters are significant different ($P < 0.05$).

Table 5.3 Power law model parameters of arabinoxylan at the concentration of 3% (*w/v*)[c].

Samples	Model parameters		
	K(Pa s^n)	**n**	**R^2**
CAX-LFA, pH 5	0.016	0.922	0.999
CAX-LFA, pH 2	0.014	0.945	0.999
SCCAX-LFA, pH 5	0.024	0.900	0.999
SCCAX-LFA, pH 2	0.773	0.548	0.997
CAX-HFA, pH 5	0.012	0.948	0.999
CAX-HFA, pH 2	0.012	0.949	0.999
SCCAX-HFA, pH 5	0.017	0.954	0.999
SCCAX-HFA, pH 2	0.701	0.593	0.999

[c]CAX-LFA and CAX-HFA stand for corn bran arabinoxylan extracted by 1.5 M and 0.25 M NaOH, respectively; SCCAX-LFA and SCCAX-HFA stand for crosslinked CAX-LFA and CAX-HFA, respectively.

Table 5.4 Zeta-potential of arabinoxylan samples[d].

Samples	CAX-LFA	SCCAX-LFA	CAX-HFA	SCCAX-HFA
zeta potential (mV)	-11.1c ± 0.8	-13.4b ± 0.4	-11.6c ± 0.9	-15.2a ± 0.1

[d]CAX-LFA and CAX-HFA stand for corn bran arabinoxylan extracted by 1.5 M and 0.25 M NaOH, respectively; SCCAX-LFA and SCCAX-HFA stand for crosslinked CAX-LFA and CAX-HFA, respectively. Data are expressed as mean ± SD (n = 3). Sample values marked by the different letters are significant different ($P < 0.05$).

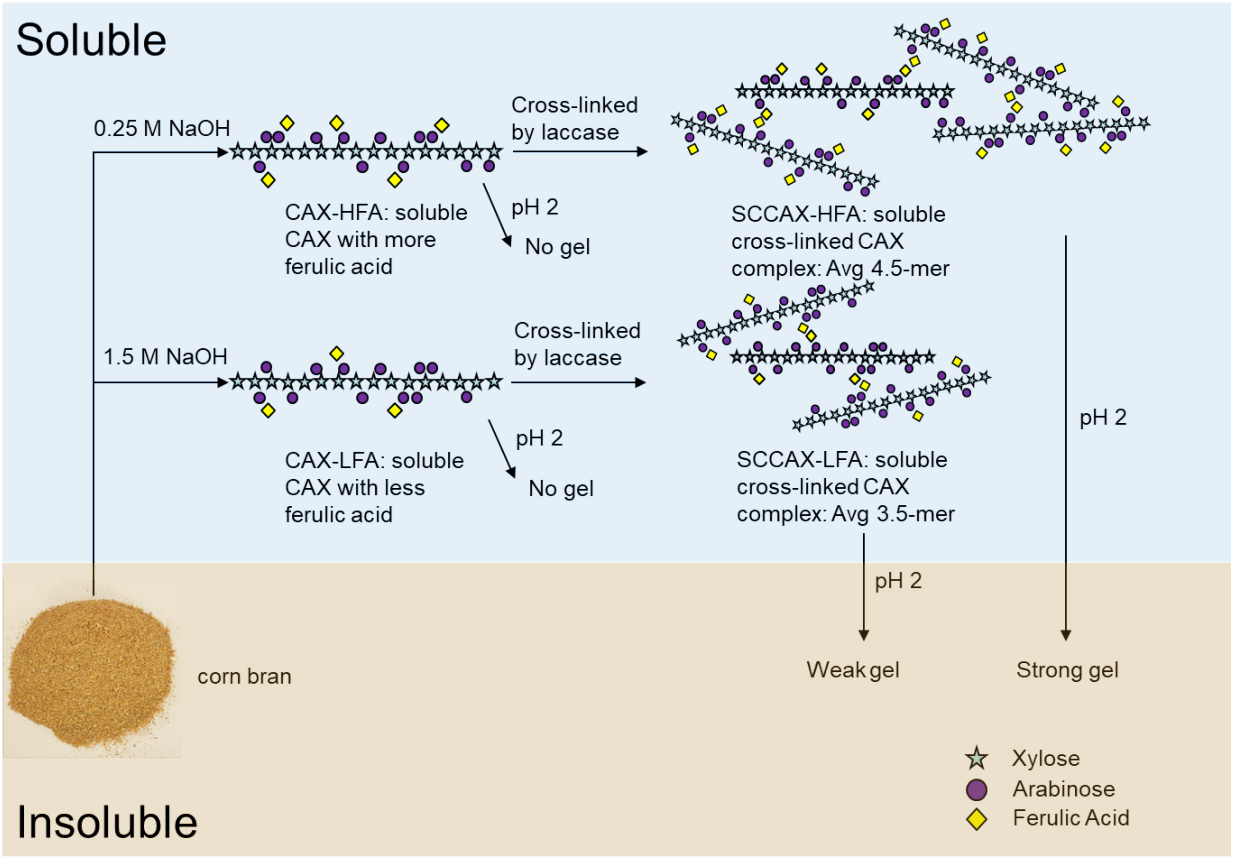

Figure 5.1 Illustration of novel gel formation of corn arabinoxylan. Alkali-extracted CAX was treated with laccase to form soluble crosslinked CAX (SCCAX) complex, which then formed gels when pH was reduced to 2.

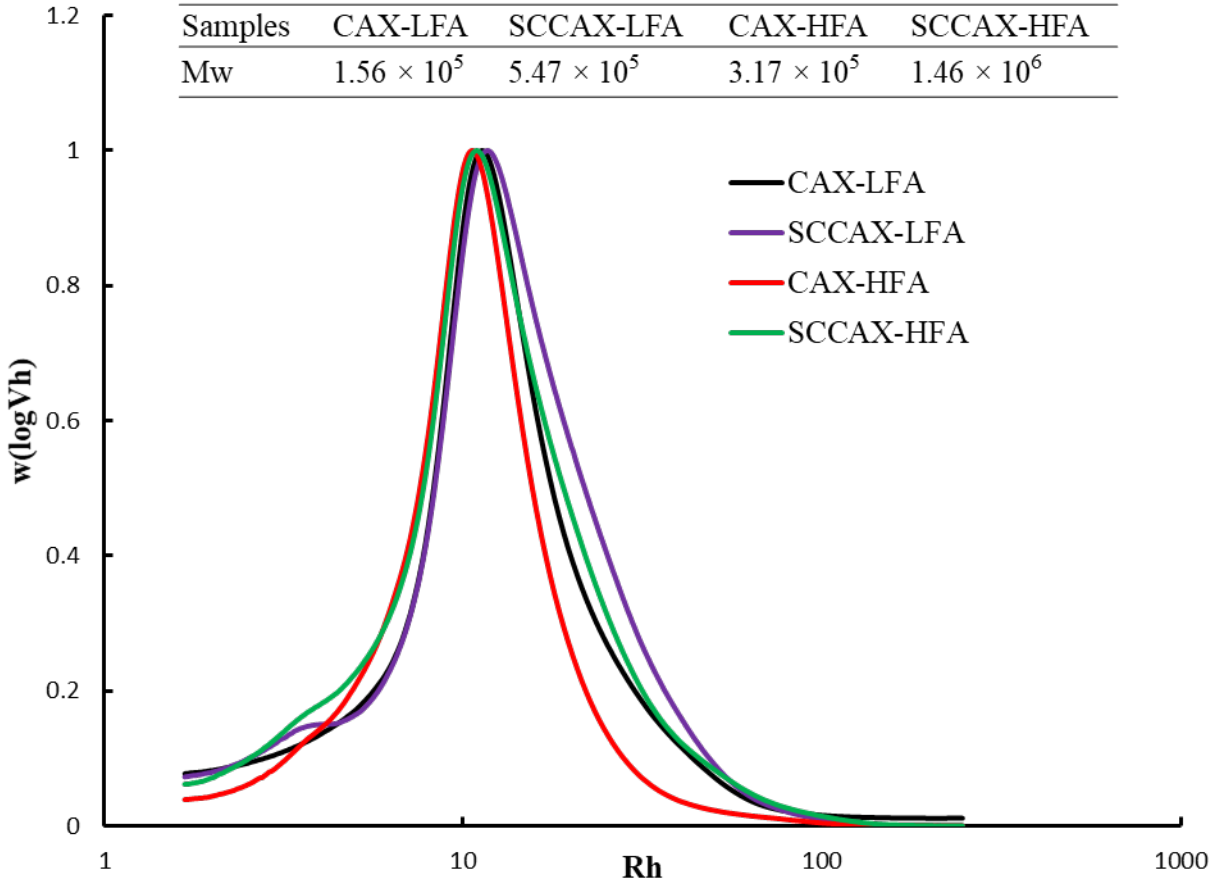

Figure 5.2 Size exclusion chromatography of arabinoxylan samples. CAX-LFA and CAX-HFA are corn bran arabinoxylans extracted in 1.5 M and 0.25 M NaOH, respectively; SCCAX-LFA and SCCAX-HFA are soluble crosslinked CAX-LFA and CAX-HFA, respectively.

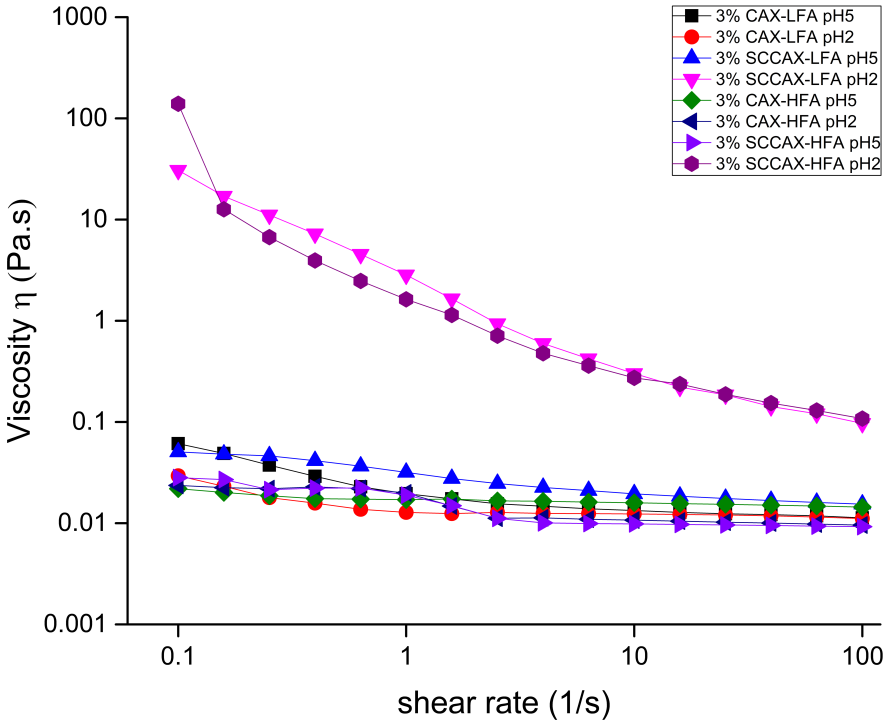

Figure 5.3 Shear rate dependence of viscosity for arabinoxylans at a concentration of 3 wt%. CAX-LFA and CAX-HFA are corn bran arabinoxylans extracted in 1.5 M and 0.25 M NaOH, respectively. SCCAX-LFA and SCCAX-HFA are soluble crosslinked CAX-LFA and CAX-HFA, respectively.

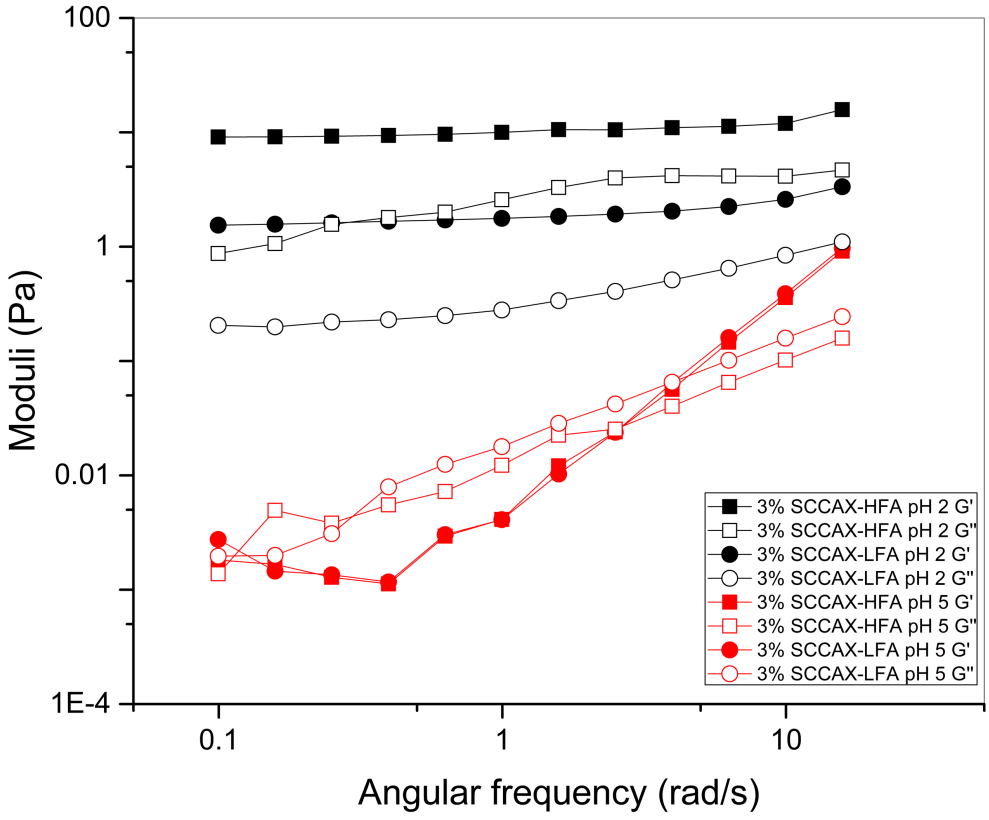

Figure 5.4 Mechanical spectra of SCCAX-HFA and SCCAX-LFA at pH 2 and 5 at a concentration of 3 wt%. CAX-LFA and CAX-HFA are corn bran arabinoxylans extracted in 1.5 M and 0.25 M NaOH, respectively. SCCAX-LFA and SCCAX-HFA are soluble crosslinked CAX-LFA and CAX-HFA, respectively.

A)

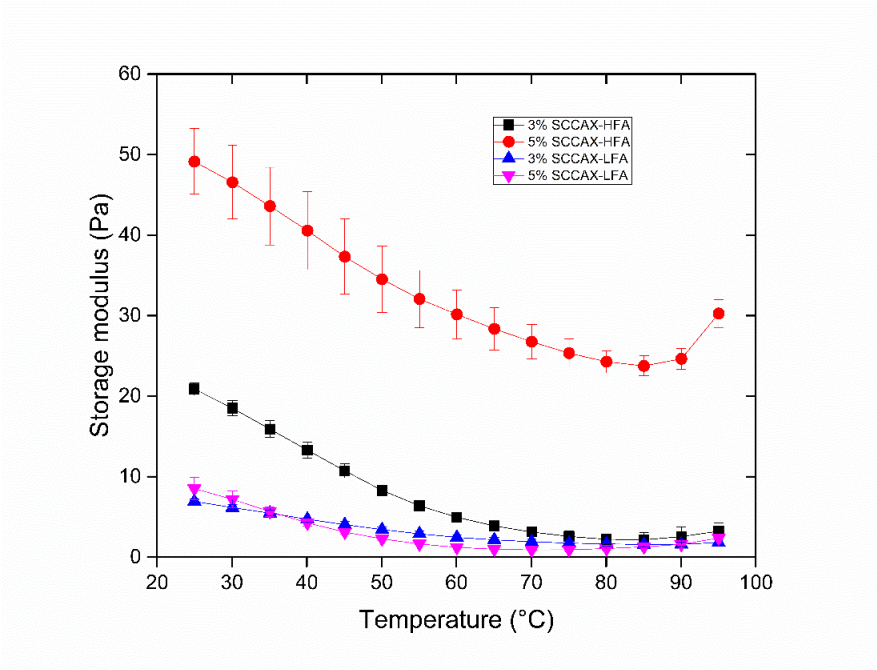

B)

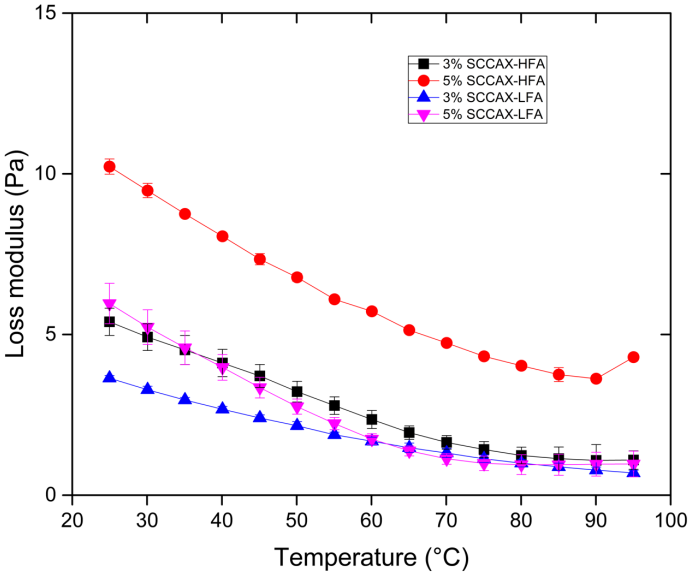

Figure 5.5 The A) storage (G') and B) loss (G") moduli as a function of temperature for crosslinked arabinoxylan at pH 2 at a concentration of 3 wt% and 5 wt%. CAX-LFA and CAX-HFA are corn bran arabinoxylans extracted in 1.5 M and 0.25 M NaOH, respectively.

A)

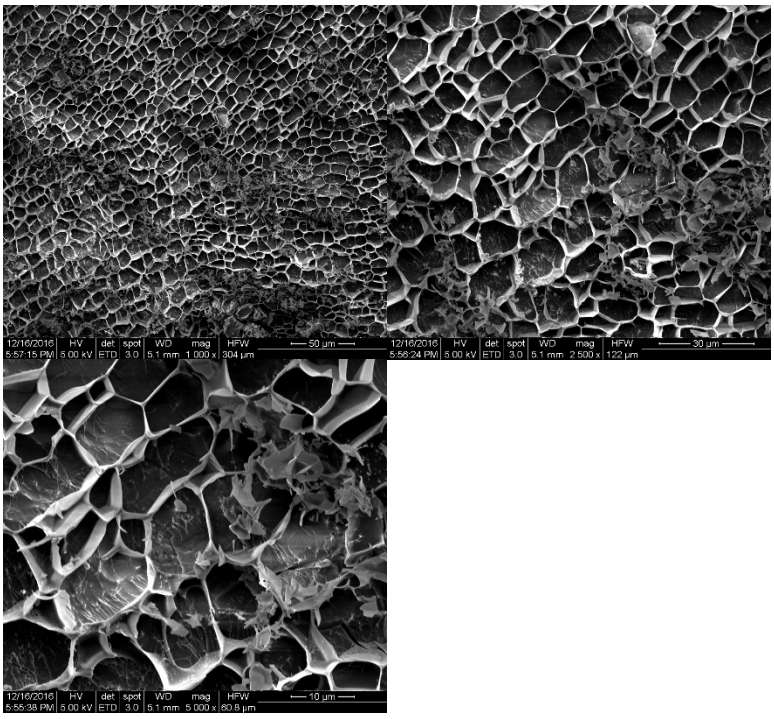

B)

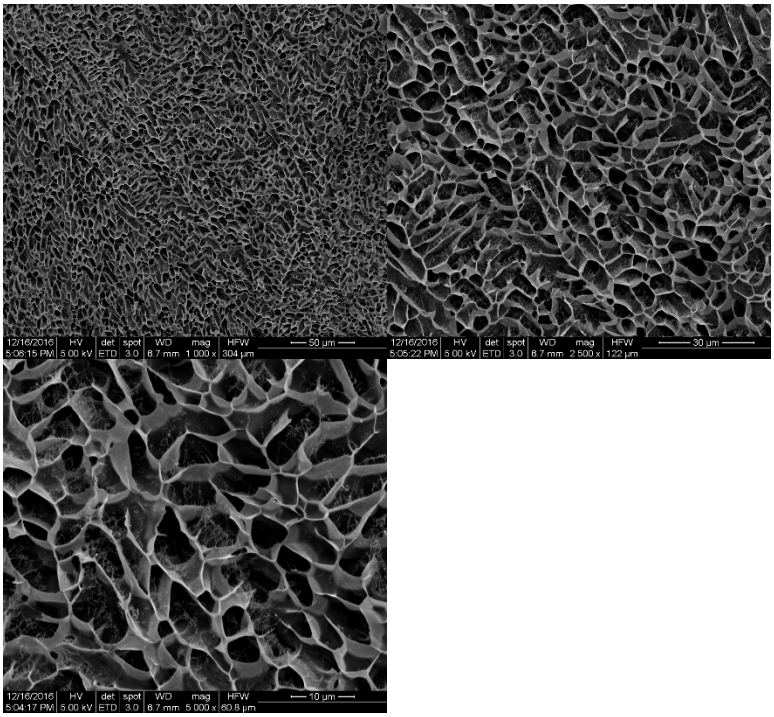

Figure 5.6 Scanning electron micrograph image of A) SCCAX-LFA at pH 2; B) SCCAX-HFA at pH2. SCCAX-LFA is crosslinked corn bran arabinoxylan extracted in 1.5 M NaOH; SCCAX-HFA is crosslinked corn bran arabinoxylan extracted in 0.25 M NaOH.

A)

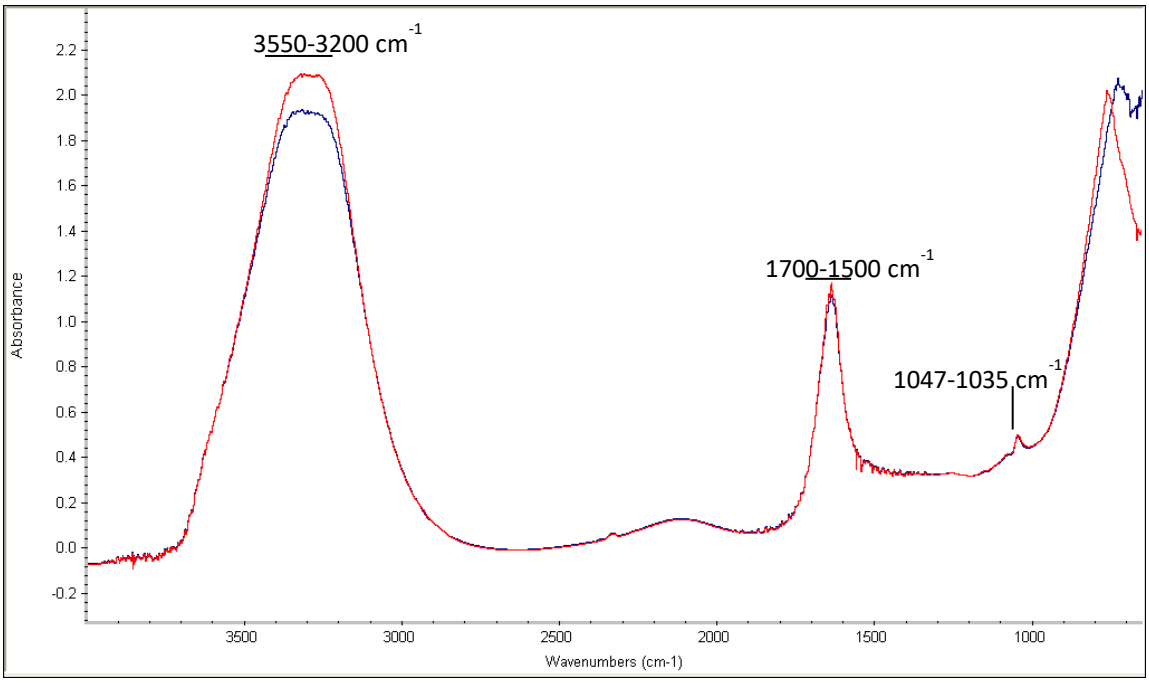

B)

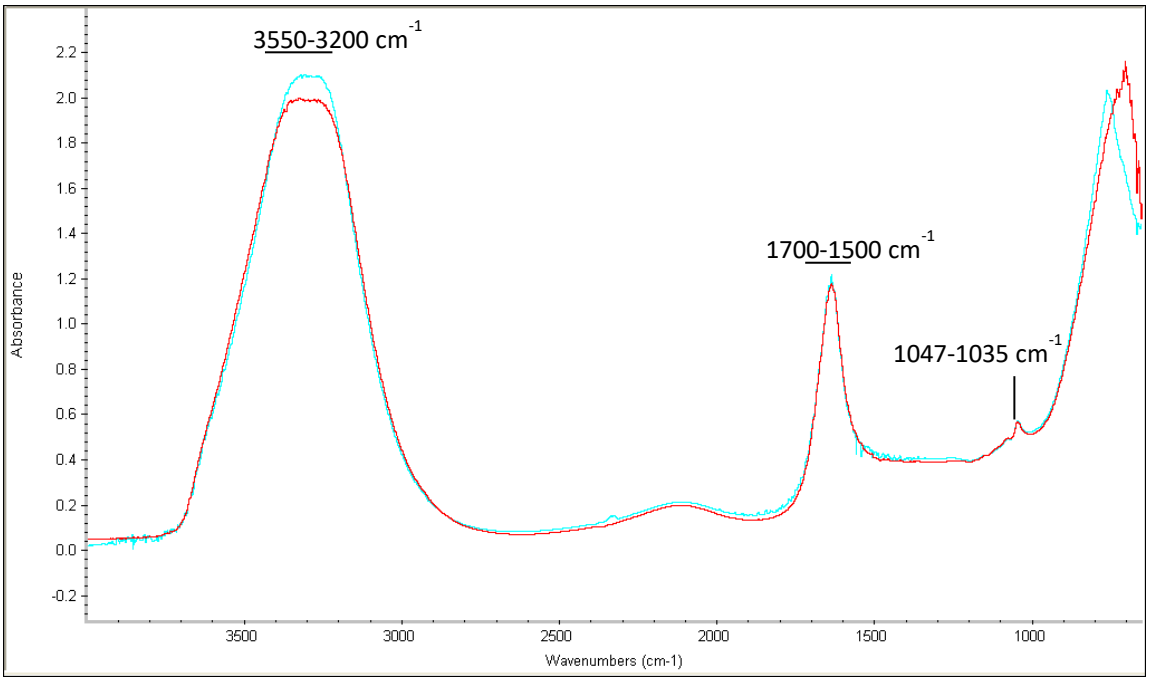

Figure 5.7 FT-IR spectra of A) SCCAX-HFA at pH 2 and 5. The red line represents SCCAX-HFA at pH 5 and the blue line represents SCCAX-HFA at pH 2; B) SCCAX-LFA at pH 2 and 5. The green line represents SCCAX-LFA at pH 2 and the red line represents SCCAX-LFA at pH 5.

CHAPTER 6. OVERALL CONCLUSION AND FUTURE WORK

In the first genotype x environment study, monosaccharide and linkage analysis revealed that CAXs had different structures and the differences were genotype-specific, but not significantly due to environment. PCA analysis revealed that both short chain fatty acid production and microbial community shifted also in a genotype-specific way. Thus, small structural changes, in terms of sugar and linkage compositions, cause significant changes in fermentation response and show very high specificity of structure to gut microbiota function. Future work should evaluate whether gut microbiota will also respond in the genotype-specific way and exhibited different biological functions in an *in vivo* study. Thus, the results might highlight the importance of crops genotype on the modulation of gut microbiota.

In the second study, a soluble fiber matrix was developed that exhibited a similar butyrogenic effect to fermentable insoluble fiber. Low arabinose/xylose ratio corn bran arabinoxylan (CAX) was extracted with two concentrations of sodium hydroxide to give soluble polymers with relatively low and high residual ferulic acid (CAX-LFA and CAX-HFA). After laccase treatment to make diferulate crosslinks, soluble matrices were formed with average 3.5 to 4.5 mer. *In vitro* human fecal fermentation of CAX-LFA, CAX-HFA, soluble crosslinked ~3.5 mer CAX-LFA (SCCAX-LFA), and ~4.5 mer SCCAX-HFA revealed that the SCCAX matrices had slower fermentation property and higher butyrate proportion in SCCAX-HFA. 16S rRNA gene sequencing showed that SCCAX-HFA promoted OTUs associated with butyrate production including Unassigned *Ruminococcaceae*, Unassigned *Blautia*, *Fecalibacterium prausnitzii*, and Unassigned *Clostridium*. Future work should focus on amplifying of the butyrogenic effects of SCCAX. The possible solution would be fabricating denser polymers through chemical modification to the CAX with higher degrees of esterified FA. These polymers would still have

low A/X ratio, but higher FA amount, thus denser polymers would be generated by laccase treatment.

In the third study, we investigated the interesting gel forming property of SCCAXs on simple pH reduction. Both of the SCCAXs formed gels at pH 2, with SCCAX-HFA forming the stronger gel. Gels showed shear-thinning behavior and a thermal and pH reversible property. A gel forming mechanism was proposed involving noncovalent crosslinking including hydrogen bonds and hydrophobic interaction among the SCCAX complexes. This mechanism was supported by structural characterization of SCCAX complexes using a Zeta-sizer and FT-IR spectroscopy. Future work could investigate possible applications of SCCAX, such as their drug delivery efficiency, or their effects on gastric emptying and satiety control. Moreover, as discussed above, the rheological property of the denser SCCAX should be further explored to illustrate the gelling property of SCCAX.

REFERENCES

Akhtar, M. F., Hanif, M., & Ranjha, N. M. (2016). Methods of synthesis of hydrogels ... A review. *Saudi Pharmaceutical Journal, 24*(5), 554-559. doi:10.1016/j.jsps.2015.03.022

Arumugam, M., Raes, J., Pelletier, E., Le Paslier, D., Yamada, T., Mende, D. R., . . . Meta, H. I. T. C. (2011). Enterotypes of the human gut microbiome. *Nature, 473*(7346), 174-180. doi:10.1038/nature09944

Ayala-Soto, F. E., Serna-Saldivar, S. O., Garcia-Lara, S., & Perez-Carrillo, E. (2014). Hydroxycinnamic acids, sugar composition and antioxidant capacity of arabinoxylans extracted from different maize fiber sources. *Food Hydrocolloids, 35*, 471-475. doi:10.1016/j.foodhyd.2013.07.004

Baldrian, P. (2006). Fungal laccases - occurrence and properties. *Fems Microbiology Reviews, 30*(2), 215-242. doi:10.1111/j.1574-4976.2005.00010.x

Benus, R. F. J., van der Werf, T. S., Welling, G. W., Judd, P. A., Taylor, M. A., Harmsen, H. J. M., & Whelan, K. (2010). Association between Faecalibacterium prausnitzii and dietary fibre in colonic fermentation in healthy human subjects. *British Journal of Nutrition, 104*(5), 693-700. doi:10.1017/s0007114510001030

Broekaert, W. F., Courtin, C. M., Verbeke, K., Van de Wiele, T., Verstraete, W., & Delcour, J. A. (2011). Prebiotic and Other Health-Related Effects of Cereal-Derived Arabinoxylans, Arabinoxylan-Oligosaccharides, and Xylooligosaccharides. *Critical Reviews in Food Science and Nutrition, 51*(2), 178-194. doi:10.1080/10408390903044768

Brown, A. J., Goldsworthy, S. M., Barnes, A. A., Eilert, M. M., Tcheang, L., Daniels, D., . . . Dowell, S. J. (2003). The orphan G protein-coupled receptors GPR41 and GPR43 are activated by propionate and other short chain carboxylic acids. *Journal of Biological Chemistry, 278*(13), 11312-11319. doi:10.1074/jbc.M211609200

Buchanan, C. M., Buchanan, N. L., Debenham, J. S., Gatenholm, P., Jacobsson, M., Shelton, M. C., . . . Wood, M. D. (2003). Preparation and characterization of arabinoxylan esters and arabinoxylan ester/cellulose ester polymer blends. *Carbohydrate Polymers, 52*(4), 345-357. doi:10.1016/s0144-8617(02)00290-4

Canani, R. B., Di Costanzo, M., Leone, L., Pedata, M., Meli, R., & Calignano, A. (2011). Potential beneficial effects of butyrate in intestinal and extrainitestinal diseases. *World Journal of Gastroenterology, 17*(12), 1519-1528. doi:10.3748/wjg.v17.i12.1519

Cani, P. D. (2017). Gut microbiota - at the intersection of everything? *Nature Reviews Gastroenterology & Hepatology, 14*(6), 321-322. doi:10.1038/nrgastro.2017.54

Cantu-Jungles, T. M., Ruthes, A. C., El-Hindawy, M., Moreno, R. B., Zhang, X. W., Cordeiro, L. M. C., . . . Iacomini, M. (2018). In vitro fermentation of Cookeina speciosa glucans stimulates the growth of the butyrogenic Clostridium cluster XIVa in a targeted way. *Carbohydrate Polymers, 183*, 219-229. doi:10.1016/j.carbpol.2017.12.020

Cao, L., Liu, X. Z., Qian, T. X., Sun, G. B., Guo, Y., Chang, F. J., . . . Sun, X. B. (2011). Antitumor and immunomodulatory activity of arabinoxylans: A major constituent of wheat bran. *International Journal of Biological Macromolecules, 48*(1), 160-164. doi:10.1016/j.ijbiomac.2010.10.014

Caporaso, J. G., Kuczynski, J., Stombaugh, J., Bittinger, K., Bushman, F. D., Costello, E. K., . . . Knight, R. (2010). QIIME allows analysis of high-throughput community sequencing data. *Nature Methods, 7*(5), 335-336. doi:10.1038/nmeth.f.303

Carvajal-Millan, E., Guigliarelli, B., Belle, V., Rouau, X., & Micard, V. (2005). Storage stability of laccase induced arabinoxylan gels. *Carbohydrate Polymers, 59*(2), 181-188. doi:10.1016/j.carbpol.2004.09.008

Carvajal-Millan, E., Landillon, V., Morel, M. H., Rouau, X., Doublier, J. L., & Micard, V. (2005). Arabinoxylan gels: Impact of the feruloylation degree on their structure and properties. *Biomacromolecules, 6*(1), 309-317. doi:10.1021/bm049629a

Carvalho-Wells, A. L., Helmolz, K., Nodet, C., Molzer, C., Leonard, C., McKevith, B., . . . Tuohy, K. M. (2010). Determination of the in vivo prebiotic potential of a maize-based whole grain breakfast cereal: a human feeding study. *British Journal of Nutrition, 104*(9), 1353-1356. doi:10.1017/s0007114510002084

Chambers, E. S., Viardot, A., Psichas, A., Morrison, D. J., Murphy, K. G., Zac-Varghese, S. E. K., . . . Frost, G. (2015). Effects of targeted delivery of propionate to the human colon on appetite regulation, body weight maintenance and adiposity in overweight adults. *Gut, 64*(11), 1744-1754. doi:10.1136/gutjnl-2014-307913

Chassard, C., Goumy, V., Leclerc, M., Del'homme, C., & Bernalier-Donadille, A. (2007). Characterization of the xylan-degrading microbial community from human faeces. *Fems Microbiology Ecology, 61*(1), 121-131. doi:10.1111/j.1574-6941.2007.00314.x

Chen, T. T., Long, W. M., Zhang, C. H., Liu, S., Zhao, L. P., & Hamaker, B. R. (2017). Fiber-utilizing capacity varies in Prevotella- versus Bacteroides- dominated gut microbiota. *Scientific Reports, 7*. doi:10.1038/s41598-017-02995-4

Chriett, S., Dabek, A., Wojtala, M., Vidal, H., Balcerczyk, A., & Pirola, L. (2019). Prominent action of butyrate over beta-hydroxybutyrate as histone deacetylase inhibitor, transcriptional modulator and anti-inflammatory molecule. *Scientific Reports, 9*. doi:10.1038/s41598-018-36941-9

Christensen, L., Roager, H. M., Astrup, A., & Hjorth, M. F. (2018). Microbial enterotypes in personalized nutrition and obesity management. *American Journal of Clinical Nutrition, 108*(4), 645-651. doi:10.1093/ajcn.nqy175

Costabile, A., Klinder, A., Fava, F., Napolitano, A., Fogliano, V., Leonard, C., . . . Tuohy, K. M. (2008). Whole-grain wheat breakfast cereal has a prebiotic effect on the human gut microbiota: a double-blind, placebo-controlled, crossover study. *British Journal of Nutrition, 99*(1), 110-120. doi:10.1017/s0007114507793923

Costabile, A., Kolida, S., Klinder, A., Gietl, E., Bauerlein, M., Frohberg, C., . . . Gibson, G. R. (2010). A double-blind, placebo-controlled, cross-over study to establish the bifidogenic effect of a very-long-chain inulin extracted from globe artichoke (Cynara scolymus) in healthy human subjects. *British Journal of Nutrition, 104*(7), 1007-1017. doi:10.1017/s0007114510001571

Courtin, C. M., & Delcour, J. A. (2002). Arabinoxylans and endoxylanases in wheat flour bread-making. *Journal of Cereal Science, 35*(3), 225-243. doi:10.1006/jcrs.2001.0433

Cummings, J. H., Pomare, E. W., Branch, W. J., Naylor, C. P. E., & Macfarlane, G. T. (1987). SHORT CHAIN FATTY-ACIDS IN HUMAN LARGE-INTESTINE, PORTAL, HEPATIC AND VENOUS-BLOOD. *Gut, 28*(10), 1221-1227. doi:10.1136/gut.28.10.1221

Cushing, K., Alvarado, D. M., & Ciorba, M. A. (2015). Butyrate and Mucosal Inflammation: New Scientific Evidence Supports Clinical Observation. *Clin Transl Gastroenterol, 6*, e108. doi:10.1038/ctg.2015.34

Damen, B., Verspreet, J., Pollet, A., Broekaert, W. F., Delcour, J. A., & Courtin, C. M. (2011). Prebiotic effects and intestinal fermentation of cereal arabinoxylans and arabinoxylan oligosaccharides in rats depend strongly on their structural properties and joint presence. *Molecular Nutrition & Food Research, 55*(12), 1862-1874. doi:10.1002/mnfr.201100377

David, L. A., Maurice, C. F., Carmody, R. N., Gootenberg, D. B., Button, J. E., Wolfe, B. E., . . . Turnbaugh, P. J. (2014). Diet rapidly and reproducibly alters the human gut microbiome. *Nature, 505*(7484), 559-+. doi:10.1038/nature12820

De Filippis, F., Vitaglione, P., Cuomo, R., Canani, R. B., & Ercolini, D. (2018). Dietary Interventions to Modulate the Gut Microbiome-How Far Away Are We From Precision Medicine. *Inflammatory Bowel Diseases, 24*(10), 2142-2154. doi:10.1093/ibd/izy080

De Filippo, C., Cavalieri, D., Di Paola, M., Ramazzotti, M., Poullet, J. B., Massart, S., . . . Lionetti, P. (2010). Impact of diet in shaping gut microbiota revealed by a comparative study in children from Europe and rural Africa. *Proceedings of the National Academy of Sciences of the United States of America, 107*(33), 14691-14696. doi:10.1073/pnas.1005963107

De Vadder, F., Kovatcheva-Datchary, P., Goncalves, D., Vinera, J., Zitoun, C., Duchampt, A., . . . Mithieux, G. (2014). Microbiota-Generated Metabolites Promote Metabolic Benefits via Gut-Brain Neural Circuits. *Cell, 156*(1-2), 84-96. doi:10.1016/j.cell.2013.12.016

Doco, T., O'Neill, M. A., & Pellerin, P. (2001). Determination of the neutral and acidic glycosyl-residue compositions of plant polysaccharides by GC-EI-MS analysis of the trimethylsilyl methyl glycoside derivatives. *Carbohydrate Polymers, 46*(3), 249-259. doi:10.1016/s0144-8617(00)00328-3

Dornez, E., Gebruers, K., Delcour, J. A., & Courtin, C. A. (2009). Grain-associated xylanases: occurrence, variability, and implications for cereal processing. *Trends in Food Science & Technology, 20*(11-12), 495-510. doi:10.1016/j.tifs.2009.05.004

Duncan, S. H., Holtrop, G., Lobley, G. E., Calder, A. G., Stewart, C. S., & Flint, H. J. (2004). Contribution of acetate to butyrate formation by human faecal bacteria. *British Journal of Nutrition, 91*(6), 915-923. doi:10.1079/bjn20041150

Duncan, S. H., Russell, W. R., Quartieri, A., Rossi, M., Parkhill, J., Walker, A. W., & Flint, H. J. (2016). Wheat bran promotes enrichment within the human colonic microbiota of butyrate-producing bacteria that release ferulic acid. *Environmental Microbiology, 18*(7), 2214-2225. doi:10.1111/1462-2920.13158

Dynkowska, W. M., Cyran, M. R., & Ceglinska, A. (2015). Soluble and cell wall-bound phenolic acids and ferulic acid dehydrodimers in rye flour and five bread model systems: insight into mechanisms of improved availability. *Journal of the Science of Food and Agriculture, 95*(5), 1103-1115. doi:10.1002/jsfa.7007

Eckburg, P. B., Bik, E. M., Bernstein, C. N., Purdom, E., Dethlefsen, L., Sargent, M., . . . Relman, D. A. (2005). Diversity of the human intestinal microbial flora. *Science, 308*(5728), 1635-1638. doi:10.1126/science.1110591

Everard, A., & Cani, P. D. (2013). Diabetes, obesity and gut microbiota. *Best Practice & Research in Clinical Gastroenterology, 27*(1), 73-83. doi:10.1016/j.bpg.2013.03.007

Fadel, A., Mahmoud, A. M., Ashworth, J. J., Li, W. L., Ng, Y. L., & Plunkett, A. (2018). Health-related effects and improving extractability of cereal arabinoxylans. *International Journal of Biological Macromolecules, 109*, 819-831. doi:10.1016/j.ijbiomac.2017.11.055

Figueroa-Espinoza, M. C., & Rouau, X. (1998). Oxidative cross-linking of pentosans by a fungal laccase and horseradish peroxidase: Mechanism of linkage between feruloylated arabinoxylans. *Cereal Chemistry, 75*(2), 259-265. doi:10.1094/cchem.1998.75.2.259

Flint, H. J., Scott, K. P., Duncan, S. H., Louis, P., & Forano, E. (2012). Microbial degradation of complex carbohydrates in the gut. *Gut Microbes, 3*(4), 289-306. doi:10.4161/gmic.19897

Frederix, S. A., Van Hoeymissen, K. E., Courtin, C. M., & Delcour, J. A. (2004). Water-extractable and water-unextractable arabinoxylans affect gluten agglomeration behavior during wheat flour gluten-starch separation. *Journal of Agricultural and Food Chemistry, 52*(26), 7950-7956. doi:10.1021/jf049041v

Gemen, R., de Vries, J. F., & Slavin, J. L. (2011). Relationship between molecular structure of cereal dietary fiber and health effects: focus on glucose/insulin response and gut health. *Nutrition Reviews, 69*(1), 22-33. doi:10.1111/j.1753-4887.2010.00357.x

Geraylou, Z., Souffreau, C., Rurangwa, E., Maes, G. E., Spanier, K. I., Courtin, C. M., . . . Ollevier, F. (2013). Prebiotic effects of arabinoxylan oligosaccharides on juvenile Siberian sturgeon (Acipenser baerii) with emphasis on the modulation of the gut microbiota using 454 pyrosequencing. *Fems Microbiology Ecology, 86*(2), 357-371. doi:10.1111/1574-6941.12169

Graf, D., Di Cagno, R., Fåk, F., Flint, H. J., Nyman, M., Saarela, M., & Watzl, B. (2015). Contribution of diet to the composition of the human gut microbiota. *Microb Ecol Health Dis, 26*, 26164. doi:10.3402/mehd.v26.26164

Guglielmetti, S., Fracassetti, D., Taverniti, V., Del Bo, C., Vendrame, S., Klimis-Zacas, D., . . . Porrini, M. (2013). Differential Modulation of Human Intestinal Bifidobacterium Populations after Consumption of a Wild Blueberry (Vaccinium angustifolium) Drink. *Journal of Agricultural and Food Chemistry, 61*(34), 8134-8140. doi:10.1021/jf402495k

Hamaker, B. R., & Tuncil, Y. E. (2014). A Perspective on the Complexity of Dietary Fiber Structures and Their Potential Effect on the Gut Microbiota. *Journal of Molecular Biology, 426*(23), 3838-3850. doi:10.1016/j.jmb.2014.07.028

Hand, T. W., Vujkovic-Cvijin, I., Ridaura, V. K., & Belkaid, Y. (2016). Linking the Microbiota, Chronic Disease, and the Immune System. *Trends Endocrinol Metab, 27*(12), 831-843. doi:10.1016/j.tem.2016.08.003

Handbook of Hydrocolloids, 2nd Edition. (2009). *Handbook of Hydrocolloids, 2nd Edition*(173), 1-924. doi:10.1533/9781845695873

Heintz-Buschart, A., & Wilmes, P. (2018). Human Gut Microbiome: Function Matters. *Trends in Microbiology, 26*(7), 563-574. doi:10.1016/j.tim.2017.11.002

Hjorth, M. F., Blaeel, T., Bendtsen, L. Q., Lorenzen, J. K., Holm, J. B., Kiilerich, P., . . . Astrup, A. (2019). Prevotella-to-Bacteroides ratio predicts body weight and fat loss success on 24-week diets varying in macronutrient composition and dietary fiber: results from a post-hoc analysis. *International Journal of Obesity, 43*(1), 149-157. doi:10.1038/s41366-018-0093-2

Hjorth, M. F., Roager, H. M., Larsen, T. M., Poulsen, S. K., Licht, T. R., Bahl, M. I., . . . Astrup, A. (2018). Pre-treatment microbial Prevotella-to-Bacteroides ratio, determines body fat loss success during a 6-month randomized controlled diet intervention. *International Journal of Obesity, 42*(3), 580-583. doi:10.1038/ijo.2017.220

Iiyama, K., Lam, T. B. T., & Stone, B. A. (1994). COVALENT CROSS-LINKS IN THE CELL-WALL. *Plant Physiology, 104*(2), 315-320. doi:10.1104/pp.104.2.315

Iqbal, M. S., Akbar, J., Hussain, M. A., Saghir, S., & Sher, M. (2011). Evaluation of hot-water extracted arabinoxylans from ispaghula seeds as drug carriers. *Carbohydrate Polymers, 83*(3), 1218-1225. doi:10.1016/j.carbpol.2010.09.024

Iravani, S., Fitchett, C. S., & Georget, D. M. R. (2011). Physical characterization of arabinoxylan powder and its hydrogel containing a methyl xanthine. *Carbohydrate Polymers, 85*(1), 201-207. doi:10.1016/j.carbpol.2011.02.017

Islam, K., Fukiya, S., Hagio, M., Fujii, N., Ishizuka, S., Ooka, T., . . . Yokota, A. (2011). Bile Acid Is a Host Factor That Regulates the Composition of the Cecal Microbiota in Rats. *Gastroenterology, 141*(5), 1773-1781. doi:10.1053/j.gastro.2011.07.046

Izydorczyk, M. S., & Biliaderis, C. G. (1994). STUDIES ON THE STRUCTURE OF WHEAT-ENDOSPERM ARABINOXYLANS. *Carbohydrate Polymers, 24*(1), 61-71. doi:10.1016/0144-8617(94)90118-x

Izydorczyk, M. S., & Biliaderis, C. G. (1995). Cereal arabinoxylans: Advances in structure and physicochemical properties. *Carbohydrate Polymers, 28*(1), 33-48. doi:10.1016/0144-8617(95)00077-1

Izydorczyk, M. S., & Dexter, J. E. (2008). Barley beta-glucans and arabinoxylans: Molecular structure, physicochemical properties, and uses in food products-a Review. *Food Research International, 41*(9), 850-868. doi:10.1016/j.foodres.2008.04.001

Jalanka, J., Major, G., Murray, K., Singh, G., Nowak, A., Kurtz, C., . . . Spiller, R. (2019). The Effect of Psyllium Husk on Intestinal Microbiota in Constipated Patients and Healthy Controls. *Int J Mol Sci, 20*(2). doi:10.3390/ijms20020433

Jaskari, J., Kontula, P., Siitonen, A., Jousimies-Somer, H., Mattila-Sandholm, T., & Poutanen, K. (1998). Oat beta-glucan and xylan hydrolysates as selective substrates for Bifidobacterium and Lactobacillus strains. *Applied Microbiology and Biotechnology, 49*(2), 175-181. doi:10.1007/s002530051155

Kale, M. S., Hamaker, B. R., & Campanella, O. H. (2013). Alkaline extraction conditions determine gelling properties of corn bran arabinoxylans. *Food Hydrocolloids, 31*(1), 121-126. doi:10.1016/j.foodhyd.2012.09.011

Kaur, A., Rose, D. J., Rumpagaporn, P., Patterson, J. A., & Hamaker, B. R. (2011). In Vitro Batch Fecal Fermentation Comparison of Gas and Short-Chain Fatty Acid Production Using "Slowly Fermentable" Dietary Fibers. *Journal of Food Science, 76*(5), H137-H142. doi:10.1111/j.1750-3841.2011.02172.x

Koh, A., De Vadder, F., Kovatcheva-Datchary, P., & Backhed, F. (2016). From Dietary Fiber to Host Physiology: Short-Chain Fatty Acids as Key Bacterial Metabolites. *Cell, 165*(6), 1332-1345. doi:10.1016/j.cell.2016.05.041

Koropatkin, N. M., Cameron, E. A., & Martens, E. C. (2012). How glycan metabolism shapes the human gut microbiota. *Nature Reviews Microbiology, 10*(5), 323-335. doi:10.1038/nrmicro2746

Larsbrink, J., Rogers, T. E., Hemsworth, G. R., McKee, L. S., Tauzin, A. S., Spadiut, O., . . . Brumer, H. (2014). A discrete genetic locus confers xyloglucan metabolism in select human gut Bacteroidetes. *Nature, 506*(7489), 498-+. doi:10.1038/nature12907

Lebet, V., Arrigoni, E., & Amado, R. (1998). Digestion procedure using mammalian enzymes to obtain substrates for in vitro fermentation studies. *Food Science and Technology-Lebensmittel-Wissenschaft & Technologie, 31*(6), 509-515.

Leitch, E. C. M., Walker, A. W., Duncan, S. H., Holtrop, G., & Flint, H. J. (2007). Selective colonization of insoluble substrates by human faecal bacteria. *Environmental Microbiology, 9*(3), 667-679. doi:10.1111/j.1462-2920.2006.01186.x

Li, J., Hou, Q. C., Zhang, J. C., Xu, H. Y., Sun, Z. H., Menghe, B., & Zhang, H. P. (2017). Carbohydrate Staple Food Modulates Gut Microbiota of Mongolians in China. *Frontiers in Microbiology, 8*. doi:10.3389/fmicb.2017.00484

Li, Y., & Yang, C. (2016). Synthesis and properties of feruloyl corn bran arabinoxylan esters. *International Journal of Cosmetic Science, 38*(3), 238-245. doi:10.1111/ics.12281

Louis, P., & Flint, H. J. (2009). Diversity, metabolism and microbial ecology of butyrate-producing bacteria from the human large intestine. *Fems Microbiology Letters, 294*(1), 1-8. doi:10.1111/j.1574-6968.2009.01514.x

Louis, P., Hold, G. L., & Flint, H. J. (2014). The gut microbiota, bacterial metabolites and colorectal cancer. *Nature Reviews Microbiology, 12*(10), 661-672. doi:10.1038/nrmicro3344

Makki, K., Deehan, E. C., Walter, J., & Backhed, F. (2018). The Impact of Dietary Fiber on Gut Microbiota in Host Health and Disease. *Cell Host & Microbe, 23*(6), 705-715. doi:10.1016/j.chom.2018.05.012

Marquez-Escalante, J. A., Carvajal-Millan, E., Yadav, M. P., Kale, M., Rascon-Chu, A., Gardea, A. A., . . . Faulds, C. B. (2018). Rheology and microstructure of gels based on wheat arabinoxylans enzymatically modified in arabinose to xylose ratio. *Journal of the Science of Food and Agriculture, 98*(3), 914-922. doi:10.1002/jsfa.8537

Martens, E. C., Kelly, A. G., Tauzin, A. S., & Brumer, H. (2014). The Devil Lies in the Details: How Variations in Polysaccharide Fine-Structure Impact the Physiology and Evolution of Gut Microbes. *Journal of Molecular Biology, 426*(23), 3851-3865. doi:10.1016/j.jmb.2014.06.022

Martens, E. C., Lowe, E. C., Chiang, H., Pudlo, N. A., Wu, M., McNulty, N. P., . . . Gordon, J. I. (2011). Recognition and Degradation of Plant Cell Wall Polysaccharides by Two Human Gut Symbionts. *Plos Biology, 9*(12). doi:10.1371/journal.pbio.1001221

Martinez, I., Kim, J., Duffy, P. R., Schlegel, V. L., & Walter, J. (2010). Resistant Starches Types 2 and 4 Have Differential Effects on the Composition of the Fecal Microbiota in Human Subjects. *Plos One, 5*(11). doi:10.1371/journal.pone.0015046

Martinez, I., Lattimer, J. M., Hubach, K. L., Case, J. A., Yang, J. Y., Weber, C. G., . . . Walter, J. (2013). Gut microbiome composition is linked to whole grain-induced immunological improvements. *Isme Journal, 7*(2), 269-280. doi:10.1038/ismej.2012.104

Martinez-Lopez, A. L., Carvajal-Millan, E., Micard, V., Rascon-Chu, A., Brown-Bojorquez, F., Sotelo-Cruz, N., . . . Lizardi-Mendoza, J. (2016). In vitro degradation of covalently cross-linked arabinoxylan hydrogels by bifidobacteria. *Carbohydrate Polymers, 144*, 76-82. doi:10.1016/j.carbpol.2016.02.031

Martinez-Lopez, A. L., Carvajal-Millan, E., Rascon-Chu, A., Marquez-Escalante, J., & Martinez-Robinson, K. (2013). Gels of ferulated arabinoxylans extracted from nixtamalized and non-nixtamalized maize bran: rheological and structural characteristics. *Cyta-Journal of Food, 11*, 22-28. doi:10.1080/19476337.2013.781679

McDonald, D., Price, M. N., Goodrich, J., Nawrocki, E. P., DeSantis, T. Z., Probst, A., . . . Hugenholtz, P. (2012). An improved Greengenes taxonomy with explicit ranks for ecological and evolutionary analyses of bacteria and archaea. *Isme Journal, 6*(3), 610-618. doi:10.1038/ismej.2011.139

Mendez-Encinas, M. A., Carvajal-Millan, E., Rascon-Chu, A., Astiazaran-Garcia, H. F., & Valencia-Rivera, D. E. (2018). Ferulated Arabinoxylans and Their Gels: Functional Properties and Potential Application as Antioxidant and Anticancer Agent. *Oxidative Medicine and Cellular Longevity*. doi:10.1155/2018/2314759

Mendis, M., Leclerc, E., & Simsek, S. (2016). Arabinoxylans, gut microbiota and immunity. *Carbohydrate Polymers, 139*, 159-166. doi:10.1016/j.carbpol.2015.11.068

Meyvis, T. K. L., De Smedt, S. C., Demeester, J., & Hennink, W. E. (2000). Influence of the degradation mechanism of hydrogels on their elastic and swelling properties during degradation. *Macromolecules, 33*(13), 4717-4725. doi:10.1021/ma992131u

Michlmayr, H., Hell, J., Lorenz, C., Bohmdorfer, S., Rosenau, T., & Kneifel, W. (2013). Arabinoxylan Oligosaccharide Hydrolysis by Family 43 and 51 Glycosidases from Lactobacillus brevis DSM 20054. *Applied and Environmental Microbiology, 79*(21), 6747-6754. doi:10.1128/aem.02130-13

Morales-Burgos, A. M., Carvajal-Millan, E., Lopez-Franco, Y. L., Rascon-Chu, A., Lizardi-Mendoza, J., Sotelo-Cruz, N., . . . Pedroza-Montero, M. (2017). Syneresis in Gels of Highly Ferulated Arabinoxylans: Characterization of Covalent Cross-Linking, Rheology, and Microstructure. *Polymers, 9*(5). doi:10.3390/polym9050164

Ndeh, D., & Gilbert, H. J. (2018). Biochemistry of complex glycan depolymerisation by the human gut microbiota. *Fems Microbiology Reviews, 42*(2), 146-164. doi:10.1093/femsre/fuy002

Neacsu, M., McMonagle, J., Fletcher, R. J., Scobbie, L., Duncan, G. J., Cantlay, L., . . . Russell, W. R. (2013). Bound phytophenols from ready-to-eat cereals: Comparison with other plant-based foods. *Food Chemistry, 141*(3), 2880-2886. doi:10.1016/j.foodchem.2013.05.023

Neyrinck, A. M., Possemiers, S., Druart, C., van de Wiele, T., De Backer, F., Cani, P. D., . . . Delzenne, N. M. (2011). Prebiotic Effects of Wheat Arabinoxylan Related to the Increase in Bifidobacteria, Roseburia and Bacteroides/Prevotella in Diet-Induced Obese Mice. *Plos One, 6*(6). doi:10.1371/journal.pone.0020944

Neyrinck, A. M., Possemiers, S., Verstraete, W., De Backer, F., Cani, P. D., & Delzenne, N. M. (2012). Dietary modulation of clostridial cluster XIVa gut bacteria (Roseburia spp.) by chitin-glucan fiber improves host metabolic alterations induced by high-fat diet in mice. *Journal of Nutritional Biochemistry, 23*(1), 51-59. doi:10.1016/j.jnutbio.2010.10.008

Nishinari, K., Zhang, H., & Ikeda, S. (2000). Hydrocolloid gels of polysaccharides and proteins. *Current Opinion in Colloid & Interface Science, 5*(3-4), 195-201. doi:10.1016/s1359-0294(00)00053-4

Ordaz-Ortiz, J. J., Devaux, M. F., & Saulnier, L. (2005). Classification of wheat varieties based on structural features of arabinoxylans as revealed by endoxylanase treatment of flour and grain. *Journal of Agricultural and Food Chemistry, 53*(21), 8349-8356. doi:10.1021/jf050755v

Ou, J. H., Carbonero, F., Zoetendal, E. G., DeLany, J. P., Wang, M., Newton, K., . . . O'Keefe, S. J. D. (2013). Diet, microbiota, and microbial metabolites in colon cancer risk in rural Africans and African Americans. *American Journal of Clinical Nutrition, 98*(1), 111-120. doi:10.3945/ajcn.112.056689

Patterson, E., Ryan, P. M., Cryan, J. F., Dinan, T. G., Ross, R. P., Fitzgerald, G. F., & Stanton, C. (2016). Gut microbiota, obesity and diabetes. *Postgraduate Medical Journal, 92*(1087), 286-300. doi:10.1136/postgradmedj-2015-133285

Peng, H., Wang, N., Hu, Z. R., Yu, Z. P., Liu, Y. H., Zhang, J. S., & Ruan, R. (2012). Physicochemical characterization of hemicelluloses from bamboo (Phyllostachys pubescens Mazel) stem. *Industrial Crops and Products, 37*(1), 41-50. doi:10.1016/j.indcrop.2011.11.031

Pettolino, F. A., Walsh, C., Fincher, G. B., & Bacic, A. (2012). Determining the polysaccharide composition of plant cell walls. *Nature Protocols, 7*(9), 1590-1607. doi:10.1038/nprot.2012.081

Pollet, A., Van Craeyveld, V., Van de Wiele, T., Verstraete, W., Delcour, J. A., & Courtin, C. M. (2012). In Vitro Fermentation of Arabinoxylan Oligosaccharides and Low Molecular Mass Arabinoxylans with Different Structural Properties from Wheat (Triticum aestivum L.) Bran and Psyllium (Plantago ovata Forsk) Seed Husk. *Journal of Agricultural and Food Chemistry, 60*(4), 946-954. doi:10.1021/jf203820j

Queipo-Ortuno, M. I., Boto-Ordonez, M., Murri, M., Gomez-Zumaquero, J. M., Clemente-Postigo, M., Estruch, R., . . . Tinahones, F. J. (2012). Influence of red wine polyphenols and ethanol on the gut microbiota ecology and biochemical biomarkers. *American Journal of Clinical Nutrition, 95*(6), 1323-1334. doi:10.3945/ajcn.111.027847

Reynolds, A., Mann, J., Cummings, J., Winter, N., Mete, E., & Te Morenga, L. (2019). Carbohydrate quality and human health: a series of systematic reviews and meta-analyses. *Lancet*.

Riviere, A., Gagnon, M., Weckx, S., Roy, D., & De Vuyst, L. (2015). Mutual Cross-Feeding Interactions between Bifidobacterium longum subsp longum NCC2705 and Eubacterium rectale ATCC 33656 Explain the Bifidogenic and Butyrogenic Effects of Arabinoxylan Oligosaccharides. *Applied and Environmental Microbiology, 81*(22), 7767-7781. doi:10.1128/aem.02089-15

Riviere, A., Selak, M., Lantin, D., Leroy, F., & De Vuyst, L. (2016). Bifidobacteria and Butyrate-Producing Colon Bacteria: Importance and Strategies for Their Stimulation in the Human Gut. *Frontiers in Microbiology, 7*. doi:10.3389/fmicb.2016.00979

Roager, H. M., Licht, T. R., Poulsen, S. K., Larsen, T. M., & Bahl, M. I. (2014). Microbial Enterotypes, Inferred by the Prevotella-to-Bacteroides Ratio, Remained Stable during a 6-Month Randomized Controlled Diet Intervention with the New Nordic Diet. *Applied and Environmental Microbiology, 80*(3), 1142-1149. doi:10.1128/aem.03549-13

Rose, D. J., Demeo, M. T., Keshavarzian, A., & Hamaker, B. R. (2007). Influence of dietary fiber on inflammatory bowel disease and colon cancer: Importance of fermentation pattern. *Nutrition Reviews, 65*(2), 51-62. doi:10.1301/nr.2007.feb.51-62

Rose, D. J., Patterson, J. A., & Hamaker, B. R. (2010). Structural Differences among Alkali-Soluble Arabinoxylans from Maize (Zea mays), Rice (Oryza sativa), and Wheat (Triticum aestivum) Brans Influence Human Fecal Fermentation Profiles. *Journal of Agricultural and Food Chemistry, 58*(1), 493-499. doi:10.1021/jf9020416

Rossmurphy, S. B., & Shatwell, K. P. (1993). POLYSACCHARIDE STRONG AND WEAK GELS. *Biorheology, 30*(3-4), 217-227.

Rowland, I., Gibson, G., Heinken, A., Scott, K., Swann, J., Thiele, I., & Tuohy, K. (2018). Gut microbiota functions: metabolism of nutrients and other food components. *European Journal of Nutrition, 57*(1), 1-24. doi:10.1007/s00394-017-1445-8

Rumpagaporn, P., Reuhs, B. L., Kaur, A., Patterson, J. A., Keshavarzian, A., & Hamaker, B. R. (2015). Structural features of soluble cereal arabinoxylan fibers associated with a slow rate of in vitro fermentation by human fecal microbiota. *Carbohydrate Polymers, 130*, 191-197. doi:10.1016/j.carbpol.2015.04.041

Sanchez, J. I., Marzorati, M., Grootaert, C., Baran, M., Van Craeyveld, V., Courtin, C. M., . . . Van de Wiele, T. (2009). Arabinoxylan-oligosaccharides (AXOS) affect the protein/carbohydrate fermentation balance and microbial population dynamics of the Simulator of Human Intestinal Microbial Ecosystem. *Microbial Biotechnology, 2*(1), 101-113. doi:10.1111/j.1751-7915.2008.00064.x

Saulnier, L., Marot, C., Chanliaud, E., & Thibault, J. F. (1995). CELL-WALL POLYSACCHARIDE INTERACTIONS IN MAIZE BRAN. *Carbohydrate Polymers, 26*(4), 279-287. doi:10.1016/0144-8617(95)00020-8

Saulnier, L., & Thibault, J. F. (1999). Ferulic acid and diferulic acids as components of sugar-beet pectins and maize bran heteroxylans. *Journal of the Science of Food and Agriculture, 79*(3), 396-402.

Saulnier, L., Vigouroux, J., & Thibault, J. F. (1995). ISOLATION AND PARTIAL CHARACTERIZATION OF FERULOYLATED OLIGOSACCHARIDES FROM MAIZE BRAN. *Carbohydrate Research, 272*(2), 241-253. doi:10.1016/0008-6215(95)00053-v

Schooneveld-Bergmans, M. E. F., Beldman, G., & Voragen, A. G. J. (1999). Structural features of (glucurono)arabinoxylans extracted from wheat bran by barium hydroxide. *Journal of Cereal Science, 29*(1), 63-75. doi:10.1006/jcrs.1998.0222

Sharma, V. K., Vasudeva, R., & Howden, C. W. (2000). Changes in colorectal cancer over a 15-year period in a single United States city. *American Journal of Gastroenterology, 95*(12), 3615-3619.

Sharon, G., Garg, N., Debelius, J., Knight, R., Dorrestein, P. C., & Mazmanian, S. K. (2014). Specialized Metabolites from the Microbiome in Health and Disease. *Cell Metabolism, 20*(5), 719-730. doi:10.1016/j.cmet.2014.10.016

Sheridan, P. O., Martin, J. C., Lawley, T. D., Browne, H. P., Harris, H. M. B., Bernalier-Donadille, A., . . . Flint, H. J. (2016). Polysaccharide utilization loci and nutritional specialization in a dominant group of butyrate-producing human colonic Firmicutes. *Microbial Genomics, 2*(2). doi:10.1099/mgen.0.000043

Shreiner, A. B., Kao, J. Y., & Young, V. B. (2015). The gut microbiome in health and in disease. *Current Opinion in Gastroenterology, 31*(1), 69-75. doi:10.1097/mog.0000000000000139

Simren, M., Barbara, G., Flint, H. J., Spiegel, B. M. R., Spiller, R. C., Vanner, S., . . . Zoetendal, E. G. (2013). Intestinal microbiota in functional bowel disorders: a Rome foundation report. *Gut, 62*(1), 159-176. doi:10.1136/gutjnl-2012-302167

Simsek, S., & Ohm, J. B. (2009). Structural changes of arabinoxylans in refrigerated dough. *Carbohydrate Polymers, 77*(1), 87-94. doi:10.1016/j.carbpol.2008.12.012

Singh, N. K., & Lee, D. S. (2014). In situ gelling pH- and temperature-sensitive biodegradable block copolymer hydrogels for drug delivery. *Journal of Controlled Release, 193*, 214-227. doi:10.1016/j.jconrel.2014.04.056

Skendi, A., Biliaderis, C. G., Izydorczyk, M. S., Zervou, M., & Zoumpoulakis, P. (2011). Structural variation and rheological properties of water-extractable arabinoxylans from six Greek wheat cultivars. *Food Chemistry, 126*(2), 526-536. doi:10.1016/j.foodchem.2010.11.038

Slavin, J. (2013). Fiber and Prebiotics: Mechanisms and Health Benefits. *Nutrients, 5*(4), 1417-1435. doi:10.3390/nu5041417

Snelders, J., Dornez, E., Delcour, J. A., & Courtin, C. M. (2013). Ferulic Acid Content and Appearance Determine the Antioxidant Capacity of Arabinoxylanoligosaccharides. *Journal of Agricultural and Food Chemistry, 61*(42), 10173-10182. doi:10.1021/jf403160x

Snelders, J., Olaerts, H., Dornez, E., Van de Wiele, T., Aura, A. M., Vanhaecke, L., . . . Courtin, C. M. (2014). Structural features and feruloylation modulate the fermentability and evolution of antioxidant properties of arabinoxylanoligosaccharides during in vitro fermentation by human gut derived microbiota. *Journal of Functional Foods, 10*, 1-12. doi:10.1016/j.jff.2014.05.011

Sonnenburg, E. D., & Sonnenburg, J. L. (2014). Starving our Microbial Self: The Deleterious Consequences of a Diet Deficient in Microbiota-Accessible Carbohydrates. *Cell Metabolism, 20*(5), 779-786. doi:10.1016/j.cmet.2014.07.003

Sonnenburg, E. D., Zheng, H. J., Joglekar, P., Higginbottom, S. K., Firbank, S. J., Bolam, D. N., & Sonnenburg, J. L. (2010). Specificity of Polysaccharide Use in Intestinal Bacteroides Species Determines Diet-Induced Microbiota Alterations. *Cell, 141*(7), 1241-U1256. doi:10.1016/j.cell.2010.05.005

Sonnenburg, J. L., & Backhed, F. (2016). Diet-microbiota interactions as moderators of human metabolism. *Nature, 535*(7610), 56-64. doi:10.1038/nature18846

Tazoe, H., Otomo, Y., Kaji, I., Tanaka, R., Karaki, S. I., & Kuwahara, A. (2008). ROLES OF SHORT-CHAIN FATTY ACIDS RECEPTORS, GPR41 AND GPR43 ON COLONIC FUNCTIONS. *Journal of Physiology and Pharmacology, 59*, 251-262.

Tuncil, Y. E., Thakkar, R. D., Arioglu-Tuncil, S., Hamaker, B. R., & Lindemann, S. R. (2018). Fecal Microbiota Responses to Bran Particles Are Specific to Cereal Type and In Vitro Digestion Methods That Mimic Upper Gastrointestinal Tract Passage. *Journal of Agricultural and Food Chemistry, 66*(47), 12580-12593. doi:10.1021/acs.jafc.8b03469

Ukhanova, M., Wang, X. Y., Baer, D. J., Novotny, J. A., Fredborg, M., & Mai, V. (2014). Effects of almond and pistachio consumption on gut microbiota composition in a randomised cross-over human feeding study. *British Journal of Nutrition, 111*(12), 2146-2152. doi:10.1017/s0007114514000385

Van Craeyveld, V., Swennen, K., Dornez, E., Van de Wiele, T., Marzorati, M., Verstraete, W., . . . Courtin, C. M. (2008). Structurally Different Wheat-Derived Arabinoxylooligosaccharides Have Different Prebiotic and Fermentation Properties in Rats. *Journal of Nutrition, 138*(12), 2348-2355. doi:10.3945/jn.108.094367

Van den Abbeele, P., Belzer, C., Goossens, M., Kleerebezem, M., De Vos, W. M., Thas, O., . . . Van de Wiele, T. (2013). Butyrate-producing Clostridium cluster XIVa species specifically colonize mucins in an in vitro gut model. *Isme Journal, 7*(5), 949-961. doi:10.1038/ismej.2012.158

Van den Abbeele, P., Gerard, P., Rabot, S., Bruneau, A., El Aidy, S., Derrien, M., . . . Possemiers, S. (2011). Arabinoxylans and inulin differentially modulate the mucosal and

luminal gut microbiota and mucin-degradation in humanized rats. *Environmental Microbiology, 13*(10), 2667-2680. doi:10.1111/j.1462-2920.2011.02533.x

Van Den Broek, L. A. M., & Voragen, A. G. J. (2008). Bifidobacterium glycoside hydrolases and (potential) prebiotics. *Innovative Food Science & Emerging Technologies, 9*(4), 401-407. doi:10.1016/j.ifset.2007.12.006

Vansteenkiste, E., Babot, C., Rouau, X., & Micard, V. (2004). Oxidative gelation of feruloylated arabinoxylan as affected by protein. Influence on protein enzymatic hydrolysis. *Food Hydrocolloids, 18*(4), 557-564. doi:10.1016/j.foodhyd.2003.09.004

Vardakou, M., Palop, C. N., Christakopoulos, P., Faulds, C. B., Gasson, M. A., & Narbad, A. (2008). Evaluation of the prebiotic properties of wheat arabinoxylan fractions and induction of hydrolase activity in gut microflora. *International Journal of Food Microbiology, 123*(1-2), 166-170. doi:10.1016/j.ijfoodmicro.2007.11.007

Velasquez-Manoff, M. (2015). The Peacekeepers. *Nature, 518*(7540), S3-+. doi:10.1038/518S3a

Vendrame, S., Guglielmetti, S., Riso, P., Arioli, S., Klimis-Zacas, D., & Porrini, M. (2011). Six-Week Consumption of a Wild Blueberry Powder Drink Increases Bifidobacteria in the Human Gut. *Journal of Agricultural and Food Chemistry, 59*(24), 12815-12820. doi:10.1021/jf2028686

Vieira-Silva, S., Falony, G., Darzi, Y., Lima-Mendez, G., Yunta, R. G., Okuda, S., . . . Raes, J. (2016). Species-function relationships shape ecological properties of the human gut microbiome. *Nature Microbiology, 1*(8). doi:10.1038/nmicrobiol.2016.88

Waitzberg, D. L., Pereira, C. C. A., Logullo, L., Jacintho, T. M., Almeida, D., da Silva, M. D. T., & Torrinhas, R. (2012). Microbiota benefits after inulin and partially hydrolized guar gum supplementation - a randomized clinical trial in constipated women. *Nutricion Hospitalaria, 27*(1), 123-129. doi:10.3305/nh.2012.27.1.5445

Walker, A. W., Ince, J., Duncan, S. H., Webster, L. M., Holtrop, G., Ze, X. L., . . . Flint, H. J. (2011). Dominant and diet-responsive groups of bacteria within the human colonic microbiota. *Isme Journal, 5*(2), 220-230. doi:10.1038/ismej.2010.118

Whistler, R., & BeMiller, J. (2008). Carbohydrate chemistry for food scientists. *Food Australia, 60*(4), 146-146.

Wu, F. F., Guo, X. F., Zhang, J. C., Zhang, M., Ou, Z. H., & Peng, Y. Z. (2017). Phascolarctobacterium faecium abundant colonization in human gastrointestinal tract. *Experimental and Therapeutic Medicine, 14*(4), 3122-3126. doi:10.3892/etm.2017.4878

Wu, G. D., Chen, J., Hoffmann, C., Bittinger, K., Chen, Y. Y., Keilbaugh, S. A., . . . Lewis, J. D. (2011). Linking Long-Term Dietary Patterns with Gut Microbial Enterotypes. *Science, 334*(6052), 105-108. doi:10.1126/science.1208344

Yatsunenko, T., Rey, F. E., Manary, M. J., Trehan, I., Dominguez-Bello, M. G., Contreras, M., . . . Gordon, J. I. (2012). Human gut microbiome viewed across age and geography. *Nature, 486*(7402), 222-+. doi:10.1038/nature11053

Zeng, H. Y., Xue, Y. M., Peng, T. T., & Shao, W. L. (2007). Properties of xylanolytic enzyme system in bifidobacteria and their effects on the utilization of xylooligosaccharides. *Food Chemistry, 101*(3), 1172-1177. doi:10.1016/j.foodchem.2006.03.019

Zhang, C. H., Zhang, M. H., Pang, X. Y., Zhao, Y. F., Wang, L. H., & Zhao, L. P. (2012). Structural resilience of the gut microbiota in adult mice under high-fat dietary perturbations. *Isme Journal, 6*(10), 1848-1857. doi:10.1038/ismej.2012.27

Zhang, Z. X., Smith, C., & Li, W. L. (2014). Extraction and modification technology of arabinoxylans from cereal by-products: A critical review. *Food Research International, 65*, 423-436. doi:10.1016/j.foodres.2014.05.068

Zhao, L. P., Zhang, F., Ding, X. Y., Wu, G. J., Lam, Y. Y., Wang, X. J., . . . Zhang, C. H. (2018). Gut bacteria selectively promoted by dietary fibers alleviate type 2 diabetes. *Science, 359*(6380), 1151-+. doi:10.1126/science.aao5774

Zu, Y. G., Zhang, Y., Zhao, X. H., Shan, C., Zu, S. C., Wang, K. L., . . . Ge, Y. L. (2012). Preparation and characterization of chitosan-polyvinyl alcohol blend hydrogels for the controlled release of nano-insulin. *International Journal of Biological Macromolecules, 50*(1), 82-87. doi:10.1016/j.ijbiomac.2011.10.006

PUBLICATIONS

Book Chapters

1. **Zhang, X. *et al.*** Food safety control technologies of 3-MCPD fatty acid esters and derivatives in the processing of edible oils. In Yu, L.; Wang, S.; & Sun, B. (eds) *Food Safety Chemistry*. Shanghai Jiao Tong University Press. Shanghai 200030, China.
2. Jala, R.C.R.; **Zhang, X.**; Huang, H.; Gao. B.; Yu, L; Xu, X. Chemistry and safety of 3-MCPD fatty acid esters in Yu, L.; Wang, S.; & Sun, B. (eds) *Food Safety Chemistry-Toxicant Occurrence, Analysis and Mitigation.* Taylor & Francis Group, Inc. Boca Raton, FL 33487, USA.

Refereed Journal Articles

1. **Zhang, X.,** Chen, T., Lim, J., Gu, F., Fang, F., Cheng, L., Campanella, O. H., Hamaker, R. B. Acid Gelation of Soluble Laccase-crosslinked Corn Bran Arabinoxylan and Possible Gel Formation mechanism. ***Food Hydrocoll.*** **2019**, 92: 1-9.
2. Lim, J., **Zhang, X.,** Ferruzzi., M. G., Hamaker, R. B. Starch digested product analysis by HPAEC reveals structural specificity of flavonoids in the inhibition of mammalian α-amylase and α-glucosidases. ***Food Chem.*** **2019,** doi: 10.1016/j.foodchem.2019.02.117
3. Liu, J., Johnson, R., Dillon, S., Kroehl, M., Frank, D. N., Tuncil, Y. E., **Zhang, X.,** Ir, D., Roberson, C. E., Seifert, S., Higgins, J., Hamaker, B., Wilson, C. C., Erlandson, K. M., Among Older Adults, Age-related Changes in the Stool Microbiome Differ by HIV-1 Serostatus. ***EBioMedicine. 2019.***
4. Liu, S., Xiao, Y., Shen, M., **Zhang, X.,** Wang, W., Xie, J. Effect of Sodium Carbonate on the Gelation, Rheology, Texture and Structural Properties of Maize Starch-*Mesona chinensis* Polysaccharide Gel. ***Food Hydrocoll. 2019*****,** 87: 943-951
5. Hunag, L., Shen, M., **Zhang, X.,** Jiang, L., Song, Q., Xie, J. Effect of High-pressure Microfluidization Treatment on the Physicochemical Properties and Antioxidant Activities of Polysaccharide from *Mesona chinesis* Benth. ***Carbohydr Polym. 2018****,* 191-199.
6. Cantu-Jungles, T. M., Ruthes, A. C., El-Hindawy, M., Moreno, R. B., **Zhang, X.,** Cordeiro, L. M. C., Hamaker, R. B., Iacomini, M., *In vitro* Fermentation of *Cookeina speciosa* Glucans Stimulates the Growth of the Butyrogenic *Clostridium* Cluster XIVa in a Target Way. ***Carbohydr Polym. 2018****,* 183: 219-229.
7. Cantu-Jungles, T. M., do Nascimento G. E., **Zhang, X.,** Iacomini, M., Cordeiro, L. M. C., Hamaker, R. B. Soluble Xyloglucan Generates Bigger Bacterial Community Shifts than Pectic Polymers during *in vitro* Fecal Fermentation. ***Carbohydr Polym. 2019****,* 206: 389-395.
8. Zhang, Z.; Gao, B.; **Zhang, X.;** Jiang, Y.; Xu, X.; Yu, L. Formation of 3-Monochloro-1,2-propanediol (3-MCPD) Di- and Monoesters from Tristearoylglycerol (TSG) and Potential Catalytic Effect of Fe^{2+} and Fe^{3+}. ***J. Agric. Food Chem.*** **2015,** 62: 3783-3790
9. Niu, Y.; Shang, P.; Chen, L.; Zhang, H.; Gong, L.; **Zhang, X.;** Wu, W.; Xu, Y.; Wang, Q.; Yu, L. Characterization of a Novel Alkali-Soluble Heteropolysaccharide from Tetraploid

Gynostemma pentaphyllum Makino and Its Potential Anti-inflammatory and Antioxidant Properties. ***J. Agric. Food Chem.*** **2014,** 62: 3783-3790

10. **Zhang, X.**; Gao, B.; Qin, F.; Shi, H.; Jiang, Y.; Xu, X.; Yu, L. Free Radical Mediated Formation of 3-Monochloropropanediol (3-MCPD) Fatty Acid Diesters. ***J. Agric. Food Chem.*** **2013**, 61: 2548-2555.
11. **Zhang, X.**; Shang, P.; Qin, F.; Zhou, Q.; Gao, B.; Huang, H.; Yang, H.; Shi, H.; Yu, L.; Chemical composition and antioxidative and anti-inflammatory properties of ten commercial mung bean samples. ***LWT-Food Sci. Technol.*** **2013**, 54: 171-178.
12. Zhou, Q.; Lu, W.; Niu, Y.; Liu, J.; **Zhang, X.;** Gao, B.; Akoh, C. C.; Shi, H.; Yu, L.; Identification and Quantification of Phytochemical Composition and Anti-inflammatory, Cellular Antioxidant, and Radical Scavenging Activities of 12 Plantago Species. ***J. Agric. Food Chem.*** **2013**, 61: 6693-6702.
13. Yang, F.; Shi, H.; **Zhang, X.;** Yang, H.; Zhou, Q.; Yu, L. Two new saponins from tetraploid jiaogulan (Gynostemma pentaphyllum), and their anti-inflammatory and α-glucosidase inhibitory activities. ***Food Chem.*** **2013**, 141: 3606-3613.
14. Niu, Y.; Gao, B.; Slavin, M.; **Zhang, X.;** Yang, F.; Bao, J.; Shi, H.; Xie, Z.; Yu, L. Phytochemical compositions, and antioxidant and anti-inflammatory properties of twenty-two red rice samples grown in Zhejiang. ***LWT-Food Sci. Technol.*** **2013**, 54: 521-527.
15. Yang, F.; Shi, H.; **Zhang, X.;** Yu, L. Two Novel Anti-inflammatory 21-Nordammarane Saponins from Tetraploid Jiaogulan (Gynostemma pentaphyllum). ***J. Agric. Food Chem.*** **2013**, 61: 12646-12652.
16. **Zhang, X.**; Gao, B.; Shi, H.; Slavin, M.; Huang, H.; Whent, M.; Sheng, Y.; Yu, L. Chemical Composition of 13 Commercial Soybean Samples and Their Antioxidant and Anti-inflammatory Properties. ***J. Agric. Food Chem.*** **2012**, 60: 10027-10034.
17. Shi, H.; Yang, H.; **Zhang, X.;** Sheng, Y.; Huang, H.; Yu, L. Isolation and Characterization of Five Glycerol Esters from Wuhan Propolis and Their Potential Anti-Inflammatory Properties. ***J. Agric. Food Chem.*** **2012**, 60:10041-10047.
18. Shi, H.; Yang, H.; **Zhang, X.;** Yu, L. Identification and Quantification of Phytochemical Composition and Anti-inflammatory and Radical Scavenging Properties of Methanolic Extracts of Chinese Propolis. ***J. Agric. Food Chem.*** **2012**, 60: 12403-12410.